



THE HONG KONG
POLYTECHNIC UNIVERSITY

香港理工大學

Pao Yue-kong Library

包玉剛圖書館

Copyright Undertaking

This thesis is protected by copyright, with all rights reserved.

By reading and using the thesis, the reader understands and agrees to the following terms:

1. The reader will abide by the rules and legal ordinances governing copyright regarding the use of the thesis.
2. The reader will use the thesis for the purpose of research or private study only and not for distribution or further reproduction or any other purpose.
3. The reader agrees to indemnify and hold the University harmless from and against any loss, damage, cost, liability or expenses arising from copyright infringement or unauthorized usage.

IMPORTANT

If you have reasons to believe that any materials in this thesis are deemed not suitable to be distributed in this form, or a copyright owner having difficulty with the material being included in our database, please contact lbsys@polyu.edu.hk providing details. The Library will look into your claim and consider taking remedial action upon receipt of the written requests.

**TO ELUCIDATE THE STRUCTURE AND FUNCTION OF
P. FALCIPARUM CHLOROQUINE RESISTANCE
TRANSPORTER (PFCRT) USING THE SUBSTITUTED-
CYSTEINE ACCESSIBILITY METHOD (SCAM)**

LIANG GUOQING

Ph.D

The Hong Kong Polytechnic University

2010

The Hong Kong Polytechnic University

Department of Applied Biology and Chemical Technology

**To Elucidate the Structure and Function of *P. falciparum*
Chloroquine Resistance Transporter (PfCRT) Using the
Substituted-Cysteine Accessibility Method (SCAM)**

Liang Guoqing

A thesis submitted in partial fulfillment of the requirements for the
degree of Doctor of Philosophy

October 2009

Certification of Originality

I hereby declare that this thesis is my own work and that, of the best of my knowledge and belief, it reproduces no material previously published or written, nor material that has been accepted for the award of any other degree or diploma, except where due acknowledgement has been made in the text.

_____ (Signed)

Liang Guoging (Name of student)

Abstract

Malaria is a major public health problem in the world. Using multiple site-directed mutagenesis, cysteine-less *pfcr*t on Dd2 genetic background and thirty-one single cysteine substituted *pfcr*t within TMD1 and TMD4 were constructed. Twenty one substituted PfCRT within TMD1 and seven in TMD4 were expressed successfully in *Pichia pastoris*.

The microsomes isolated from *Pichia pastoris* were used to determine the transport activities of PfCRT. Cysteine substitution of obligate amino acids of PfCRT affects the function of PfCRT. Modified by MTSES, Dd2-Cys-less-T76C PfCRT microsomes can accumulate more CQ when the concentration of MTSES increases. Meanwhile, MTSET and MTSEA lead to a decrease in specific CQ accumulation as the concentration of these two MTS reagents increase. This suggests that the charged 76th amino acid affects the CQ accumulation.

Substrate protection of MTS reagents modification was carried out in the presence of non-radiolabelled CQ. In these assays, only the 76th showed protection effects. This result strongly suggests that the 76th is a binding site of CQ in PfCRT.

Reconstituted proteoliposomes were used to study the PfCRT. Dd2-Cys-less reconstituted proteoliposomes have significant specific CQ accumulation activities. Modification of Dd2-Cys-less-T76C by MTSES demonstrated a higher relative activity and showed that the 76th, 73rd and 67th are accessible to MTS. In the CQ protection assay, CQ impedes the 76th from modification by MTSES and the 76th amino acid of PfCRT may be involved in the position where MTSET modification takes place.

In the modification of TMD4 by MTSET, only S163C displays a lower relative activity. This suggests that inducing a positive charge at the 163rd may decrease CQ accumulation.

Our results showed that the CQ accumulation ability of the 163rd was not affected by CQ protection. This suggests that the 163rd is different from the 76th, which may be a CQ binding site within PfCRT.

Acknowledgements

First of all, I would like to express my deepest sense of gratitude to my supervisor Dr. Larry M. C. Chow for his kindness, encouragement, patient guidance and excellent advice throughout this study.

I am thankful to Miss Yunzhe Zhao, Dr. Weiqi Tan, Dr. Iris Wang and Miss Kitying Choy, Mr. Tebris Choy and Mr. C. M. Lau for their generous assistance during this time.

I am thankful to Mr. CHIA Keng Kia for his close collaboration with me in this study.

I thank all the technicians in the Department of Applied Biology and Chemical Technology, especially Miss Mabel Yau and Miss Sarah Yeung for their technical support.

I also thank PolyU SEM Christian Fellowship for prayers and support to my family and me.

Finally, I take this opportunity to express my profound gratitude to my beloved parents, my brother, my wife and my son for their moral support and patience during my study in PolyU.

Table of Contents

Certification of Originality	III
Abstract	IV
Acknowledgements	VI
Table of Contents	VII
List of Figures	XIV
List of Tables	XVIII
List of Abbreviations	XIX
1 Chapter 1	2 -
<i>1.1 Malaria and Antimalarial Drugs</i>	<i>3 -</i>
1.1.1 Life cycle of <i>P. falciparum</i>	5 -
1.1.2 Hemoglobin degradation and DV	9 -
1.1.3 Free heme detoxification systems of <i>P. falciparum</i>	10 -
1.1.4 Antimalarial drugs	13 -
1.1.5 The mechanisms of resistance of chloroquine	15 -
<i>1.2 Mechanism of Action of Chloroquine</i>	<i>17 -</i>
1.2.1 The energy-dependent rapid efflux mechanism	19 -

1.2.2	The reduced import of CQ mechanism	21 -
1.2.3	The plasmodial Na ⁺ /H ⁺ exchanger model	22 -
1.2.4	The trapping of weak-base CQ in the acidic environment mechanism.....	23 -
1.2.5	Binding affinity of chloroquine.....	25 -
1.3	<i>The pfcrt Gene Associated with CQR in P. falciparum</i>	26 -
1.3.1	Mutations distinguished CQR from CQS.....	27 -
1.3.2	Is PfCRT a member of the Drug/Metabolite transporter superfamily?.....	32 -
1.3.3	Proposed function of PfCRT	35 -
1.3.4	S163R mutation of PfCRT restores susceptibility from CQR.....	36 -
1.4	<i>Expression of PfCRT in a Heterologous System</i>	37 -
1.5	<i>The Substituted-cysteine Accessibility Method (SCAM) to Elucidate Membrane Protein Structure</i>	38 -
1.5.1	The substituted-cysteine accessibility method (SCAM)	39 -
1.5.2	The strategy for performing SCAM.....	42 -
1.5.3	Characterization and applications of charged and neutral MTS reagents ..	44 -
1.5.4	The limitations of SCAM	47 -
	Objectives	48 -
2	Chapter 2	49 -
	Abstract	50 -

2.1	<i>Introduction</i>	51 -
2.1.1	The features of the <i>Pichia pastoris</i> expression system	52 -
2.1.2	Cell lines constructed in this project	54 -
2.2	<i>Materials and Methods</i>	56 -
2.2.1	Materials	56 -
2.2.2	Construction strategy of cysteine-less <i>pfcr1</i>	57 -
2.2.3	Site-directed mutagenesis of single cysteine-substituted <i>pfcr1</i>	60 -
2.2.4	Cloning of genes for expression	62 -
2.2.5	Transformation of <i>Pichia pastoris</i> and confirmation of <i>pfcr1</i> integration ..	63 -
2.2.6	Growth of <i>Pichia pastoris</i>	65 -
2.2.7	Preparation of microsomes from <i>Pichia pastoris</i>	65 -
2.2.8	Detection of expressed PfCRT with Western blot	66 -
2.2.9	Solubilization of PfCRT and purification by Ni ²⁺ -NTA agarose	67 -
2.3	<i>Results</i>	68 -
2.3.1	Construction of cysteine-less and single cysteine <i>pfcr1</i> gene mutants	68 -
2.3.2	Expression of PfCRT derivatives in <i>P. pastoris</i>	71 -
2.3.3	Microsome preparation and purification of PfCRT	73 -
2.4	<i>Discussion</i>	73 -
3	Chapter 3	77 -
	Abstract	78 -

3.1	<i>Introduction</i>	79 -
3.1.1	Conversion of lysine 76 to threonine in TMD1 confers CQR phenotype ..	79 -
3.1.2	PfCRT is a putative transporter	80 -
3.1.3	Characterization of PfCRT by heterologous expression system	81 -
3.1.4	Use of microsomes in CQ transport analysis of PfCRT	82 -
3.2	<i>Materials and Methods</i>	84 -
3.2.1	Materials	84 -
3.2.2	Culture of <i>P. pastoris</i> cells and preparation of microsomes from <i>P. pastoris</i>	84 -
3.2.3	Determination of the orientation of PfCRT in the membrane of microsomes	85 -
3.2.4	Assay of the accumulation of ³ H-CQ in microsomes	85 -
3.2.5	Treatment with MTS reagents	86 -
3.3	<i>Results</i>	88 -
3.3.1	Determination of the orientation of PfCRT across microsomes	88 -
3.3.2	PfCRT microsomes transport CQ in a saturable manner	89 -
3.3.3	Dependence of ³ H-CQ uptake on microsome concentration and incubation time	91 -
3.3.4	The specific ³ H-CQ accumulation activity of single cysteine-substituted mutants	93 -
3.3.5	MTS concentration-dependence modification	94 -

3.3.6	The sensitivity of single cysteine-substituted mutants to MTSES	97 -
3.3.7	The sensitivity of single cysteine substitution mutants to MTSET	98 -
3.3.8	The sensitivity of single cysteine substitution mutants to MTSEA	99 -
3.3.9	CQ protection of MTSES modification	100 -
3.3.10	CQ protection of MTSET modification	103 -
3.3.11	CQ protection of MTSEA modification	104 -
3.4	<i>Discussion</i>	105 -
4	Chapter 4	110 -
	Abstract	111 -
4.1	<i>Introduction</i>	112 -
4.1.1	Reasons for reconstitution of proteoliposomes	112 -
4.1.2	Characteristics of liposomes	113 -
4.1.3	Application of proteoliposome reconstitution in basic research	115 -
4.2	<i>Materials and Methods</i>	117 -
4.2.1	Materials	117 -
4.2.2	Preparation of liposomes	117 -
4.2.3	Reconstitution of PfCRT	118 -
4.2.4	Assay of the accumulation of ³ H-CQ in proteoliposomes	119 -
4.2.5	Treatment with MTS-linked reagents	119 -
4.3	<i>Results</i>	121 -

4.3.1	Reconstitution of PfCRT	121 -
4.3.2	Reconstituted proteoliposomes transport CQ in a saturable manner	122 -
4.3.3	Dependence of ³ H-CQ uptake on proteoliposome concentration and incubation time	124 -
4.3.4	The specific ³ H-CQ accumulation activity of single cysteine substitution mutants	126 -
4.3.5	MTS concentration dependence modification	127 -
4.3.6	The sensitivity of single cysteine substitution mutants to MTSES	130 -
4.3.7	The sensitivity of single cysteine substitution mutants to MTSET	132 -
4.3.8	CQ protection of MTS modification	133 -
4.3.9	CQ protection to MTSET modification	134 -
4.4	<i>Discussion</i>	136 -
5	Chapter 5	138 -
	Abstract	139 -
5.1	<i>Introduction</i>	140 -
5.2	<i>Materials and Methods</i>	142 -
5.2.1	Materials	142 -
5.2.2	Culture of <i>P. pastoris</i> cells and preparation of microsomes from <i>P. pastoris</i>	142 -

5.2.3	Determination of the orientation of PfCRT within membrane of microsomes ..	142 -
5.2.4	Assay of the accumulation of ³ H-CQ in microsomes	142 -
5.2.5	Treatment with MTS-linked reagents	142 -
5.3	<i>Results</i>	143 -
5.3.1	The specific ³ H-CQ accumulation activity of single cysteine substitution mutants	143 -
5.3.2	The sensitivity of single cysteine substitution mutants to MTSES and MTSET	144 -
5.3.3	CQ protection to MTSES modification	146 -
5.3.4	CQ protection of MTSET modification	147 -
5.4	<i>Discussion</i>	149 -
	Conclusion	151 -
	Summary	156 -
	Future Work	161 -
	Appendix	165 -
	<i>Solution</i>	165 -
	<i>Drug Structure</i>	167 -
	References	169 -

List of Figures

Figure 1-1	Life cycle of <i>Plasmodium</i>	- 8 -
Figure 1-2	Possible mechanisms of free heme toxicity in malaria parasite.....	- 11 -
Figure 1-3	Quinoline and its derivatives	- 15 -
Figure 1-4	The concentration–effect relationship of drug resistance to an antimalarial compound.....	- 17 -
Figure 1-5	Capping model of quinoline action	- 18 -
Figure 1-6	Proposed model of chloroquine resistance in <i>P. falciparum</i>	- 21 -
Figure 1-7	Charge distribution, topology, and putative roles of the TMDs of PfCRT .-	- 27 -
Figure 1-8	A model for the mechanism of PfCRT-mediated CQ-resistance.....	- 34 -
Figure 1-9	Thiol-modifying reagents widely used in SCAM	- 41 -
Figure 1-10	Schematic representation of the reaction of an MTS reagent with a cysteine exposed in the binding-site crevice.....	- 43 -
Figure 2-1	Features of the pPICZA, B, C.....	- 53 -
Figure 2-2	The procedure of multiple site-directed mutagenesis.....	- 59 -
Figure 2-3	The sequence of cysteine-less <i>pfCRT</i>	- 69 -
Figure 2-4	The expression of PfCRT derivatives demonstrated by western blot.	- 72 -
Figure 2-5	Time course of PfCRT expression in Yeast-Dd2-Cys-less	- 73 -

Figure 2-6 SDS-PAGE of purified PfCRTs.....	- 75 -
Figure 3-1 Western blot of orientation of PfCRT in microsomes.....	- 89 -
Figure 3-2 Dependence of ³ H-CQ uptake on ³ H-CQ concentration	- 90 -
Figure 3-3 Dependence of ³ H-CQ uptake on concentration of microsomes	- 92 -
Figure 3-4 Time course of ³ H-CQ accumulation in microsomes of mutated PfCRT	- 93 -
Figure 3-5 The Specific ³ H-CQ accumulation of PfCRT of Dd2-Cys-less parent and 21 single cysteine recovery mutants within TMD1.....	- 94 -
Figure 3-6 MTSES concentration dependence of the ability of CQ accumulation of microsomes containing mutagenic PfCRT.....	- 95 -
Figure 3-7 MTSET concentration dependence of the ability of CQ accumulation of microsomes containing mutagenic PfCRT.....	- 96 -
Figure 3-8 MTSEA concentration dependence of the ability of CQ accumulation of microsomes containing mutagenic PfCRT.....	- 97 -
Figure 3-9 Sensitivity of single cysteine substitution mutants to MTSES.....	- 98 -
Figure 3-10 Sensitivity of single cysteine substitution mutants to MTSET.....	- 99 -
Figure 3-11 Sensitivity of single cysteine substitution mutants to MTSEA.....	- 100 -
Figure 3-12 Specific ³ H-CQ accumulation by microsomes of Dd2-Cys-less with pre- incubation of non-radiolabeled CQ	- 102 -
Figure 3-13 CQ protection to MTSES modification.....	- 102 -
Figure 3-14 CQ protection to MTSET modification.....	- 103 -
Figure 3-15 CQ protection to MTSEA modification	- 104 -

Figure 3-16 Role of PfCRT in chloroquine resistance in <i>P. falciparum</i>	107 -
Figure 3-17 Integrated view of TMD1 of PfCRT	109 -
Figure 4-1 Schematic illustration of liposomes of different size and number of lamellae.....	
.....	114 -
Figure 4-2 Typical western blot results of PfCRT mutants using anti-his antibody.....	121 -
Figure 4-3 Dependence of ³ H-CQ uptake on ³ H-CQ concentration in proteoliposome.....	
.....	124 -
Figure 4-4 Dependence of ³ H-CQ uptake on concentration of proteoliposomes.....	125 -
Figure 4-5 Time course of ³ H-CQ accumulation in proteoliposomes	126 -
Figure 4-6 The specific ³ H-CQ accumulation activity of proteoliposomes.....	127 -
Figure 4-7 MTSES concentration dependence of the ability of CQ accumulation of	
proteoliposomes containing mutagenic PfCRT.....	129 -
Figure 4-8 MTSET concentration dependence of the ability of CQ accumulation of	
proteoliposomes containing mutagenic PfCRT.....	129 -
Figure 4-9 MTSEA concentration dependence of the ability of CQ accumulation of	
reconstituted proteoliposomes.....	130 -
Figure 4-10 Sensitivity of single cysteine substitution mutants to MTSES	131 -
Figure 4-11 Sensitivity of single cysteine substitution mutants to MTSET	132 -
Figure 4-12 CQ protection to MTSES modification	134 -
Figure 4-13 CQ protection to MTSET modification.....	135 -
Figure 5-1 PfCRT point mutations and drug effects in <i>P. falciparum</i>	141 -

Figure 5-2 The specific ³H-CQ accumulation of Pfcrf of Dd2-Cys-less seven single
cysteine recovery mutants within TM4..... - 143 -

Figure 5-3 Sensitivity of single cysteine substitution mutants to MTSES - 145 -

Figure 5-4 Sensitivity of single cysteine substitution mutants to MTSET - 146 -

Figure 5-5 CQ protection to MTSES modification - 147 -

Figure 5-6 CQ protection to MTSET modification..... - 148 -

List of Tables

Table 1-1 Classification of antimalarial drugs	- 14 -
Table 1-2: Mutant forms of PfCRT and complete association of the K76T marker with chloroquine-resistant <i>P. falciparum</i> parasites from different geographic regions. .	- 28 -
Table 1-3 Summary of charged MTS reagents	- 44 -
Table 2-1 Cell lines expressed in this project	- 55 -
Table 2-2 cysteine-less mutagenic oligonucleotide primers	- 58 -
Table 2-3 Anchor oligonucleotide primers	- 58 -
Table 2-4 Sequence primers used for single-cysteine recoveries in TMD1	- 61 -
Table 2-5 Plasmids of single cysteine mutants	- 70 -
Table 3-1 Summary of Vmax values of microsomes containing Dd2-Cys-less, Dd2-Cys- less-I59C and Dd2-Cys-less-T76C	- 91 -
Table 4-1 Reconstitution efficiency of mutagenic PfCRT proteins in reconstituted proteoliposomes.....	- 122 -

List of Abbreviations

ABC	ATP-binding cassette
ADP	Adenosine diphosphate
AM	Amantadine
AO	Acridine orange
AOX	Alcohol oxidase
<i>A. thaliana</i>	<i>Arabidopsis thaliana</i>
ATP	Adenosine triphosphate
BCECF	2',7'-bis-(2-carboxyethyl)-5-(and -6)-carboxyfluorescein
<i>C. elegans</i>	<i>Caenorhabditis elegans</i>
CEO	<i>C. elegans</i> ORF
CFTR	Cystic fibrosis transmembrane regulator
<i>C. parvum</i>	<i>Cryptosporidium parvum</i>
CQ	Chloroquine
CQR	Chloroquine resistance
CQS	Chloroquine sensitive
CRT	Chloroquine resistance transporter
CSA	Chondroitin sulphate A
<i>D. discoideum</i>	<i>Dictyostelium discoideum</i>
DDM	Dodecyl- β -D-maltoside
DME	Drug/Metabolite effluxer
DMT	Drug/Metabolite Transporter
DO	Dissolved oxygen

DTT	Dithiothreitol
DV	Digestive food vacuole
Egg PC	Egg phosphatidylcholine
Fe(III)PPIX	Fe (III)-protoporphyrin-IX
FPIX	Iron (III) Ferriprotoporphyrin IX
FV	Food vacuole
Gcat	Cation conductance
GRP	Glucose/Ribose permease
GSH	Glutathione
H ⁺	Proton
H ⁺ -ATPase	Proton-translocating ATPase
Hb	Haemoglobin
HF	Halofantrine
H ⁺ -PPase	Proton-translocating pyrophosphatase
IMAC	Immobilized metal affinity chromatography
ISOV	Inside-out vesicles
MDR	Multidrug resistance
MGYH	Minimal glycerol medium with histidine
MMH	Minimal methanol with histidine
MTS	methanethiosulphonates
MTSEA	2-Aminoethyl methanethiosulfonate hydrobromide
MTSES	Sodium (2-sulfonatoethyl) methanethiosulfonate
MTSET	Trimethylammonium ethylmethanethiosulfonate bromide
MRP	Multidrug resistance related protein
Mut ⁺	Methanol utilization plus

Mut ^S	Methanol utilization slow
NHE	Na ⁺ /H ⁺ exchanger
NST	Nucleotide sugar transporter
ORF	Open-reading-frame
PC	Phosphatidylcholine
PfCRT	<i>Plasmodium falciparum</i> chloroquine resistance transporter
PfEMP1	<i>P. falciparum</i> -infected erythrocyte membrane protein 1
<i>Pfmdr</i>	<i>Plasmodium falciparum</i> Multiple-drug Resistant Gene
Pgp	P-glycoprotein
Pgh	P-glycoprotein homology
pH	pH gradient
pHi	Internal pH
pH _{vac}	Internal pH of food vacuole
POP	Plant organization permease
<i>P. pastoris</i>	<i>Pichia pastoris</i>
PVDF	Polyvinylidene fluoride
QNR	Quinine resistance
RBC	Red blood cells
RhaT	L-Rhamnose symporter
ROV	Right-side-out Vesicles
SCAM	Substituted-cysteine accessibility method
SDS-PAGE	Sodium dodecyl sulphate-polyacrylamide gel electrophoresis
TEMED	N,N,N',N'-tetramethylethylenediamine
TMD	Transmembrane domain

TPT	Triose-phosphate transporter
TTBS	Tween-tris buffered saline
VPL	verapamil
WHO	World Health Organization
YPD	Yeast peptone dextrose
	Membrane potential

Chapter 1

Introduction

1.1 Malaria and Antimalarial Drugs

Malaria is a major public health problem in the world. It contributes to a considerable burden in endemic communities with premature deaths, disability from illness and impedes social and economic development. There were an estimated 247 million malaria cases among 3.3 billion people in 2006, causing nearly a million deaths, mostly children under 5 years old. A total of 109 countries and areas were considered to have malaria zones in 2008, 45 within the African region (WHO, 2008). Malaria is also an important cause of death and illness in children and adults in tropical countries.

Malaria transmission occurs in large areas of Central and South America, the island of Hispaniola (the Dominican Republic and Haiti), Africa, Asia (including South Asia, Southeast Asia, and the Middle East), Eastern Europe, and the South Pacific. Malaria transmission differs in intensity and regularity depending on local factors such as rainfall patterns, proximity of mosquito breeding sites, mosquito species, and the vector of malaria (WHO, 2008). Some regions experience a fairly constant number of cases throughout the year. Climate changes associated with global warming could bring malaria to parts of the world that are currently malaria-free. Of the numerous challenges faced by malaria control in all regions, the most daunting include insecticide resistant mosquitoes and parasites that have developed resistance to most antimalarial medicines. Travelers going from malaria-free regions to areas where there is malaria transmission are highly vulnerable; they have little or no immunity and are often exposed to delayed or wrong malaria diagnosis when returning to their home country.

Chapter 1 Antimalarial and CQ Resistance

Malaria is a hematoprotzoan parasitic infection transmitted by the female *Anopheles* mosquito. It is a disease that can be treated in just 48 hours, yet it can cause fatal complications if the diagnosis and treatment are delayed. Malaria was nearly eradicated from most parts of the world by the early 60's, owing largely to concerted antimalarial campaigns under the guidance of the WHO (Greenwood and Mutabingwa, 2002). But now, it is re-emerging as the number one infectious killer and the number one priority tropical disease of the WHO.

Malaria is caused by the parasite called *Plasmodium*. Four species of protozoal parasites that belong to the genus *Plasmodium* infect humans, though there are more than 100 species of *Plasmodium* in nature. *Plasmodium falciparum*, which is found worldwide in tropical and subtropical areas, is the only species that can cause severe, potentially fatal malaria. *P. falciparum* is regarded as the greater menace because of its widespread resistance to antimalarial drugs. It is also the predominant species, especially in Africa. *Plasmodium vivax* is found mostly in Asia, Latin America, and in some parts of Africa. *P. vivax* has also placed huge burdens on the health, longevity, and general prosperity of large sections of the human population, especially in Asia. It is probably the most prevalent human malaria parasite. The two other species are less frequently encountered: *Plasmodium ovale* is found mostly in Africa. *Plasmodium malariae*, found worldwide, is the only human malaria parasite species that has a quartan cycle (three-day cycle), while the three other species have a tertian, two-day cycle.

WHO forecasts a 16% growth in malaria cases annually. About 1.5 million to 3 million people die of malaria every year (85% of these occur in Africa), accounting for about 4-5% of all fatalities in the world (Trape et al., 1998; Trape et al., 2002; WHO). A persistent effort to control malaria worldwide has been carried out the latest two decades

Chapter 1 Antimalarial and CQ Resistance

for effective tools and methods for prevention and cure. The combination of tools and methods to combat malaria now includes long-lasting insecticidal nets and artemisinin-based combination therapy, supported by indoor residual spraying of insecticide and intermittent preventive treatment in pregnancy. The procurement of antimalarial medicines through public health services increased sharply between 2001 and 2006, but access to treatment, especially of artemisinin-based combination therapy, was inadequate in all countries surveyed in 2006.

We should remember that one child dies of malaria somewhere in Africa every 20 seconds, and there is one malarial death every 12 sec somewhere in the world. Malaria kills in 1 year what AIDS killed in 15 years. In 15 years, if 5 million have died of AIDS, 50 million have died of malaria (WHO, 2008; Wiesner et al., 2003). After pneumococcal acute respiratory infections and tuberculosis, Malaria ranks the third among the major infectious diseases in causing deaths. It is expected that malaria will be the number one infectious killer disease in the world.

1.1.1 Life cycle of *P. falciparum*

Malaria is caused by several species of obligate intracellular protozoa from the genus *Plasmodium*. *P. falciparum* is the most deadly of these. *Plasmodium* is a very small, single-cell blood organism, or 'protozoan'. The parasites have a complicated life cycle that requires a vertebrate host for the asexual cycle and a female *Anopheles* mosquito, which is the only species capable of serving as host for it, for completion of the sexual cycle. Sixty species of *Anopheles* mosquito vectors exist worldwide and mosquito

Chapter 1 Antimalarial and CQ Resistance

species vary by region. It has three to four different forms. Each form is specialized in living in a certain place.

When the mosquito has sucked blood containing gametocytes, these pass into the salivary glands of the mosquito, where they develop into a new form, the sporozoite. The sporozoite can be passed on to man when the mosquito bites, injecting its saliva into the blood vessels. The sporozoites travel with the blood to the liver and enter the liver cells. In infected liver cells sporozoites mature into schizonts, which rupture and release merozoites. After this exo-erythrocytic schizogony cycle replication in the liver, the parasites undergo erythrocytic schizogony asexual multiplication in the erythrocytes. The merozoites are released from the liver to the blood where they are taken up by the red corpuscles. Some of these turn into ring-formed trophozoites. After the ring stage, trophozoites mature into schizonts, which rupture and release merozoites. In this stage some parasites differentiate into sexual erythrocytic stages, the gametocytes. Blood stage parasites are responsible for the clinical manifestations of the disease. Schizonts burst the red corpuscles at a certain moment, releasing the merozoites. This release coincides with the violent rises in temperature during the attacks seen in malaria. The incubation period, time from infection to development of the disease, is usually about 10 to 15 days. This period can be much longer depending on whether any antimalarial medication has been taken.

The male gametocytes (microgametocytes) and female gametocytes (macrogametocytes) are ingested by an *Anopheles* mosquito during a blood meal. The parasites' multiplication in the mosquito is known as the sporogonic cycle. In the mosquito's stomach, the microgametocytes penetrate the macrogametocytes generating zygotes. The zygotes in turn become motile and elongated to ookinetes. The ookinetes invade the

Chapter 1 Antimalarial and CQ Resistance

midgut wall of the mosquito where they develop into oocysts. The oocysts grow, rupture, and release sporozoites, which make their way to the mosquito's salivary glands. Inoculation of the sporozoites into a new human host perpetuates the malaria life cycle. (Figure 1-1).

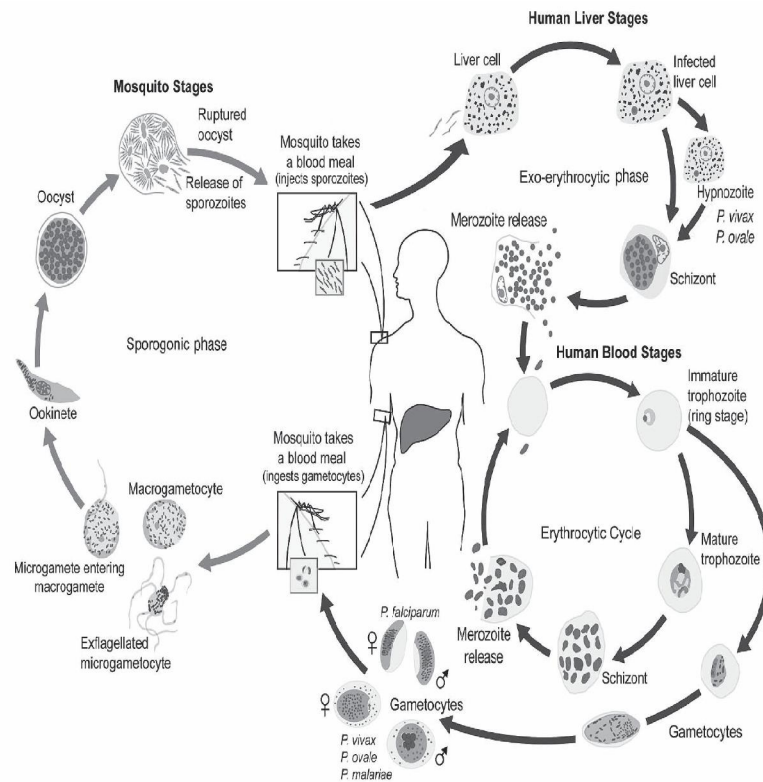


Figure 1-1 Life cycle of *Plasmodium*

The mosquito injects sporozoites into the host, which are carried through the blood to the liver, where they invade hepatocytes and undergo a process of asexual (mitotic) replication to give rise to an exoerythrocytic schizont. Up to this point, the infection is non-pathogenic and clinically silent. After about seven days, the liver schizonts rupture to release many thousands of merozoites into the blood. Each merozoite invades an erythrocyte and divides mitotically to form an erythrocytic schizont, containing up to 20 daughter merozoites. These merozoites can re-infect fresh erythrocytes, giving rise to a cyclical blood-stage infection with a periodicity of 48-72 hours, depending on the *Plasmodium* species. As-yet-unknown factors trigger a subset of developing merozoites to differentiate into male and female gametocytes, which, when taken up by a feeding mosquito, give rise to extracellular gametes. In the mosquito mid-gut, the gametes fuse to form a motile zygote (ookinete), which penetrates the mid-gut wall and forms an oocyst, within which meiosis takes place and haploid sporozoites develop. The immune responses known to be protective at each main stage of the life cycle are shown. (Hill, 2006)

1.1.2 Hemoglobin degradation and DV

The malaria parasite requires amino acids for the synthesis of its proteins. The three sources of amino acids are *de novo* synthesis, imported from host plasma, and digestion of host hemoglobin. Hemoglobin is an extremely abundant protein in the erythrocyte cytoplasm and serves as the major source of amino acids for the parasite. It is present at a concentration of 5 mM. During the intraerythrocytic cycle, the host cell cytoplasm is consumed and an estimated 60–80% of the hemoglobin is degraded.

During the early ring stage, the parasite takes up the host cell cytoplasm by pinocytosis thus resulting in double membrane vesicles. The inner membrane rapidly disappears and the digestion of hemoglobin takes place within these small vesicles during the early trophozoite stage. As the parasite matures, it develops a special organelle, the cytostome, for the uptake of host cytoplasm. And the small pigment-containing vesicles fuse to form a large digestive vacuole (DV, also known as food vacuole). Double-membrane vesicles pinch off from the base of the cytostome and fuse with the DV. The inner membrane is degraded and the hemoglobin is released into the DV.

The DV has an acidic compartment with physiological pH 5.0-5.4. It contains proteases. The hemoglobin-laden endocytic vesicles mature into DVs (Bannister and Mitchell, 2003; Slomianny et al., 1985), which probably are the equivalent of acidic late endosomes or lysosomes in other eukaryotic cells. Whether DVs mature directly from endosomes that have docked and fused with each other or whether endosomes dock and fuse with lysosomes to acquire degradative capabilities has not been determined.

Hemoglobin proteolysis releases heme and generates amino acids. The heme moiety does not appear to be metabolized or recycled, but instead, is stored as an inert polymer

known as the malaria pigment hemozoin. Sooner or later, the DVs containing hemozoin dock and fuse with each other, presumably to permit membrane recycling. The resulting residual vacuoles continue to collect and store hemozoin until the schizont matures, ruptures, and dumps its waste into the circulatory system of the host. Each of the steps is comprised of a series of molecular events (Bannister and Mitchell, 2003).

The globin is degraded to peptides by parasite aspartic proteinase enzymes called plasmepsins I (Goldberg et al., 1997) and II (Gluzman et al., 1990) and a cysteine proteinase enzyme called falcipain (Francis et al., 1996) in DVs (Krogstad et al., 1987). In collaboration with plasmepsins, falcipain cleaves the large globin fragments into smaller polypeptides of up to 20 residues and into short peptide fragments of 6-8 amino acids.

These peptides are then assumed to be transported out of the DV to the parasite cytoplasm by a peptide transporter located in the DV membrane (Kolakovich et al., 1997; Rubio and Cowman, 1996). Peptides are hydrolyzed to amino acids by cytosolic exopeptidase and the released amino acids are used by the parasites for their protein synthesis and growth.

1.1.3 Free heme detoxification systems of *P. falciparum*

In the process of hemoglobin degradation, heme is released from the hemoglobin and autooxidised to hematin, namely ferriprotoporphyrin IX (Fe(III)PPIX). This leads to the production of hydrogen peroxide through the one-electron oxidation of Fe (II) (Figure 1-2). In addition to this oxidative assault, if the released heme accumulates within the DV, the concentration of free heme may reach 300 – 500 mM (Wright et al., 2001). Free heme

(Fe^{3+}) is very toxic because it can generate reactive oxygen species (Kumar et al., 2006) and may induce oxidative stress leading to parasite death (Schmitt and Burckhardt, 1993). Since free heme is a lipophilic molecule, it can easily intercalate in the membrane and may cause changes in membrane permeability and lipid organization, and induces lipid peroxidation of the parasite membrane (Begum et al., 2003). Oxidation of membrane components induced by free heme promotes cell lysis and ultimately death of the parasite (Schmitt and Burckhardt, 1993).

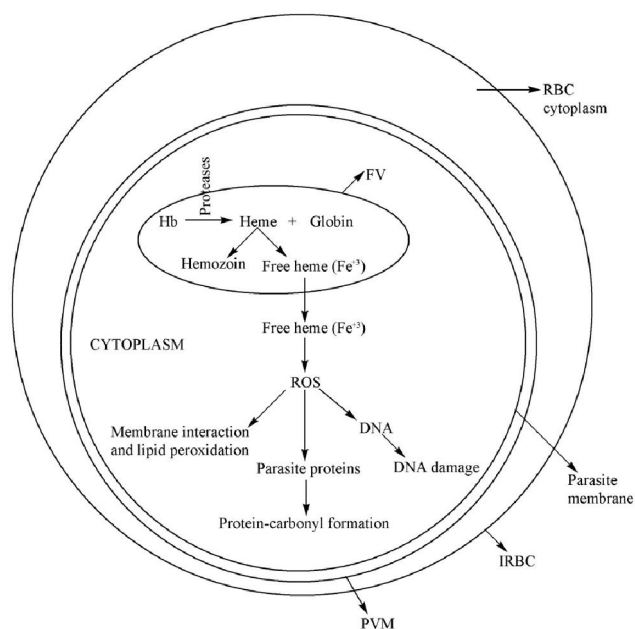


Figure 1-2 Possible mechanisms of free heme toxicity in malaria parasite
Hb, hemoglobin; FV, DV; IRBC, infected red blood cell; PVM, parasitophorous vacuolar membrane;
ROS, reactive oxygen species (Kumar et al., 2007).

Chapter 1 Antimalarial and CQ Resistance

The Malaria parasite possesses efficient heme detoxification mechanisms to protect itself from heme-induced oxidative stress. There are several possible processes of heme detoxification: (1) sequestration of the free heme into hemozoin, namely malarial pigment; (2) degradation facilitated by hydrogen peroxide within the DV; (3) glutathione-dependent degradation which occurs in the parasite's cytoplasm; (4) and possibly a heme oxygenase which has been found in *P. berghei* (rodent parasite) and *P. knowlesi* (simian parasite). These four processes take the reactive heme species out of solution chemically. As *P. falciparum* lacks heme oxygenase and cannot degrade heme by macrocycle cleavage, it uniquely makes a heme crystal called hemozoin or malarial pigment for heme detoxification.

During its pathogenic blood stage, the malaria parasite *P. falciparum* digests a large proportion of host red blood cell hemoglobin. Only a small quantity of heme released is oxidised to ferriprotoporphyrin IX (Fe(III)PPIX) and at least 95% is sequestered in the form of hemozoin (malaria pigment) (Kumar et al., 2006). Formation of hemozoin is the primary process of detoxification of heme. The mechanism of hemozoin formation is not yet very clear. Several hypotheses have been offered to explain hemozoin crystallization in malaria parasites (Slater and Cerami, 1992; Sullivan et al., 1996; Egan, 2004; Tekwani and Walker, 2005; Pagola et al., 2000; Egan, 2001, 2002).

Heme metabolism in humans is an oxygenase pathway. In this process, the porphyrin ring of heme opens to form less toxic by-products, i.e. the bile pigments. The parasite detoxifies Fe(III)PPIX by converting it into an insoluble, inert crystalline material called malaria pigment or hemozoin. This brown-colored pigment accumulated in the DV also offers one of the most characteristic morphological features of malaria infection. The presence of this brown birefringent crystal also demarcates the transition from a non-

pigmented ring-stage to the pigmented trophozoite stage (Bruce, 1993). The observation of these kinds of black dots within infected RBC is clinical confirmation of active malarial infection.

1.1.4 Antimalarial drugs

Antimalarial drugs can be classified according to anti-malarial activity and structure. According to anti-malarial activity, tissue schizonticides, applied for causal prophylaxis, act on the primary tissue forms of the plasmodia. After growth within the liver, schizonts initiate the erythrocytic stage. Theoretically, by blocking this stage, further development of the infection can be prevented. Pyrimethamine and Primaquine have this activity. Since it is impossible to predict the infection before clinical symptoms, this mode of therapy is more theoretical than practical. Tissue schizonticides for preventing relapse act on the hypnozoites of *P. vivax* and *P. ovale* in the liver that cause relapse of symptoms on reactivation. Primaquine is the prototype drug and pyrimethamine also has such activity.

Blood schizonticides act on the blood forms of the parasite and thereby terminate clinical attacks of malaria. These are the most important drugs in antimalarial chemotherapy. Quinoline and its derivatives (Table 1-1, Figure 1-3 Quinoline and its derivatives) represent a very important class of antimalarial drugs that function by targeting the parasite-specific hemoglobin breakdown pathway. Important members of this class are chloroquine, amodiaquine, amopyroquine, tebuquine, mepacrine, pyronaridine, halofantrine, quinine, epiquinine, quinidine and bisquinoline.

Chapter 1 Antimalarial and CQ Resistance

Gametocytocides destroy the sexual forms of the parasite in the blood and thereby prevent transmission of the infection to the mosquito. Chloroquine and quinine have gametocytocidal activity against *P. vivax* and *P. malariae*, but not against *P. falciparum*. Primaquine has gametocytocidal activity against all plasmodia, including *P. falciparum*. Sporontocides prevent the development of oocysts in the mosquito and thus ablate the transmission. Primaquine and chloroguanide have this action. Thus in effect, treatment of malaria would include a blood schizonticide, a gametocytocide and a tissue schizonticide (in case of *P. vivax* and *P. ovale*). A combination of chloroquine and primaquine is thus needed in all cases of malaria. Other than this classification, antimalarial drugs can be divided into 8 groups according to the chemical structure. (Table 1-1)

Table 1-1 Classification of antimalarial drugs.

Aryl amino alcohols:	Quinine, quinidine (cinchona alkaloids), mefloquine, halofantrine.
4-aminoquinolines:	Chloroquine, amodiaquine.
Folate synthesis inhibitors:	Type 1 - competitive inhibitors of dihydropteroate synthase - sulphones, sulphonamides. Type 2 - inhibit dihydrofolate reductase - biguanides like proguanil and chlorproguanil; diaminopyrimidine like pyrimethamine.
8-aminoquinolines:	Primaquine, WR238, 605.
Antimicrobials:	Tetracycline, doxycycline, clindamycin, azithromycin, fluoroquinolones.
Peroxides:	Artemisinin (Qinghaosu) derivatives and analogues - artemether, arteether, artesunate, artelinic acid.
Naphthoquinones:	Atovaquone.
Iron chelating agents:	Desferrioxamine.

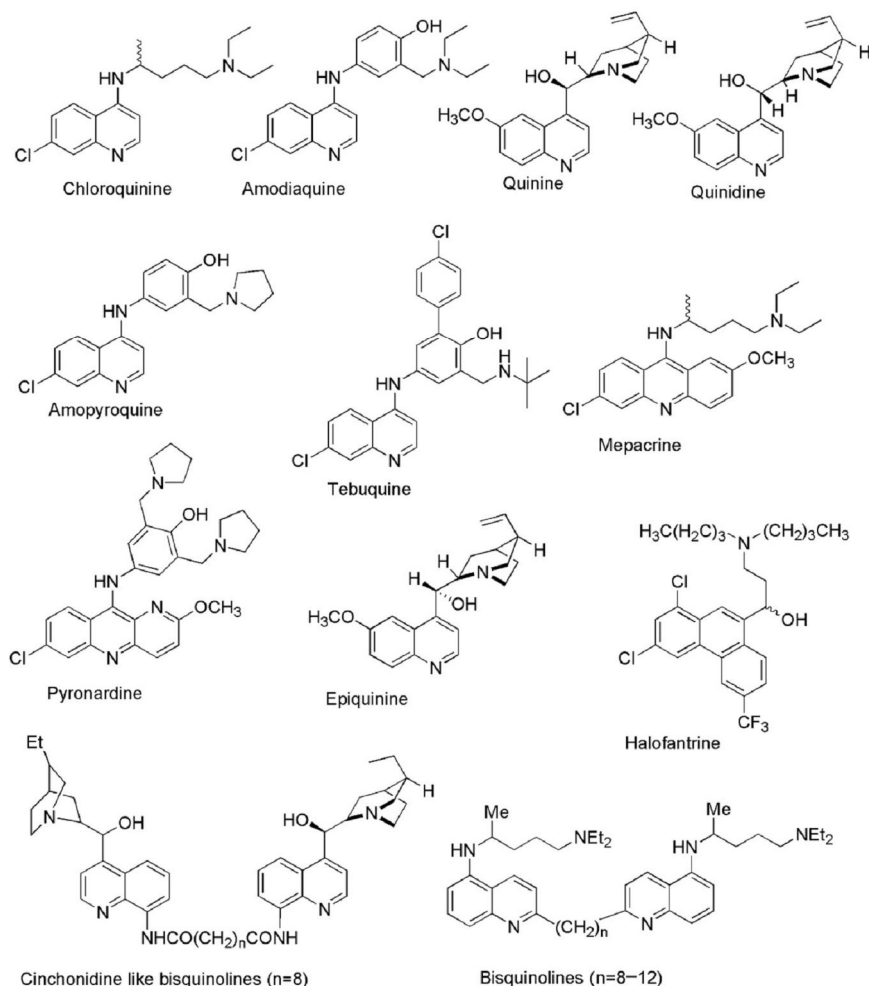


Figure 1-3 Quinoline and its derivatives

1.1.5 The mechanisms of resistance of chloroquine

Based on genetic diversity, the malaria parasite has evolved an ability to resist drug therapy. As the sensitive organisms die off, the resistant genotypes escape unharmed and pass along their resistance to their progeny. To date, the vast majority of antimalarial therapies widely used have lost their usefulness over time. Resistance to antimalarial drugs has increased the global cost of controlling the disease. Drug resistance occurring with *P. falciparum* remains the greatest problem, because of the enormous burden of

Chapter 1 Antimalarial and CQ Resistance

disease caused by this species, its lethal potential, the propensity for epidemics, and the cost of candidate replacement drugs for areas with established drug resistance. Chloroquine resistance does occur in *P. vivax*, especially in western Oceania, but there are very few reports of resistance in *P. malariae* or *P. ovale*.

Antimalarial drug resistance is defined as the ability of a parasite strain to survive and/or multiply despite the proper administration and absorption of an antimalarial drug in the dose normally recommended. Drug resistance to an antimalarial compound results in a right shift in the concentration–effect (dose–response) relationship (Figure 1-4). The development of resistance can be considered in two parts: the initial genetic event, which produces the resistant mutant; and the subsequent selection process in which the survival advantage in the presence of the drug leads to preferential transmission of resistant mutants and thus the spread of resistance.

Since the appearance of Chloroquine-resistance (CQR) 20 years ago, various CQR mechanisms have been proposed. Almost all of these models focus on two distinct characteristics of CQR. The first one is based on the understanding of diminished CQ accumulation in CQR parasites (Fitch, 1970; Krogstad et al., 1987). The other is based on the chemosensitisation of verapamil and other agents (Martin et al., 1987; Peters et al., 1989). The mechanism underpinning chloroquine drug resistance has remained controversial. Currently considered models to explain the resistance phenotype include acquisition of a chloroquine efflux pump, changes in intracellular chloroquine partitioning, diminished binding affinity of chloroquine to its intracellular target, heme, and changes in heme crystallization.

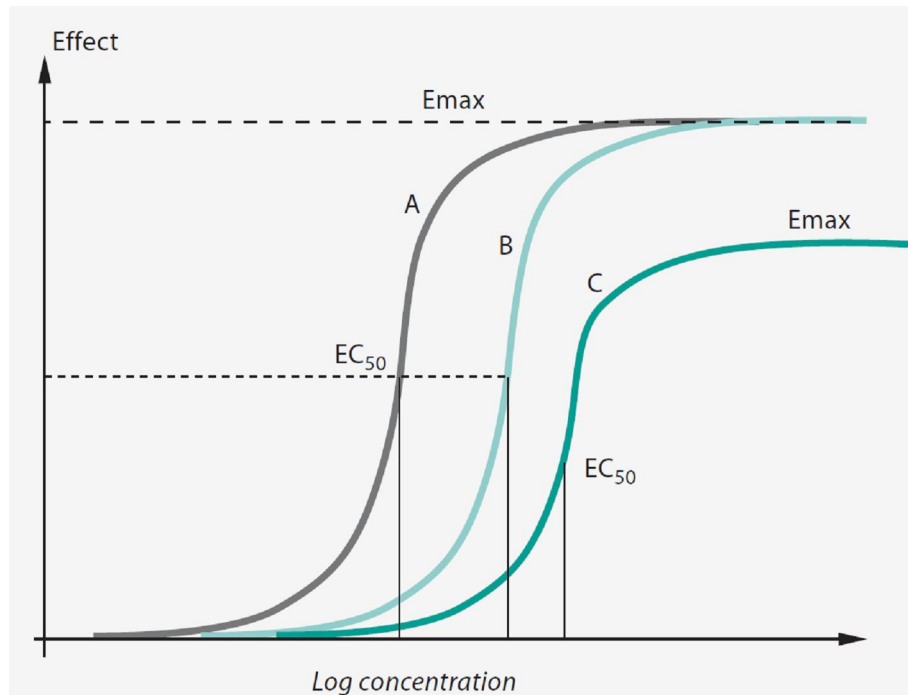


Figure 1-4 The concentration–effect relationship of drug resistance to an antimalarial compound. Resistance is a rightward shift in the concentration–effect relationship for a particular parasite population. This may be a parallel shift (B) from the “normal” profile (A) or, in some circumstances, the slope changes, and/or the maximum achievable effect is reduced (C). The effect is parasite killing.

1.2 Mechanism of Action of Chloroquine

CQ remains one of the best antimalarial drugs because of its high efficacy, its relative safety and its low cost. Various mechanisms have been proposed for the action of CQ (Akompang et al., 2002; Blauer and Akkawi, 2000; Bonday et al., 1997; Choi et al., 1999; Shear et al., 1998). The most spectacular characteristic of chloroquine is its capacity to concentrate itself from nanomolar levels outside the parasite to millimolar levels in the DV of the intraerythrocytic trophozoite. It is here that it inhibits hemoglobin degradation and forms complexes with hemozoin (Figure 1-5) (Sullivan et al., 1996a; Trager, 2003; Winograd et al., 1999).

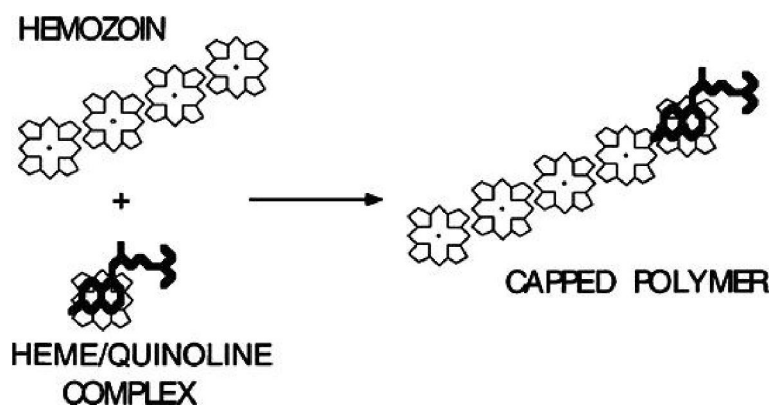


Figure 1-5 Capping model of quinoline action

Quinoline binds heme to form a drug-heme complex that adds on to the growing hemozoin chain, which prevents further polymerization and promotes toxic monomeric heme accumulation (Sullivan et al., 1996b).

CQ inhibits heme crystallization and heme decomposition mediated by glutathione or hydrogen peroxide. Some mechanisms have been proposed to explain how CQ prevents hemozoin formation (Demirev, 2004; Fitch, 1998; Hanscheid et al., 2000; Kumar et al., 2007; Schumann, 2007; Ziegler et al., 2001). *In vitro*, the polymerization of heme is blocked under approximately physiological conditions by chloroquine, quinine, mefloquine, and related quinolines (Bendrat et al., 1995; Cole et al., 2000; Dorn et al., 1995; Nalbandian et al., 1995; Orjih, 1996; Platel et al., 1999). It has therefore been proposed that drugs like chloroquine act by forming a complex with heme in the DV (Slater, 1993) and incorporating into the growing polymer as a drug-heme complex (Sullivan et al., 1996a) (Figure 1-5). This cap blocks further extension, resulting in accumulation of toxic free heme and initiating the irreversible demise of the parasite. These drugs thus appear to turn the organism's own hemoglobin degradation pathway against itself, poisoning the parasite by preventing waste removal (Bendrat et al., 1995; Cole et al., 2000; Nalbandian et al., 1995; Orjih, 1996; Platel et al., 1999).

Although the extension of a growing heme polymer is capped by a preformed CQ-heme complex (Dorn et al., 1998b), it is difficult to imagine how the limited number of CQ-heme complexes could inhibit the growth of hemozoin crystals (Loria et al., 1999). And if CQ inhibits a protein that catalyses hemozoin formation (Slater and Cerami, 1992), it is difficult to explain how hemozoin growth occurs *in vitro* without proteins (Dorn et al., 1998). The absorption of CQ onto the surface of the hemozoin crystal, which would inhibit further heme crystallization, seems the most likely scenario of how CQ inhibits hemozoin crystallization (Pagola et al., 2000). It is also suggested that CQ prevents glutathione and hydrogen peroxide from reacting with the complexed heme moiety to result in inhibiting heme degradation. As a result, membrane-toxic CQ-heme complexes accumulate.

1.2.1 The energy-dependent rapid efflux mechanism

Chloroquine-resistant *P. falciparum* accumulate significantly less chloroquine than susceptible parasites, and this is thought to be the basis of their resistance (Fitch, 1970; Krogstad et al., 1987). CQR parasites accumulate approximately four to ten times less CQ than susceptible ones (Ayesh et al., 1997; Becker and Kirk, 2004; Bray et al., 1999), thus keeping the intracellular CQ concentration below toxic levels. The resistant parasite was found to release chloroquine 40 to 50 times more rapidly than the susceptible parasite, although their initial rates of chloroquine accumulation are the same. These results suggest that a higher rate of chloroquine release explains the lower chloroquine accumulation, and thus the resistance observed in resistant *P. falciparum*. Verapamil and two other calcium channel blockers, as well as vinblastine and daunomycin, each slowed the release and increased the accumulation of chloroquine by resistant *P. falciparum*

Chapter 1 Antimalarial and CQ Resistance

(Krogstad and Herwaldt, 1988; Krogstad and Schlesinger, 1987). Based on these observations, together with the discovery that verapamil partially reverses CQR *in vitro*, the energy-dependent rapid efflux mechanism was proposed. According to this model, CQR parasites can pump out CQ more quickly than sensitive parasites, therefore accumulating less CQ, and so are more resistant to CQ.

There are several experiments that support this energy-dependent rapid efflux model. It was found that chloroquine-resistant *P. falciparum* isolates release pre-accumulated ³H chloroquine more rapidly than sensitive isolates. The chloroquine-sensitive parasites retain 2-3 times more chloroquine than resistant parasites (Bayoumi et al., 1994). The steady-state uptake of ³H chloroquine appears to be enhanced by verapamil and desipramine in the chloroquine-resistant clones, while the opposite is observed with sensitive clones. This supports the suggestion that verapamil inhibits the rapid efflux in CQR parasites resulting in a readily detectable increase in chloroquine accumulation.

The chloroquine efflux carrier could be a primary active transporter, such as a pump, or a secondary active transporter that co- or counter-transport chloroquine with or against a substrate (Figure 1-6) (Sanchez et al., 2007a; Sanchez et al., 2003; Sanchez et al., 2007b).

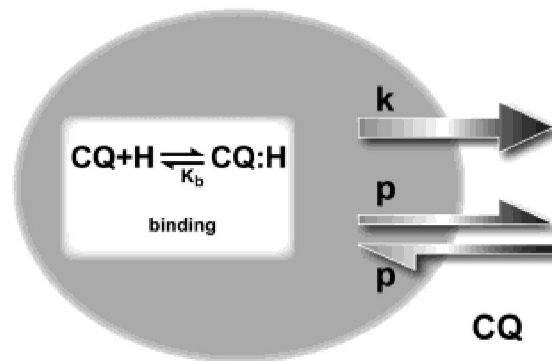


Figure 1-6 Proposed model of chloroquine resistance in *P. falciparum*

Chloroquine, CQ, enters and leaves the compartment where it accumulates by a simple bidirectional leak, having the rate constant p for drug movement in both directions. In addition, intracellular chloroquine is bound within this compartment to some binding site, H, forming a stable complex, termed CQ:H, with a binding affinity given by the dissociation constant (Michaelis constant), K_b . In chloroquine-resistant strains, chloroquine is pumped out of this compartment by an energy-dependent pump having the rate constant k . (Sanchez et al., 2003)

1.2.2 The reduced import of CQ mechanism

Other studies suggest that the lower level of CQ accumulated in CQR parasite DVs is due to reduced import of CQ rather than increased drug export. In this model, chloroquine resistance generally in *P. falciparum*, results at least in part from a change in the drug concentrating mechanism and changes in efflux rates are insufficient to explain chloroquine resistance.

With a rapid chloroquine efflux phenotype, no relationship is found between chloroquine sensitivity and the rate of 3H chloroquine efflux from isolates of *P. falciparum* with a greater than 10-fold range in sensitivity to chloroquine (Bray et al., 1992). In Bray's experiments, all the isolates tested displayed the rapid efflux phenotype, irrespective of sensitivity. Chloroquine sensitivity of these isolates was correlated with the energy-dependent rate of drug accumulation into these parasites. Verapamil and a variety of

other compounds reverse chloroquine resistance. The reversal mechanism is assumed to result from competition between verapamil and chloroquine for efflux protein translocation sites, thus causing an increase in steady-state accumulation of chloroquine and hence a return to sensitivity. Verapamil accumulation at a steady-state is increased by chloroquine, possibly indicating competition for efflux of the two substrates. Increases in steady-state verapamil concentrations caused by chloroquine are identical in sensitive and resistant strains, suggesting that similar capacity efflux pumps may exist in these isolates. Differences in steady-state chloroquine accumulation can be attributed to changes in the chloroquine concentrating mechanism rather than the efflux pump (Bray et al., 1992).

1.2.3 The plasmodial Na^+/H^+ exchanger model

A related model proposes that CQ is transported into the DV in exchange for protons by a parasite Na^+/H^+ exchanger (Bray et al., 1992). This model is based on the observation that changes in the chloroquine import kinetics play a pivotal role in constituting the resistant phenotype. The initial chloroquine uptake is temperature-dependent, saturable, and inhibitable. These features are indicative of carrier-mediated transport and clearly demonstrate the existence of a chloroquine import mechanism in *P. falciparum*. No evidence for a chloroquine concentrating mechanism was found in uninfected erythrocytes (Bray et al., 1992; Bray et al., 1999). These suggest that the factor mediating chloroquine import is encoded by *P. falciparum*. Although both chloroquine-resistant and susceptible parasite isolates exhibit facilitated chloroquine uptake, the kinetics is different. Chloroquine-resistant parasite isolates consistently have an import mechanism with a lower transport activity and a reduced affinity for chloroquine. These differences

in uptake kinetics are linked with chloroquine resistance in a genetic cross (Fidock et al., 2000a; Fidock et al., 2000b). Changes in chloroquine import kinetics constitute a minimal and necessary event in the generation of the resistant phenotype. Competitive inhibition of chloroquine uptake by amiloride derivatives further suggests that chloroquine import is mediated by a plasmodial Na^+/H^+ exchanger (Warhurst, 2002).

1.2.4 The trapping of weak-base CQ in the acidic environment mechanism

Differential accumulation of CQ in the DV of CQR and susceptible parasites could also be due simply to the trapping of weak-base CQ in the acidic environment of the DV.

CQ is a diprotic weak base. Unionized CQ is membrane permeant species (Krogstad et al., 1989). CQ is concentrated several thousand-fold inside the malaria parasite (Yayon et al., 1984). This can be explained on the basis of an ion-trapping mechanism (Hawley et al., 1996). According to this weak base model, the level of CQ accumulation depends only on the difference in pH between the external medium and the vacuole (Ferrari and Cutler, 1990). The un-protonated CQ form can transverse the parasite membrane and move down the pH gradient. Once protonated, CQ becomes membrane impermeable and is trapped inside the DV to millimolar levels (Foley and Tilley, 1998; Ward et al., 1997). This hypothesis is still controversial because passive diffusion is insufficient to account for the kinetics of CQ uptake (Ferrari and Cutler, 1990).

Indeed, there are pH differences in the DV of CQR and susceptible parasites, determined using single-cell photometric measurement of the distribution of acridine orange dye (Dzekunov et al., 2000; Ursos et al., 2000).

Chapter 1 Antimalarial and CQ Resistance

Roepe's group presented the first single cell-level analysis of digestive vacuolar pH for representative chloroquine resistant (strain Dd2) versus sensitive (strain HB3) malarial parasites (Ursos et al., 2000). Using single cell imaging and photometric techniques they found that digestive vacuolar pH (pH_{vac}) is near 5.6 for HB3 parasites, and that pH_{vac} of Dd2 is more acidic relative to HB3. *In vitro* pH titration of hemozoin confirms a very steep transition between soluble heme (capable of binding chloroquine) and insoluble hemozoin (not capable of binding chloroquine, but still capable of polymerization to hemozoin) with a distinct midpoint at pH 5.6. This suggests the similarity between the hemozoin pH titration midpoint and the measured value of HB3 pH_{vac} is not coincidental, and that decreased pH_{vac} for Dd2 titrates the limited initial drug target (i.e. soluble heme) to a lower concentration. Lowering drug target levels either would decrease the efficiency of drug or target interaction and hence the net cellular accumulation of drug over time, as is typically observed for resistant parasites. These observations contrast sharply with the common expectation that decreased chloroquine accumulation in drug resistant malarial parasites is likely linked to elevated pH_{vac} (Dzekunov et al., 2000).

To accommodate the observation of lower pH (pH 0.3-0.5 units) in CQR parasite DVs, a hypothesis was proposed that a more acidic pH would reduce the amount of soluble hemozoin to which CQ binds. This may be consistent with the model suggesting altered binding of CQ to soluble hemozoin (Bray et al., 1998). This pH hypothesis is still controversial because the use of acridine orange and dextran-tagged dyes as probes for the measurement of DV pH has been questioned (Bray et al., 2002; Kirk and Saliba, 2001).

1.2.5 Binding affinity of chloroquine

Chloroquine uptake is due to the binding of chloroquine to hemozoin rather than active uptake. In sodium-free medium, chloroquine is not directly exchanged for protons by the plasmodial Na^+/H^+ exchanger (Bray et al., 1998). Using Ro 40-4388 (a potent and specific inhibitor of hemozoin digestion), a concentration-dependent reduction in the number of chloroquine binding sites is observed. An equal number of chloroquine binding sites are found in both resistant and susceptible isolates, but the apparent affinity of chloroquine binding is found to correlate with drug activity. The activity of chloroquine is directly dependent on the saturable binding of the drugs to hemozoin and the inhibition of hemozoin polymerization may be secondary to this binding. The chloroquine-resistance mechanism regulates the access of chloroquine to hemozoin. This model is consistent with a resistance mechanism that acts specifically at the DV to alter the binding of chloroquine to hemozoin rather than changing the active transport of chloroquine across the parasite plasma membrane.

Therefore, the relationship of DV pH, CQ accumulation, and CQ response in *P. falciparum* remains uncertain. Other potential mechanisms involving parasite glutathione S-transferase or other parasite targets have also been proposed (Foley et al., 1994; Platel et al., 1999), but more work is needed in order to establish the contributions of these molecules to the CQ response. Whereas the details of the mechanism of CQR are still to be worked out, the involvement of the DV in the process is clear, supported by the DV localization of PfCRT that has been shown to play a key role in CQR and *P. falciparum*-infected erythrocyte membrane protein 1 (PfMDR1) that may contribute to CQR by modulating the parasite response to CQ.

1.3 The *pfcr*t Gene Associated with CQR in *P. falciparum*

Since the early 1990s, the genetic basis governing CQR has been a subject of much debate. A genetic determinant in a ~400 kb DNA segment on chromosome 7 was found to be associated with the CQR phenotype in a genetic cross (Fidock et al., 2000b; Wellems et al., 1991).

The *pfcr*t gene (*Plasmodium-falciparum* chloroquine resistance transporter) has a coding region of 3.1 kb with 13 exons ranging in size from 45 to 269 base pairs. Translation of the Dd2 *pfcr*t coding region predicts a 424 amino acid, 48.6 kDa protein. The protein product of *pfcr*t, PfCRT, belongs to a previously uncharacterized family of putative transporters, with 10 transmembrane segments (Figure 1-7). Database searches, alignment and prediction algorithms indicate that PfCRT belongs to a previously undescribed family of putative transporters or channels with ten transmembrane segments. These analyses show no evidence of a typical signal sequence or other recognizable features such as ATP binding motifs. Localization studies place it at the membrane of the parasite's DV (Fidock et al., 2000b).

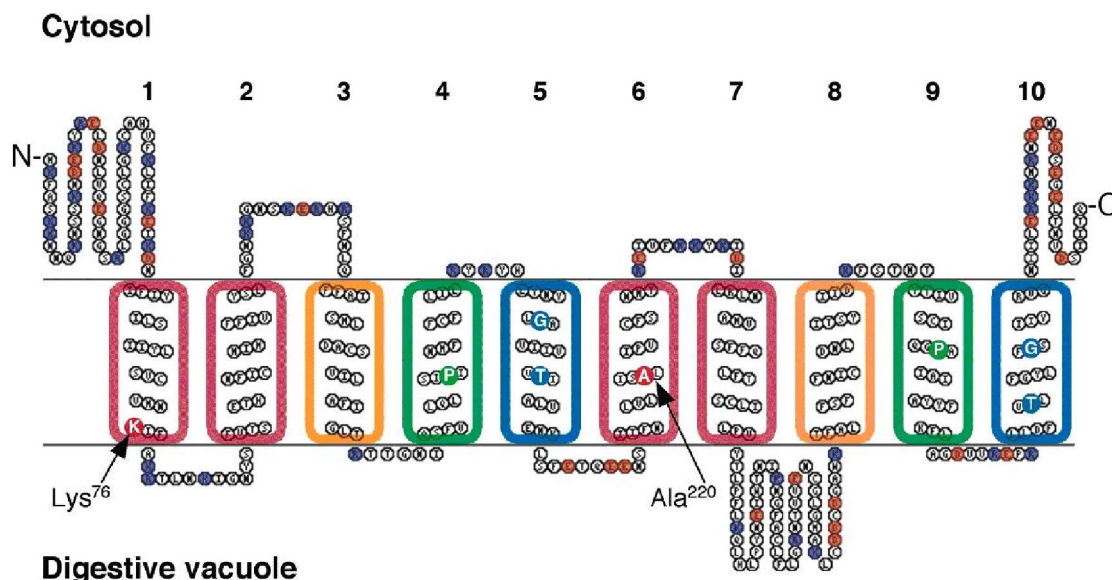


Figure 1-7 Charge distribution, topology, and putative roles of the TMDs of PfCRT

Positively charged residues (lysine or arginine) predicted to lie in the extra-membrane segments or in the termini regions are shown in black. The putative TMDs are numbered 1–10. The position of the CQ-resistance-associated K76T (TMD 1) and A220S (TMD 6) mutations (black), the conserved prolines (TMDs 4 and 9; dark grey) and the helix packing motifs (GxxxxxxT; TMDs 5 and 10; mid-grey) are highlighted. TMDs 4 and 9 (boxed in dark grey) are implicated in the binding and translocation of substrates by DMT proteins. The conserved helix packing motifs in TMDs 5 and 10 (boxed in mid-grey) play a role in the formation of homo-dimers by TPT and NST proteins. Certain residues in TMDs 3 and 8 (boxed in light grey) in DMT transporters assist in the binding and translocation of the substrate and both domains also influence the substrate specificity of the transporter. Several elements of the DMT transporter seem to be involved in recognizing and discriminating between substrates. Along with TMDs 3 and 8, TMDs 1, 2, 6, and 7 (boxed in black) also participate in determining substrate specificity. TMD: transmembrane domain; DMT: Drug/Metabolite Transporter; TPT: Triose-phosphate Transporter; NST: Nucleotide Sugar Transporter. (K. Kirk, 2002)

1.3.1 Mutations distinguished CQR from CQS

Eight point mutations in PfCRT (M74I, N75E, K76T, A220S, Q271E, N326S, I356T, and R371I) distinguish chloroquine-resistant from chloroquine-sensitive progeny of the hybridized cross (Table 1-2) (Fidock et al., 2000b). Seven of these 8 mutations are detected in each of 14 other chloroquine-resistant parasite lines from diverse regions of

Chapter 1 Antimalarial and CQ Resistance

Asia and Africa (the I356T mutation is not always detected in these parasites). PfCRT mutations, including K76T and A220S, are also detected in each of 9 chloroquine-resistant lines from South America, although the exact number and positions of all of the mutations indicate haplotypes distinct from those in Southeast Asia and Africa.

Table 1-2: Mutant forms of PfCRT and complete association of the K76T marker with chloroquine-resistant *P. falciparum* parasites from different geographic regions.

Parasite type and origin	PfCRT position and encoded amino acid									
	72	74	75	76	97	220	271	326	356	371
<u>Chloroquine sensitive</u>										
Wild type	C	M	N	K	H	A	Q	N	I	R
106/1	C	I	E	K	H	S	E	S	I	I
<u>Chloroquine resistant</u>										
Southeast Asia and Africa, type E1a	C	I	E	T	H	S	E	S	T	I
Southeast Asia and Africa, type E1b	C	I	E	T	H	S	E	S	I	I
Papua New Guinea, type P1	S	M	N	T	H	S	Q	D	L	R
South America, type W1a	S	M	N	T	H	S	Q	D	L	R
South America, type W1b	C	M	N	T	H	S	Q	D	L	R
South America, type W2	C	M	E	T	Q	S	Q	N	I	T

At least 5 amino acid substitutions are required for conversion to a CQR phenotype, with changes at codons 76 and 220 always required (Table 1-2). The number of mutations apparently required for conversion to CQR may explain why CQR took so long to appear on a large scale and why it has historically been impossible to create CQR strains from CQS in the laboratory via drug-selection pressure alone. In fact, this is now known to be

Chapter 1 Antimalarial and CQ Resistance

incorrect. If one begins with Sudan 106/1, a strain that harbors all but one of the mutations required to complete a CQR *pfcr*t allele, CQR strains can be rapidly created in the laboratory by simple selection with chloroquine (Cooper et al., 2002), and the final mutation required to complete the CQR *pfcr*t allele (Fidock et al., 2000b) is found in these selected CQR strains. In successfully performing this experiment, Cooper et al. also found other *crt* mutations that are not known to exist in the wild and that confer unusual drug resistance profiles (Cooper et al., 2002). These will be extremely informative with regard to further defining *pfcr*t protein function. Of the 16 CQS parasites tested, 15 display the canonical *pfcr*t sequence of the HB3 CQS strain (Fidock et al., 2000b). In the remaining clone, 106/1, the *pfcr*t allele shows six of the seven mutations but differs in having a K76 codon characteristic of CQS isolates. Ten point mutations were identified after comparison of *pfcr*t sequences of CQR and CQS isolates from Asia, Africa, Papua New Guinea, and South America. The substitution at amino acid position 76 (K to T) is found in all CQR isolates from various malarious regions, e.g. the mutation is 100% percent associated with the *in vitro* CQR phenotype (Djimde et al., 2001a). Genetic transformation experiments of *P. falciparum* parasites have provided further evidence that mutations in *pfcr*t can indeed affect parasite CQ response, with characteristic verapamil reversibility and reduced CQ accumulation (Leed et al., 2002). Additionally, allelic exchange of the 3' untranslated region of *pfcr*t in a CQR line (7G8) produces a marked decrease in *pfcr*t transcription and an estimated 30% to 40% decline in PfCRT protein expression. This decrease in expression leads to a ~40% decrease in CQ verapamil IC₅₀ levels compared with the 7G8 parent, although the relationship between PfCRT expression and parasite CQ response has not been established in field isolates.

Chapter 1 Antimalarial and CQ Resistance

Transfection of clone 106/1 and of 2 additional chloroquine-sensitive lines with plasmid constructs expressing resistant forms of *pfcr*t yield transformed lines that grow at drug concentrations tolerated only by natural chloroquine-resistant *P. falciparum* (Fidock et al., 2000c). In the same experiments, stepwise chloroquine pressure on the transformed 106/1 parasites eventually selected a resistant line that had lost the transfected DNA and had undergone a single K76I point mutation in the PfCRT encoded by the endogenous (chromosomal) gene. The selection of this new K76I mutation on the background of mutations already present elsewhere in PfCRT provides additional support for a determining role of residue 76 in chloroquine resistance (Fidock et al., 2000b).

It has been suggested that the codon 76 changes in PfCRT may reduce chloroquine influx into, or increase chloroquine efflux from the lysosome and/or alter drug action by pH modulation. The other codon changes in *pfcr*t are believed to be compensatory, increasing the fitness of the modified protein. It is probably significant that there are as yet only two chloroquine-sensitive and five geographically-associated chloroquine-resistant sequences of PfCRT. In all five resistant types, threonine 76 replaces lysine in transmembrane domain 1, and serine 220 replaces alanine in transmembrane domain 6. In a model, domains 1 and 6 are opposite, and residues 76 and 220 are at approximately the same level. These data demonstrate conclusively that *pfcr*t is a key gene conferring CQR in *P. falciparum*.

More and more studies now provide information on PfCRT mutations and their role in chloroquine treatment failures (Djimde et al., 2001a). These include reports of PfCRT markers and chloroquine treatment outcomes in Mali (Djimde et al., 2001a), Cameroon (Basco and Ringwald, 2001), Sudan (Babiker et al., 2001), and Mozambique (Mayor et al., 2001), where both chloroquine-sensitive and chloroquine-resistant *P. falciparum*

Chapter 1 Antimalarial and CQ Resistance

strains are still widespread. Other reports from Brazil (Vieira et al., 2001), Uganda (Dorsey et al., 2001), Laos (Pillai et al., 2001), and Thailand and Papua New Guinea (Chen et al., 2001) describe outcomes from regions where chloroquine-resistant parasites carrying the PfCRT K76T mutation are now predominant. Together, these reports provide substantial support for a sweeping association of the PfCRT K76T mutation with different foci of chloroquine resistance.

A novel mutation has been reported to restore the CQ susceptibility of the CQR line from Southeast Asia isolated under selective pressure of amantadine or halofantrine (Johnson et al., 2004). Selection for mefloquine resistance in Dd2 is accompanied by halofantrine cross-resistance, increased sensitivity to CQ and loss of the chemosensitising effect of VPL (Johnson et al., 2004). Amantadine resistance screening of CQR parasites restores CQS, while K76T remains. When halofantrine resistance screening experiments were carried out, the same results were observed. Then a common point mutation at residue 163 (S163R) was noted. This novel mutation in *pfCRT*, S163R in TMD4, resulted in both loss of chloroquine resistance and verapamil-reversible CQ resistance, despite the presence of K76T in TMD1. It was proposed that residue 163 is located on the luminal side of the PfCRT channel, the 76 and 163 residue together line the PfCRT lumen and the S163R mutation can compensate for the loss of positive charge in the K76T mutation in Dd2, thereby blocking the exit of positively charged CQ from the DV, resulting in CQS. It is thereby proposed that S163R again introduces a positive charge to the PfCRT protein and could gate the deprotonated CQ through the DV.

1.3.2 Is PfCRT a member of the Drug/Metabolite transporter superfamily?

After searching the NCBI database with PfCRT as the query sequence, a putative nucleotide sugar transporter (NST) in the drug/metabolite transporter (DMT) superfamily was uncovered (Altschul et al., 1997; Jack et al., 2001). Comparison of the putative NST against the DMT superfamily (Saier, 2000) shows strong sequence similarity with a UDP-*N*-acetylglucosamine (UDP-GlcNAc) transporter. The hypothetical NST, PfCRT, and many proteins of the DMT superfamily are predicted to have 10 transmembrane spanners (TMSs); the UDP-GlcNAc transporters as well as many other DMT superfamily members have been shown to have arisen by duplication of a primordial 5 TMS element (Jack et al., 2001).

Having established that PfCRT is a member of the DMT superfamily it is possible to assign putative functions to different regions of the PfCRT protein on the basis of previous studies of other members of the superfamily.

The orientation of the N- and C-termini

The N- and C-termini of the DMT superfamily have a preponderance of positive charge (Figure 1-7). This makes it likely that the even-numbered loops, together with the N- and C-termini, are located at the cytoplasmic face of the membrane (predicted by the positive inside rule (van Klompenburg et al., 1997) and by TMHMM (Sonnhammer et al., 1998)).

PfCRT may function as a dimer

The motif (GxxxxxxG) is a common feature of membrane proteins, and is thought to facilitate the packing of membrane-spanning helices, leading to the association of TMDs

to form oligomers. In TMDs 5 and 10 there are two conserved glycines that are separated by 6 hydrophobic residues (Knappe et al., 2003). TMDs 5 and 10 are known to have a role in mediating the formation of homo-dimers by the NST and TPT transporters (Abe et al., 1999); (Gao et al., 2001). So the presence of helix packing motifs in TMDs 5 and 10 indicates that PfCRT may function as a dimer.

Substrates effluxed by DME transporters

Substrates for DME transporters include amino acids, weak bases and organic cations. DME transporters are known to transport both weak bases and organic divalent cations, which adds support to the hypothesis that the CQ-resistant form of PfCRT transports the chloroquine in a di-cationic form. Additionally, DME systems are postulated to be proton-driven and this has been confirmed experimentally for at least one DME transporter (the *E. coli* YbiF protein) (Livshits et al., 2003).

The role of PfCRT in CQ resistance

Based on the bioinformatic analysis, Figure 1-8 shows a model for the mechanism of PfCRT-mediated CQ-resistance. The protein is shown as a dimer, functioning to export 'metabolites' from the parasite's DV. The fact that a number of related DME proteins transport amino acids, and the only known metabolite transport function of the DV is the efflux of peptides (Kolakovich et al., 1997) and perhaps amino acids, prompt the hypothesis that PfCRT is an amino acid/peptide transporter (perhaps H⁺-coupled).

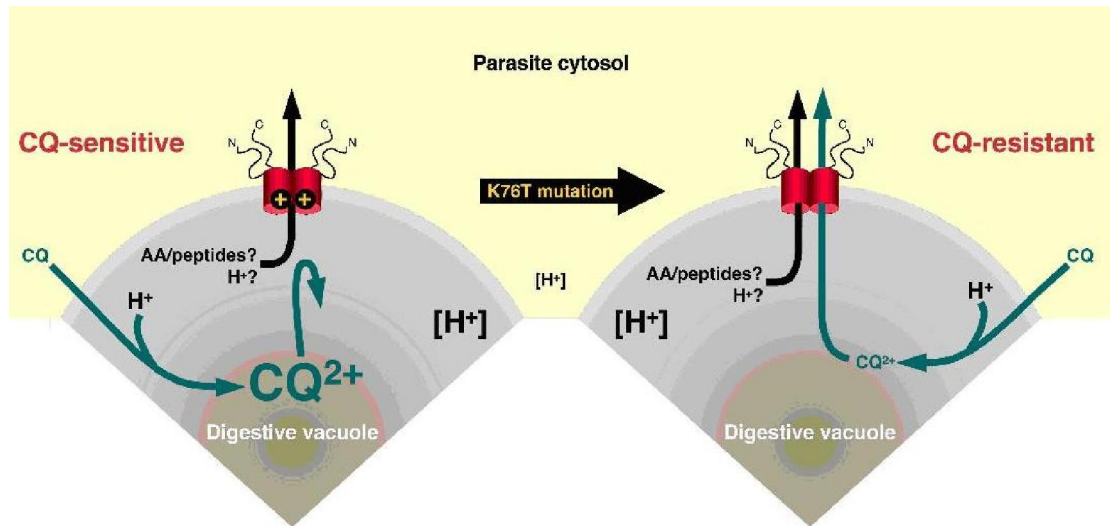


Figure 1-8 A model for the mechanism of PfCRT-mediated CQ-resistance (K. Kirk, 2002)

On the basis of the ‘positive-inside’ rule as well as by TMHMM, the protein is predicted to be oriented with the N and C termini in the parasite cytosol and the ‘compact globular domain’ of loop 7 located at the vacuolar face of the membrane. In this orientation, the crucial CQR-conferring K76T mutation lies close to the surface of the vacuolar face of the membrane, within a region of the protein postulated to be involved in substrate-selectivity. The positive charge is predicted to play a key role in repelling the protonated (cationic) form of chloroquine, and preventing it interacting with the transporter. The CQR-conferring mutation of Lys to Thr (or Ile or Asn) removes the positive charge, allowing CQ²⁺ to interact with and be transported by the protein, down the steep outward CQ²⁺ concentration gradient (perhaps in symport with H⁺)

1.3.3 Proposed function of PfCRT

Warhurst reported that the PfCRT protein sequence shows a strong resemblance to the aqueous chloride channel of *Salmonella typhimurium* (Warhurst, June 23, 2002:). And a mutated chloride channel is associated with verapamil reversibility (Martiney et al., 1995). Paul Roepe's research group also noted a mutated PfCRT mediates the chloride-dependent and verapamil-inhibitable export of acridine orange (Zhang et al., 2002).

PfCRT has multiple transmembrane domains and is located on the digestive vacuole membrane (Fidock et al., 2000b). PfCRT could be involved in binding and/or transporting CQ (Zhang et al., 2004). Indeed, evidence provided by Sanchez *et al.* (Sanchez et al., 2003) suggests that *pfcr*t is probably the molecule underlying the efflux mechanism in their model. Two of the parasites used in their study, 106/1 and FCB, have an almost identical genome except for a mutation at amino acid position 76 in *pfcr*t (K for 106/1 and T for FCB) (Wootton et al., 2002). The parasites show typical CQR (FCB) and susceptible (106/1) efflux phenotypes (Cooper et al., 2002), suggesting an association of the *pfcr*t 76T mutation with the efflux phenotype. If the rapid efflux model is correct, then PfCRT could be involved in transporting CQ across the DV membrane.

Mutations in *pfcr*t could also affect the binding of CQ to the protein, leading to altered transport efficiency (Warhurst, June 23, 2002:).

Fitting *pfcr*t into the proposed models of CQR will be the key step to a complete understanding of the mechanism of CQR in this parasite. Thus, the underlying mechanism of PfCRT may involve protein-protein interactions, as the activation of an $\text{Na}^+\text{-K}^+\text{-2Cl}^-$ cotransporter by the trout erythrocyte anion exchanger-1 (Guizouarn et al., 2004) or of channels by single membrane-spanning proteins (Sha et al., 2001). PfCRT

may also involve electric or thermodynamic coupling such as with the $\text{Na}^+\text{-K}^+\text{-2Cl}^-$ cotransporter and KCl transporter (Gillen and Forbush, 1999). It may be like amino acid transporters, coupling of transport activities may serve to recycle ions or to buffer ionic changes induced by the transporter of interest (Wagner et al., 2000). Alternatively, PfCRT may interfere with second messengers, such as Ca^{2+} , which is known to regulate the activity of numerous membrane transporters, including the NHE (Burckhardt et al., 2002) and $\text{H}^+\text{-ATPase}$.

1.3.4 S163R mutation of PfCRT restores susceptibility from CQR

When researchers focused on the 76th amino acid within TMD1, it was demonstrated that selection for mefloquine resistance in Dd2 strain is accompanied by halofantrine cross-resistance, increased sensitivity to CQ and loss of the chemosensitising effect of verapamil (VPL) (Johnson et al., 2004). This means that Amantadine resistance screening of CQR parasites restores susceptibility, while the genetic background of K76T remains. The same result was observed in halofantrine resistance screening experiments. When the *pfCRT* was sequenced, a common point mutation at codon 163 was noted (S163R, sites on TMD4). The mutation may be of selective advantage under increasing levels of amantadine or halofantrine, yet the conversion of CQR back to susceptibility by a single point mutation is astonishing. It was suggested that the gain of positive charge at residue 163, by S163R mutation, may block the efflux of positively-charged molecules from the DV, thereby trapping protonated CQ in the DV, resulting in susceptibility. This

proposed mechanism relies on the assumption that residue 163 is located on the luminal side of the PfCRT channel, the K76^h and S163 line the PfCRT lumen and the S163R mutation can compensate the loss of positive charge in the K76T mutation in Dd2, thereby blocking the exit of positively-charged CQ from the DV, resulting in susceptibility.

1.4 Expression of PfCRT in a Heterologous System

In many recent molecular level analyses of polytopic integral membrane transport proteins, heterologous expression of the transporter in either yeast or *E. coli* has proved to be invaluable. Such expression allows for detailed vesicle-based analysis of transport function, as well as more rapid and convenient purification and reconstitution of both mutant and wild-type proteins. Unfortunately, there are only few successful reports of expression of a native *P. falciparum* cDNA in either yeast or bacteria, and this yielded rather low expression for the soluble protein (Sirawaraporn et al., 1990). After optimizing codon usage, expression of native *P. falciparum* cDNA increased by at least an order of magnitude (Prapunwattana et al., 1996). Aside from codon usage, integral membrane proteins typically contain processing and translocation sequences that are frequently species-specific. Such sequences are not well defined for malarial membrane proteins.

After examining these issues, a proper synthetic *pfcr*t gene *de novo* via overlapping PCR methods was constructed, the resulting constructs cloned into a series of appropriate

yeast expression vectors, and subsequently high-level expression of PfCRT protein was achieved in the plasma membrane of *Pichia pastoris*, and there was some direct demonstration of its transport function ((Zhang et al., 2002); our laboratory, unpublished).

Expressing PfCRT in *Xenopus laevis* oocytes has been successful (Nessler et al., 2004). This is based on reconstructing the coding sequence on the basis of the yeast codon usage. The high A/T content of the *P. falciparum* sequence most likely prevents efficient translation, a problem, like in yeast and *E.coli*, often encountered when working with DNA from this parasite. The reconstructed *pfcr*t coding sequence was designed such that translation of the corresponding cRNA generated *in vitro* would produce the original full-length protein in *X. laevis* oocytes without generating any kind of fusion protein. PfCRT-expressing oocytes can be used to reveal the physiological parameters of PfCRT.

1.5 The Substituted-cysteine Accessibility Method (SCAM) to Elucidate Membrane Protein Structure

The crystallization of most membrane proteins is inherently difficult. Only a few high-resolution structures for membrane proteins have been achieved (Henderson et al., 1990; Iwata et al., 1995; Pebay-Peyroula et al., 1997). Using molecular biological techniques to engineer membrane proteins by various site-directed techniques is providing detailed information about the structure and function of membrane proteins.

Karlin and co-workers initiated the use of the substituted cysteine accessibility method (SCAM) (Karlin, 2001). In the original work, single cysteine substitutions within a target protein coupled with covalent cysteine modification by hydrophilic thiol-specific

reagents was used to study structure–function relationships and dynamics of membrane protein function. Later, SCAM was applied to study the mapping of channel gating residues, identification of residues lining a membrane channel, identification of residues involved in substrate or ligand binding, etc. Especially in recent years, coupled with biochemical and biophysical techniques, SCAM is used to elucidate membrane topology (Audia et al., 2006; Iwata et al., 1995; Kaback, 1997; Loo and Clarke, 1995a; Sun et al., 1997; Sun et al., 1996) and accessibility of intramembrane residues to the aqueous or lipid phase of the membrane (Akabas et al., 1992; Altenbach et al., 1990; Frillingos and Kaback, 1997), as well as spatial proximity between transmembrane domains (Chervitz and Falke, 1996; Karlin, 2001; Sun and Kaback, 1997).

1.5.1 The substituted-cysteine accessibility method (SCAM)

The substituted-cysteine accessibility method (SCAM) is an approach used for the characterization of channel (England et al., 1999; Ivanina et al., 1994) and binding-site structures of a protein. By mutating every residue of a protein to cysteine and by characterizing the reaction of the cysteine with sulfhydryl-specific reagents, SCAM probes the environment of any residue in the protein. SCAM has been successfully used to identify channel-lining residues, to determine the potentially different environments of these residues in the open and closed states of the channel, to locate selectivity filters and gates, and to map the binding sites of channel blockers (Karlin and Akabas, 1998).

In a membrane-spanning segment of a protein, the sulfhydryl group of a native or engineered cysteine will be either at the water-accessible surface of the protein, at the lipid-accessible surface, or in the protein interior. In the development of the theory and

Chapter 1 Antimalarial and CQ Resistance

techniques of SCAM, it is assumed that the surface of the binding-site is part of the water-accessible surface and that small, hydrophilic, charged reagents will react much faster with a sulfhydryl group at the water-accessible surface than with a sulfhydryl group facing lipid or the interior (Karlin and Akabas, 1998). As for sulfhydryl-specific reagents, the methanethiosulphonates (MTS) are attractive because of their small size and their specificity for sulfhydryls. Moreover, MTS derivatives react with the ionized thiolate (RS⁻) more than a billion times faster than with the nonionized thiol (RSH). Cysteine residues accessible to water are likely to ionize to a significant extent (Roberts et al., 1986). The intrinsic reactivity of MTS reagents with thiols is quite high, on the order of 10^5 M/sec (Stauffer and Karlin, 1994). Similar rates can often be achieved with introduced cysteines in proteins (Liu et al., 1996), meaning that complete modification can be achieved using a few seconds of application and reagent concentrations in the 10-100 μ M range. So it is assumed that slower rates of modification may suggest that the introduced cysteine is not at the freely accessible surface of the protein, but is more likely partially buried in a crevice or possibly in the pore of a channel protein. When modification is monitored by a functional measurement, no effect of an MTS reagent may suggest that the modification reaction did not occur or that even when modification does occur it produces no functional change in the assay used. Figure 1-9 displays a general reaction of thio-modification.

Sometimes an introduced cysteine may exhibit different modification rates depending on the conformational state of the protein. This phenomenon has allowed the MTS reagents to be used to analyze the nature of ion-channel gating motions (Akabas et al., 1994; Akabas et al., 1992; Liu et al., 1996).

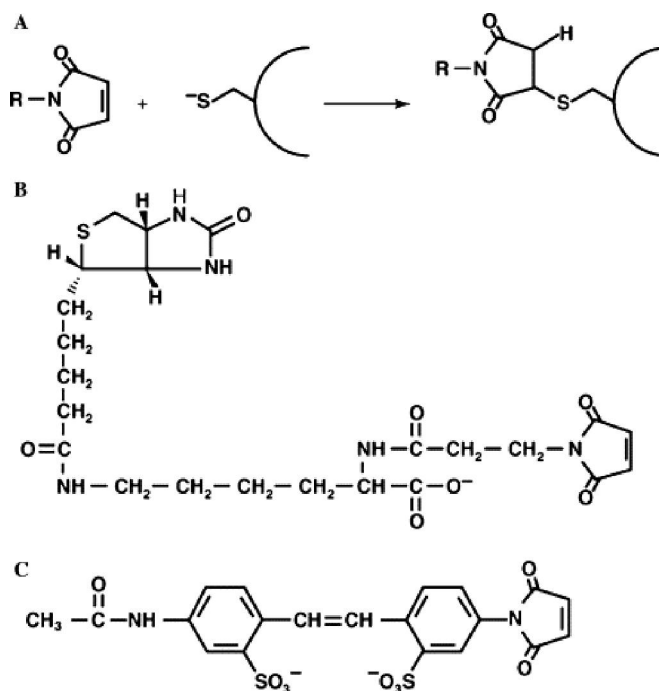


Figure 1-9 Thiol-modifying reagents widely used in SCAM

(A) The reaction of the thiolate anion of cysteine with maleimide by nucleophilic addition to the double bond of the maleimide ring. (B) The structure of the maleimide- and biotin-containing labeling reagent 3-(N-maleimidylpropionyl) biocytin (MPB). (C) The structure of the blocking reagent 4-acetamido-4'-maleimidylstilbene-2,2'-disulfonic acid (AMS). (Bogdanov, 2005)

Theoretically, to perform SCAM, every residue in a membrane-spanning segment is mutated, one at a time, to cysteine. The mutant receptors are then expressed in heterologous cells and assessed as to whether the substituted cysteine residues react with small, hydrophilic, charged sulfhydryl reagents. In most cases, the reaction of an engineered cysteine with a sulfhydryl reagent in the binding-site crevice alters ligand binding. Thus, if ligand binding is irreversibly altered by the reagents, it is inferred that covalent modification of the cysteine with an MTS reagent has taken place and that the engineered cysteine is at the water-accessible surface of the receptor. Additionally, reaction of an MTS reagent with a cysteine near a binding site should be retarded in the presence of ligand.

1.5.2 The strategy for performing SCAM

The ability to substitute cysteines for other residues and still obtain a functional receptor is central to this approach (Fu et al., 1996; Javitch et al., 1998). These tolerated substitutions are for hydrophobic residues (alanine, leucine, isoleucine, methionine, and valine), polar residues (asparagine, serine, threonine), neutral residues (proline), acidic residues (aspartate), aromatic residues (phenylalanine, tryptophan, tyrosine), and glycine. There are several reasons why cysteine substitution may be so well tolerated. Cysteine is a relatively small amino acid with a volume of 108 Å³; only glycine, alanine, and serine are smaller. In globular proteins, roughly half of the nondisulfide-linked cysteine residues are buried in the protein interior and half are on the water-accessible surface of the protein. Furthermore, cysteine has little preference for a particular secondary structure.

Only cysteine substitution mutants with near wild-type binding affinities are used, and these mutants are assumed to have near wild-type structure. It is also assumed that the substituted cysteine side chain is positioned similarly to the wild-type side chain, and that SCAM accurately reports the accessibility of the wild-type side chain.

SCAM and the charged MTS reagents have been successfully applied to the structural and functional elucidation of a number of ligand-gated ion channels, including muscle acetylcholine receptor (Akabas and Karlin, 1995; Akabas et al., 1994; Akabas et al., 1992), neuronal acetylcholine receptor (Ramirez-Latorre et al., 1996), GABA receptor (Xu and Akabas, 1993, 1996), NMDA glutamate receptor (Kuner et al., 1996), and cyclic nucleotide gated channels (Su and Wellems, 1996). This technique has also been applied to the cystic fibrosis transmembrane conductance regulator (Akabas et al., 1994), and to

voltage-gated potassium (Pascual et al., 1995) and sodium channels (Yang et al., 1996). SCAM has also been used to map the ligand-binding domain of the seven-transmembrane-helices, G-protein-linked dopamine receptor (Javitch et al., 1995).

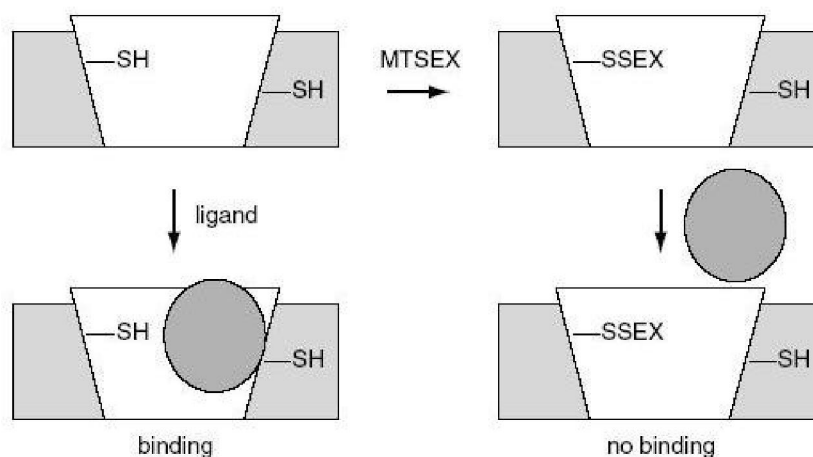


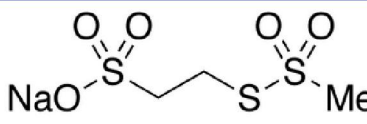
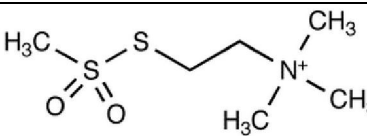
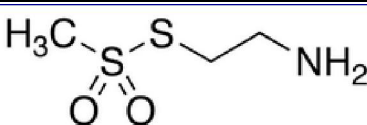
Figure 1-10 Schematic representation of the reaction of an MTS reagent with a cysteine exposed in the binding-site crevice

The membrane is represented by the shaded rectangle, the binding-site crevice by the white area within the plane of the membrane, and ligand by the solid oval. SEX represents $\text{CH}_2\text{CH}_2\text{X}$, where X is NH_3^+ , $\text{N}(\text{CH}_3)_3^+$, or SO_3^- . SEX is covalently linked to the water-accessible cysteine sulfhydryl. In the bound state (lower left panel), ligand is reversibly bound at the binding site within the binding-site crevice. In the unbound state (upper left), the binding site is unoccupied. After irreversible reaction with MTSEX (upper right), ligand can no longer bind (lower right). The cysteine sulfhydryl facing lipid or the interior of the protein does not react significantly with MTSEX. MTSEX only reacts with a sulfhydryl in the binding site crevice of ligand-free receptor. Thus, ligand binding retards the rate of reaction of receptor with MTSEX and protects subsequent ligand binding. (Javitch et al., 1995)

1.5.3 Characterization and applications of charged and neutral MTS reagents

There are typically three charged MTS reagents, 2-aminoethyl methanethiosulfonate hydrobromide (MTSEA), sodium (2-sulfonatoethyl) methanethiosulfonate (MTSES), and [2-(Trimethylammonium)ethyl] methanethiosulfonate bromide (MTSET) introduced by Karlin and his colleagues (Stauffer and Karlin, 1994) (Table 1-3). These reagents are used in conjunction with site-specific introduction of cysteines to study the structure and function of ion channel proteins. Because these reagents introduce a positive or negative charge at the position of a previously neutral cysteine residue, they frequently cause a functional change in a channel protein that can be measured by electrical recording (Akabas et al., 1992).

Table 1-3 Summary of charged MTS reagents

NAME	Chemical Name	Charge	Chemical structure
MTSES	Sodium(2-Sulfonatoethyl) methanethiosulfonate	Negatively charged reagent	
MTSET	[2-(Trimethylammonium)ethyl] methanethiosulfonate	Positively charged reagent	
MTSEA	2-Aminoethyl Methanethiosulfonate	Positively charged reagent	

SCAM and the charged MTS reagents have been successfully applied to the structural and functional elucidation of a number of ligand-gated ion channels, including muscle acetylcholine (ACh) receptor (Akabas and Karlin, 1995; Akabas et al., 1994; Akabas et al., 1992). In these studies, researchers found that in membrane-spanning segments

TMD2 and TMD1, there are some positions which are exposed to the channel lumen and suggest that TMD1 is either exposed in the channel or its exposure changes during gating or desensitization.

Fu and Kirk (Fu and Kirk, 2001) used SCAM to study the functions of the amino-terminal tail in cystic fibrosis transmembrane conductance regulator channel gating. They found that the three MTS reagents have different effects on the duration of channel openings exhibited by different mutants. They concluded that the negative charges at the N-tail appear to play a significant role in stabilizing CFTR channel openings.

Winkler and co-workers have studied the accessibility of the *Rickettsia prowazekii* ATP/ADP translocase transmembrane domains (TMs) IV-VII and IX-XII to the putative, water-filled ATP translocation pathway (Audia et al., 2006). They found that TMs IV, V, VII, X, and XI are exposed to the aqueous ATP translocation pathway. In a previous study they found that TMs I, II and VIII have a similar pattern (Alexeyev, 2004; Winkler, 2003).

The SCAM and charged MTS reagents have been widely used for many types of proteins. These include studies of the neuronal acetylcholine receptor (Ramirez-Latorre et al., 1996), GABA receptor (Xu and Akabas, 1993, 1996), NMDA glutamate receptor (Kuner et al., 1996), and cyclic nucleotide gated channels (Su and Wellems, 1996). This technique has also been applied to the cystic fibrosis transmembrane conductance regulator (Akabas et al., 1994), and to voltage-gated potassium (Pascual et al., 1995) and sodium channels (Yang et al., 1996). SCAM has also been used to map the ligand-binding domain of the seven-transmembrane-helices, G-protein-linked dopamine receptor (Javitch et al., 1995).

Chapter 1 Antimalarial and CQ Resistance

Neutral MTS reagents are uncharged sulfhydryl active probes. In Diez-Sampedro's work (Diez-Sampedro et al., 2004), coupled with charged MTS reagents, uncharged MTS reagents 2-Hydroxyethyl methanethiosulfonate (MTSHE) and Methyl methanethiosulfonate (MMTS) are used to elucidate the charge in the coordination of the cotransport mechanism of SGLT1.

While SCAM has been used as a powerful tool to study the structure and function of protein, novel thiol reagents have been produced and introduced in SCAM research. The spin labeled derivative (1-Oxyl-2,2,5,5-tetramethyl- Æ^3 -pyrrolin-3-yl)methyl methanethiosulfonate (MTSL) was described by Berliner and his colleagues (Berliner et al., 1982). This reagent exhibits high sulfhydryl selectivity and reactivity. The side-chain has a relatively small molar volume, and an EPR (electron paramagnetic resonance) spectrum. With EPR variations, the accessibility to collision with paramagnetic species in solution and the motion of the spin-labeled side-chain, which is exquisitely sensitive to structural changes, can be measured. Site-directed spin labeling (SDSL) and analysis of the EPR of spin labeled proteins can be used to map the topography of a membrane protein. It also can be used to determine secondary structure, measure the distance between two sites bearing a spin label, and identify sites of tertiary interaction. It is possible to using these methods to study protein folding both in solution and in chaperone-mediated systems.

The MTS-fluorophores could be applied in the real-time monitoring of conformational changes, since fluorophores coupled to introduced cysteines can change their fluorescence during a conformational change (Mannuzzu et al., 1996). Fluorescence lifetime may also yield information about distances and molecular motion in a protein molecule.

1.5.4 The limitations of SCAM

In spite of all the success, SCAM has several limitations. First of all, it relies on cysteine mutation and therefore is restricted by the extent of the tolerance for cysteine substitution in the protein. Second, it is limited to those positions that are accessible by the modification reagent. Furthermore, it lacks site-specificity if there is more than one cysteine in the protein. Finally, there might be complications due to side reactions related to the chemical modification. Additionally, it is important to consider the ability of MTS compounds to cross membranes. Although MTSES and MTSET are membrane impermeant, MTSEA can modify membrane proteins from the "wrong side". But the use of a thiol scavenger on the opposite side of the membrane from where the MTS reagent is applied may eliminate this "trans" modification (Holmgren et al., 1996) .

Objectives

1. Use site-directed mutagenesis to constitute Cys-less *pfert*, twenty-one cysteine substituted *pfert* within TMD1 and ten within TMD4.
2. To express PfCRT of Cys-less and single cysteine mutants within TMD1 and TMD4 in *Pichia*. Prepare microsomes of these mutants for further study.
3. Reconstitute proteoliposomes for SCAM assays.
4. Use SCAM and charged MTS reagents (MTSES, MTSET and MTSEA) to elucidate structure and functions of PfCRT.

Chapter 2

Expression of Substituted PfCRT Proteins in *Pichia pastoris*

Abstract

Pichia pastoris has many of the advantages of higher eukaryotic expression systems in protein processing, protein folding, and posttranslational modification. It is also easy to manipulate. It is faster, easier, and less expensive to use than other eukaryotic expression systems such as baculovirus or mammalian tissue culture, and generally gives higher expression levels.

Using multiple site-directed mutagenesis, cysteine-less *pfert* on a Dd2 genetic background and thirty-one single cysteine-substituted *pfcrts* within TMD1 and TMD4 were constructed. Twenty-one substituted PfCRTs within TMD1 and seven in TMD4 were expressed successfully in *Pichia pastoris*. Expression levels of these substituted PfCRT were analyzed. Microsomes of these mutants were prepared for further study.

2.1 Introduction

Pichia pastoris is a highly successful system for production of a wide variety of recombinant proteins. A yeast, *P. pastoris* is a single-celled microorganism that is easy to manipulate and culture. It is capable of many post-translational modifications found in higher eukaryotic cells such as proteolytic processing, folding, disulfide bond formation and glycosylation (Buckholz and Gleeson, 1991; Romanos et al., 1992). Thus, many proteins that end up as inactive inclusion bodies in bacterial systems are produced as biologically active molecules in *P. pastoris*. The *P. pastoris* system is also generally regarded as being faster, easier, and less expensive to use than expression systems derived from higher eukaryotes such as insect and mammalian tissue culture cell systems and usually gives higher expression levels.

PfCRT resides in a subcellular membrane within an intracellular parasite, so to study PfCRT transport function requires the transport of substrates across three membranes in a coordinated fashion. But this is extremely difficult to manipulate experimentally. In order to elucidate the molecular mechanism of CQR, it is also essential to purify and reconstitute polytopic integral membrane proteins. Heterologous expression experiments and further functional characterization should provide information about the function of PfCRT and its role in DV physiology.

2.1.1 The features of the *Pichia pastoris* expression system

P. pastoris has many of the advantages of higher eukaryotic expression systems. A yeast, it shares the advantages of molecular and genetic manipulations with *Saccharomyces*, and has the added advantage of 10- to 100-fold higher heterologous protein expression levels. These features make *Pichia* very useful as a protein expression system.

P. pastoris is a methylotrophic yeast, capable of metabolizing methanol as its sole carbon source. The first step in the metabolism of methanol is its oxidation to formaldehyde using molecular oxygen by the enzyme alcohol oxidase. This reaction generates both formaldehyde and hydrogen peroxide. Alcohol oxidase has a poor affinity for O₂, and *P. pastoris* compensates by generating large amounts of the enzyme. The promoter regulating the production of alcohol oxidase drives heterologous protein expression in *Pichia*.

Expression of the *AOX1* gene is regulated and induced by methanol to very high levels of the total soluble protein in cells grown with methanol. The isolated and a plasmid-borne version of the *AOX1* promoter is used to drive expression of the gene of interest encoding the desired heterologous protein (Tschopp et al., 1987). The strong, highly-inducible *PAOX1* promoter in vector pPICZ is used for intracellular expression of PfCRT protein. The vector pPICZ contains the ZeocinTM resistance gene for positive selection in *E. coli* and *Pichia* (Figure 2-1).

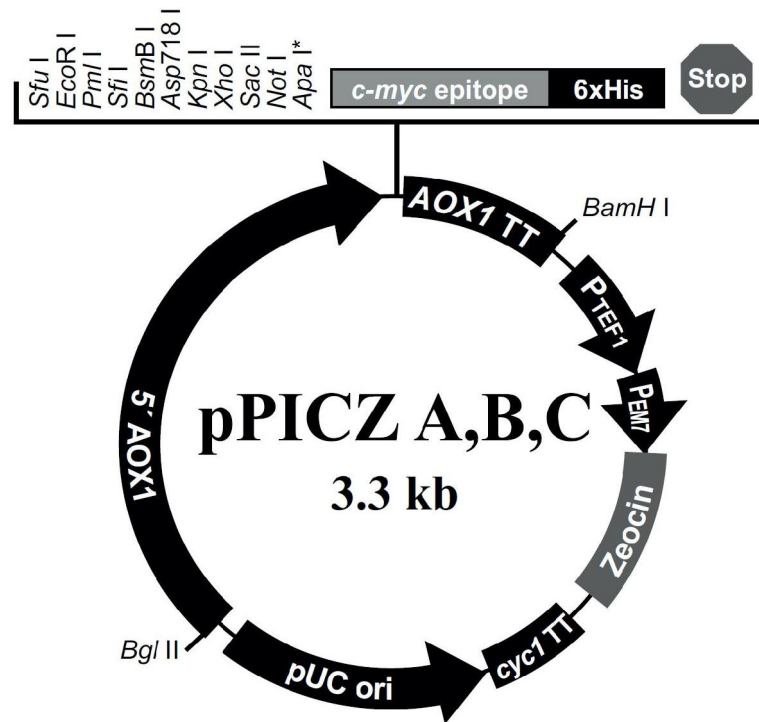


Figure 2-1 Features of the pPICZA, B, C

5' fragment containing the AOX1 promoter for tightly regulated, methanol-induced expression of the gene of interest. Zeocin™ resistant gene for selection in both *E. coli* and *P. pastoris*. C-terminal peptide containing the c-myc epitope and a polyhistidine (6XHis) tag for detection and purification of a recombinant fusion protein (if desired). * The restriction site between Not I and c-myc epitope is different in each version of pPICZ: Apa I in pPICZA, Xba I in pPICZB, and Sna I in pPICZC. Cloning modified *pfert* gene into the EcoR I and Not I sites of the vector of pPICZA. (adapted from <http://www.invitrogen.com>).

Plasmid vectors designed for heterologous protein expression in *P. pastoris* have several common features. The foreign gene expression cassette is one of those and is composed of DNA sequences containing the *P. pastoris* AOX1 promoter, followed by one or more unique restriction sites for insertion of the foreign gene, followed by the transcriptional termination sequence from the *P. pastoris* AOX1 gene that directs efficient 3' processing and polyadenylation of the mRNAs. Some vectors also contain AOX1 3' flanking sequences that are derived from a region of the *P. pastoris* genome that lies immediately

3' of the *AOX1* gene and can be used to direct fragments containing a foreign gene expression cassette to integration at the *AOX1* locus by gene replacement (or gene insertion 3' to the *AOX1* gene).

The Mut^S, namely methanol utilization slow phenotype of recombinant strains, is caused by the loss of alcohol oxidase activity encoded by the *AOX1* gene. A strain with a Mut^S phenotype has a mutant *AOX1* locus, but is wild type for *AOX2*. This results in a slow growth phenotype on methanol medium. KM71 strain is Mut^S. Transformation of KM71 with plasmid DNA linearized in the 5' *AOX1* region will yield Mut^S transformants.

P. pastoris is a cheap but powerful system for high-level heterologous gene expression. Under the control of the *AOX1* promoter, foreign genes can be maintained in an “expression-off” mode on a non-methanolic carbon source to minimize selection for non-expressed mutant strains during cell growth. It can then efficiently be switched on by shifting to methanol-containing medium. The *P. pastoris* expression system has now been successfully utilized to produce a number of heterologous proteins at the commercial scale (Cregg et al., 1993), including mammalian membrane transporters such as human PEPT1 (Doring et al., 1997), mouse MDR3 (Beaudet et al., 1998), and plasmodial apical membrane antigen1 (AMA-1) (Kocken et al., 1999). This made *P. pastoris* the main choice for the *pfCRT* gene expression system.

2.1.2 Cell lines constructed in this project

Twenty-nine *P. pastoris* cell lines were established in this project. Yeast-Dd2-Cys-less expressed Cys-less PfCRT (Refer to Section Table 2-1), in which all obligate cysteines were replaced by alanines. The other twenty-eight were single cysteine mutants of

Chapter 2 Expression of Substituted PfCRT

PfCRT. They were single cysteine PfCRT with amino acids being substituted by cysteines one by one (Table 2-1 Cell lines expressed in this project).

Table 2-1 Cell lines expressed in this project

No.	Mutant	Shortened name	Mutation position	TMD
1	Yeast-Dd2-Cys-less	yCys-less	14 cysteines	TMD1-10
2	Yeast-Dd2-Cys-less-I59C	yI59C	I59C	TMD1
3	Yeast-Dd2-Cys-less-F60C	yF60C	F60C	TMD1
4	Yeast-Dd2-Cys-less-I 61C	yI 61C	I 61C	TMD1
5	Yeast-Dd2-Cys-less-Y62C	yy62C	Y62C	TMD1
6	Yeast-Dd2-Cys-less-I63C	yI63C	I63C	TMD1
7	Yeast-Dd2-Cys-less-L64C	yL64C	L64C	TMD1
8	Yeast-Dd2-Cys-less-S65C	yS65C	S65C	TMD1
9	Yeast-Dd2-Cys-less-I66C	yI66C	I66C	TMD1
10	Yeast-Dd2-Cys-less-I67C	yI67C	I67C	TMD1
11	Yeast-Dd2-Cys-less-C68C	yC68C	C68C	TMD1
12	Yeast-Dd2-Cys-less-L69C	yL69C	L69C	TMD1
13	Yeast-Dd2-Cys-less-S70C	yS70C	S70C	TMD1
14	Yeast-Dd2-Cys-less-V71C	yV71C	V71C	TMD1
15	Yeast-Dd2-Cys-less-A72C	yA72C	A72C	TMD1
16	Yeast-Dd2-Cys-less-V73C	yV73C	V73C	TMD1
17	Yeast-Dd2-Cys-less-I74C	yI74C	I74C	TMD1
18	Yeast-Dd2-Cys-less-E75C	yE75C	E75C	TMD1
19	Yeast-Dd2-Cys-less-T76C	yI76C	I76C	TMD1
20	Yeast-Dd2-Cys-less-I77C	yI77C	I77C	TMD1
21	Yeast-Dd2-Cys-less-F78C	yF78C	F78C	TMD1
22	Yeast-Dd2-Cys-less-A79C	yA79C	A79C	TMD1
23	Yeast-Dd2-Cys-less-V159C	yV159C	V159C	TMD4
24	Yeast-Dd2-Cys-less-L160C	yL160C	L160C	TMD4
25	Yeast-Dd2-Cys-less-Q161C	yQ161C	Q161C	TMD4
26	Yeast-Dd2-Cys-less-S163C	yS163C	S163C	TMD4
27	Yeast-Dd2-Cys-less-I164C	yI164C	I164C	TMD4
28	Yeast-Dd2-Cys-less-P165C	yP165C	P165C	TMD4
29	Yeast-Dd2-Cys-less-N167C	yP167C	N167C	TMD4

2.2 Materials and Methods

2.2.1 Materials

Restriction enzymes and all other routine molecular reagents were purchased from either New England Biolabs or Gibco/BRL Life Technologies. The oligonucleotides were synthesized on a 50-nmol scale and dissolved in water to a final concentration of 100 μ M each. The Advantage[®] PCR Kit was purchased from Clontech. QuikChange[®] II Site-Directed Mutagenesis kits were purchased from Stratagene. The pGEM-T cloning kit was supplied by Promega. *E. coli* strain XL-1 Blue (Stratagene) was used for transformation and propagation of the recombinant plasmid. Mini-Plasmid and Midi-Plasmid DNA purifications were prepared by using the GFX Micro plasmid Prep Kit (Amersham Pharmacia Biotech) and Midi-Prep kit (Promega), respectively. Automated DNA sequencing was done on a Perkin-Elmer ABI 310 sequencer, using the Perkin-Elmer Big-Dye reagent kit. The *P. pastoris* expression kit containing *P. pastoris* KM71 (*his4 aox1::ARG4*) and intracellular expression vector (pPICZA) was purchased from Invitrogen (San Diego, California). Dodecyl- β -D-maltoside (DDM) was obtained from Amresco. Other chemical reagents were purchased from Sigma. Ni²⁺-NTA agarose resin was obtained from Qiagen. Anti-His polyclonal antibody, secondary goat anti-rabbit antibody, and protein G agarose were from Santa Cruz Biotechnology. The protein molecular weight marker was from Bio-Rad. The SuperSignal Substrate Western Blotting kit (Pierce) was used for detection in Western hybridization.

2.2.2 Construction strategy of cysteine-less *pfert*

There are fourteen cysteines in cysteine-less PfCRT to be substituted to alanine. To carry out this project, cysteine-less mutagenic oligonucleotide primers were synthesized (

Table 2-2). Using a plasmid of Dd2 genetic background (constructed by our group previously) as template, 11 mutagenic segments were amplified by separating PCR. Hence 11 alanine-substituted cysteine DNA segments with their 5' and 3' terminals complementarily overlapping with length equal to the two neighboring mutagenic primers were obtained (Figure 2-2. Step 1). All the segments were purified. Each segment (1 pmol) was mixed in 20 μ l of PCR assembly mixture (2 μ l 10 \times Adanvatage[®] buffer, 2.5 mM MgCl₂, 0.1% Triton X-100, 0.1 mg/ml BSA, 0.2 mM each dNTPs, 1.25 U Advantage[®] DNA polymerase). The assembly PCR program was performed with 50 cycles of 94 $^{\circ}$ C for 30 s, 55 $^{\circ}$ C for 30 s and 72 $^{\circ}$ C for 90s (Figure 2-2. Step 2). Subsequently, 2 μ l of the assembly mixture was diluted 1000-fold in 20 μ l PCR mixture (2 μ l 10 \times Advantage buffer, 1.5 mM MgCl₂, 0.1% Triton X-100, 0.1 mg/ml BSA, 0.2 mM each dNTPs, 3 U Advantage[®] DNA polymerase) with 1 μ M of each the two anchor-forward and reverse primers) (Table 2-3 Anchor oligonucleotide primers). This step PCR program was performed with 94 $^{\circ}$ C for 30 s, followed by 25 cycles of 94 $^{\circ}$ C for 30 s, 55 $^{\circ}$ C for 45 s and 72 $^{\circ}$ C for 5 min and a final incubation cycle at 72 $^{\circ}$ C for 10 min (Figure 2-2. Step 3). The PCR product was analyzed on a 1% agarose gel and then purified and cloned into pGEM-T vector. Several colonies were picked and analysed by DNA sequencing analysis.

Table 2-2 cysteine-less mutagenic oligonucleotide primers

1	Primer 01-a	GGAGGTTCTGCCCTGGGTAAGGCTGCTCATGT
	Primer 01-b	ACATGAGCAGCCTTACCCAGGGCAGAACCTCC
2	Primer 02-a	TTGTCTGTCCGCTTATGAA
	Primer 02-b	TTCATAACGGCGACAGACAA
3	Primer 03-a	AACTTCATTGCCATGATCAT
	Primer 03-b	ATGATCATGGCAATGAAGTT
4	Primer 04-a	TTGGATGCCGCTTCCGTTAT
	Primer 04-b	ATAACGGAAGCGGCATCCAA
5	Primer 05-a	CAATCAATATGTTCTTCGCTTTCCTTATTCTTAGATAC
	Primer 05-b	GTATCTAAGAATAAGGAAAGCGAAGAACATATTGATTG
6	Primer 06-a	GATCTCCGCTCTAATTCCAGTCGCTTCTCCAATATGAC
	Primer 06-b	GTCATATTGGAGAAAGCGACTGGAATTAGAGCGGAGATC
7	Primer 07-a	TTCACCAGTGCCCTAATCTT
	Primer 07-b	AAGATTAGGGCACTGGTGAA
8	Primer 09-a	TTCAACATCGCCGACAACCT
	Primer 09-b	AGGTTGTCGGCGATGTTGAA
9	Primer 10-a	ATCGTCTCTGCTATCCAGGG
	Primer 10-b	CCCTGGATAGCAGAGACGAT
10	Primer 08-a	GGATTCGCCGCTCTATTCTTGGGAAGGAACACCGTCGTCG AGAATGCTGGTCTTGGGAATGGCTAAGTTGGCTGACGATG CCGATGGTGC
	Primer 08-b	GCACCATCGGCATCGTCAGCCAACCTTAGCCATTCCAAGA CCAGCATTCTCGACGACGGTGTTTCCTTCCAAGAATAGAG CGGCGAATCC

* All the sequences is read from 5' to 3'.

Table 2-3 Anchor oligonucleotide primers

Forward linker (FL)	5' AAGCTTCGTACGGATATCCACCGACGAGTTCGAATTCACC ATGGAGTTCGC 3'
Forward anchor (FA):	5' AAGCTTCGTACGGATATCCACCGAC 3'
Reverse Linker (RL):	5' AGCATCACAGTCGAGACGATCCCTGGGTACCAAGCTTGCG GCCGCTTAC3'
Reverse anchor (RA)	5' AGCATCACAGTCGAGACGATCC3'

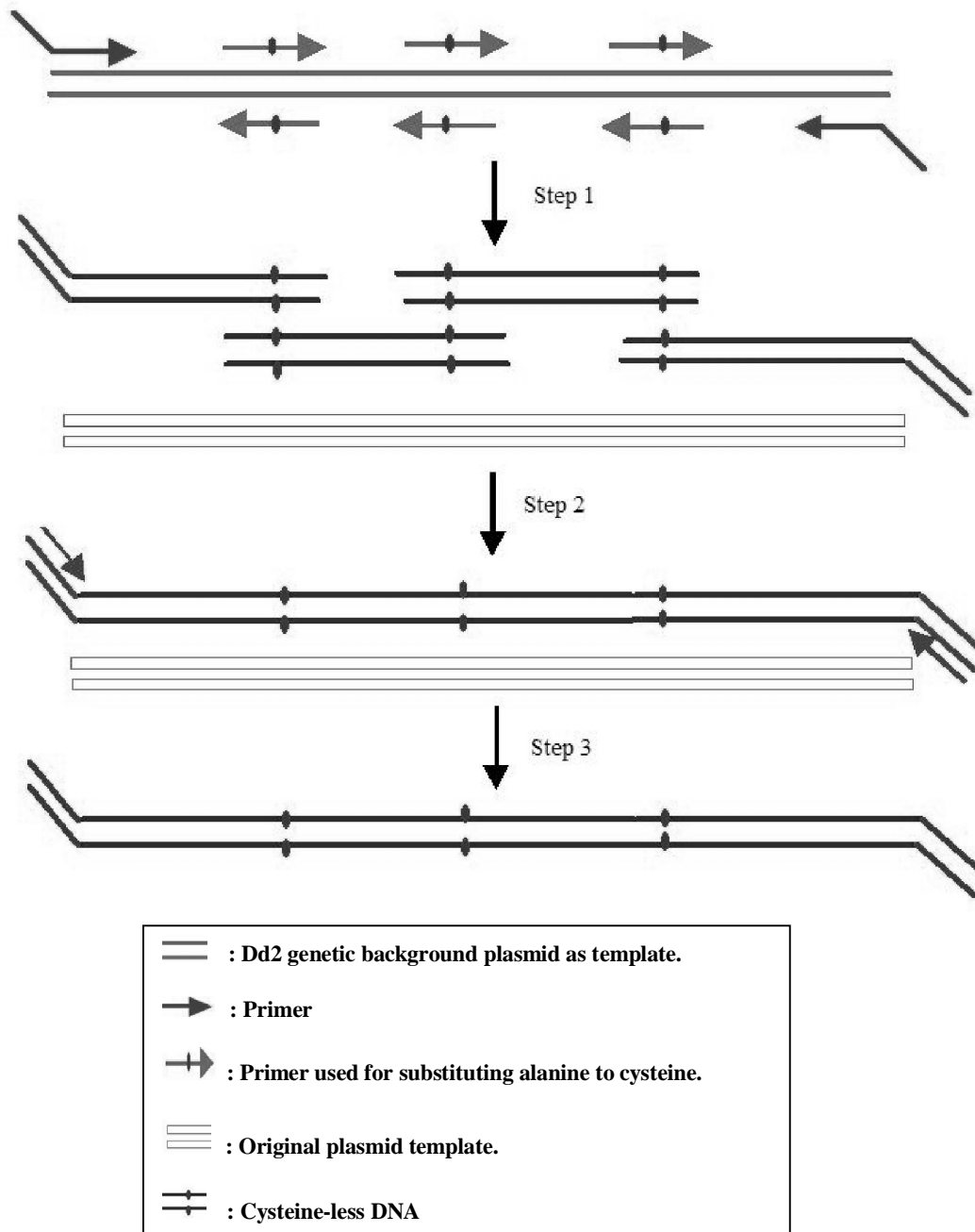


Figure 2-2 The procedure of multiple site-directed mutagenesis. Step 1 indicates that the 11 fragments were synthesized. Step 2 indicates that a 50 cycle of overlapping PCR was conducted. Step 3 indicates that the anchor primers were used to amplifying the cysteine-less DNA fragments.

2.2.3 Site-directed mutagenesis of single cysteine-substituted *pfcrt*

Site-directed mutagenesis was used to make point mutations. The site-directed mutagenesis method is performed using *PfuTurbo*[®] DNA polymerase and a temperature cycler. *PfuTurbo* DNA polymerase replicates both plasmid strands with high fidelity and without displacing the mutant oligonucleotide primers. The basic procedure utilizes a supercoiled double-stranded DNA (dsDNA) vector with an insert of interest and two synthetic oligonucleotide primers containing the desired mutation (Table 2-4 Sequence primers used for single-cysteine recoveries in TMD1). The oligonucleotide primers, each complementary to opposite strands of the vector, are extended during temperature cycling by *PfuTurbo* DNA polymerase. Incorporation of the oligonucleotide primers generates a mutated plasmid containing staggered nicks.

Following temperature cycling, the product was treated with *DpnI*. The *DpnI* endonuclease (target sequence: 5'-Gm6ATC-3') is specific for methylated and hemimethylated DNA and is used to digest the parental DNA template and to select for mutation-containing synthesized DNA. DNA isolated from *E. coli* strains is dam methylated and therefore susceptible to *Dpn I* digestion. The nicked vector DNA containing the desired mutations was then transformed into XL1-Blue competent cells. The small amount of starting DNA template required to perform this method, the high fidelity of the *PfuTurbo* DNA polymerase, and the low number of thermal cycles all contribute to the high mutation efficiency and decreased potential for generating random mutations during the reaction.

Table 2-4 Sequence primers used for single-cysteine recoveries in TMD1

No.	Mutant	Primer
1	Dd2-Cys-less-I59C	5' GAGATCAAGGACAAC TG CTTCATCTACATCCTG*
2	Dd2-Cys-less-F60C	5' ATCAAGGACAACATCTGCATCTACATCCTGTCC
3	Dd2-Cys-less-I 61C	5' AAGGACAACATCTT TG CTACATCCTGTCCATC
4	Dd2-Cys-less-Y62C	5' GACAACATCTTCATCTGCATCCTGTCCATCATC
5	Dd2-Cys-less-I63C	5' AACATCTTCATCTACT GC CCTGTCCATCATCTAC
6	Dd2-Cys-less-L64C	5' ATCTTCATCTACATCT GC TCCATCATCTACTTGT
7	Dd2-Cys-less-S65C	5' TTCATCTACATCCTGTGCATCATCTACTTGTCT
8	Dd2-Cys-less-I66C	5' ATCTACATCCTGTCC GC ATCTACTTGTCTGTCTGC
9	Dd2-Cys-less-I67C	5' TACATCCTGTCCATCT GC TACTTGTCTGTCTGC
10	Dd2-Cys-less-C68C	5' ATCCTGTCCATCATCT GC TTGTCTGTCTGC
11	Dd2-Cys-less-L69C	5' CTGTCCATCATCTACT GC TCTGTCTGC
12	Dd2-Cys-less-S70C	5' TCCATCATCTACTT GT GTCTGC
13	Dd2-Cys-less-V71C	5' ATCATCTACTTGTCT GC CGCGTTATGAACATC
14	Dd2-Cys-less-A72C	5' ATCTACTTGTCTGTCT GC CGTTATGAACATCATC
15	Dd2-Cys-less-V73C	5' TACTTGTCTGTCTGC CG TTATGAACATCATCTTC
16	Dd2-Cys-less-I74C	5' TTGTCTGTCTGC CG TTATGAACATCATCTTCGC
17	Dd2-Cys-less-E75C	5' TCTGTCTGC CG TTAT GT GTATCATCTTCGCCAA
18	Dd2-Cys-less-T76C	5' GTCGCCGTTATGAAC GC ATCTTCGCCAAGAGG
19	Dd2-Cys-less-I77C	5' GCCGTTATGAACATCT GC TTTCGCCAAGAGGACT
20	Dd2-Cys-less-F78C	5' GTTATGAACATCATCT GC CGCCAAGAGGACTCTG
21	Dd2-Cys-less-A79C	5' ATGAACATCATCTTCT GC AAGAGGACTCTGAAC
22	Dd2-Cys-less-F158C	5' GGAAACATCCAGTC CG CTTCAGTTGTCC
23	Dd2-Cys-less-V159C	5' GAAACATCCAGTC CG CTTCAGTTGTCCATC
24	Dd2-Cys-less-L160C	5' CATCCAGTCCTTCGT GC CAGTTGTCCATCCCAATC
25	Dd2-Cys-less-Q161C	5' CAGTCCTTCGTCT GC TTGTCCATCCCAATC
26	Dd2-Cys-less-L162C	5' GTCCTTCGTCTTCAG GC TCCATCCCAATCAATATG
27	Dd2-Cys-less-S163C	5' CTTCGTCTTCAGTT GC ATCCCAATCAATATG
28	Dd2-Cys-less-I164C	5' GTCCTTCAGTTGTCT GC CCAATCAATATGTTCTC
29	Dd2-Cys-less-P165C	5' CTTCAGTTGTCCATCT GC ATCAATATGTTCTTC
30	Dd2-Cys-less-I166C	5' CTTCAGTTGTCCATCT GC ATCAATATGTTCTTC
31	Dd2-Cys-less-N167C	5' GTTGTCCATCCCAATCT GC ATGTTCTTCGCTTTC

*Only coding sequences are showed.

2.2.4 Cloning of genes for expression

Colonies from the plate were inoculated into 5 ml LB medium with an appropriate amount of antibiotic (100 µg/ml Zeocin) in a universal bottle. After growing at 300 rpm at 37°C overnight, the culture became saturated. Cells were harvested by centrifugation from the culture and ready for plasmid DNA isolation using the Wizard[®] Plus SV Minipreps DNA Purification System kit (Promega).

DNA sequencing was carried out by using the ABI PRISM BigDye[™] Terminator Cycle Sequencing Kit (PE Applied Biosystem). The ABI PRISM[™] 310 Genetic Analyzer (an automated instrument) was used for analyzing fluorescently labeled DNA fragments by capillary electrophoresis. Cycle sequencing is a simple method in which successive rounds of denaturation, annealing, and extension in a thermal cycle result in linear amplification of the extension product. The procedures of DNA sequencing were carried out as recommended by the kit's manufacturer with minor modification. A 4 µl portion of the master mix, 0.5-1 µg of plasmid DNA, 0.16 µM of primers and sterile water were mixed together to make a total volume of 10 µl. Thirty cycles of amplification were carried out in a DNA thermal cycler (GenAmp PCR System 2400 or 9600, Perkin-Elmer) with the recommended conditions (96°C for 10 s, 50°C for 30 s, 60°C for 4 min). To remove unincorporated dyes, the entire contents of each extension reaction were mixed thoroughly with 1 µl of 3 M sodium acetate (pH 4.8) and 25 µl of 100% ethanol in a 0.5-ml microcentrifuge tube. After incubation at room temperature for 15 min, the extension products were precipitated by centrifugation at 14,000 g for 20 min at room temperature. The supernatant was carefully aspirated as completely as possible, and the pellet was washed with 250 µl of 70% ethanol. After the pellet was dried at 90°C for 1 min, 10 µl of template suppression reagent (TSR) was added. The products were denatured by boiling

for 3 min and then ice-chilled. The samples were loaded onto the instrument for automated electrophoresis. The results were analyzed with ABI PRISM[®] DNA Sequencing Analysis Software.

Each oligonucleotide (2.5 pmol) was mixed in 20 µl of PCR assembly mixture (2 µl 10×Advantage[®] buffer, 2.5 mM MgCl₂, 0.1% Triton X-100, 0.1 mg/ml BSA, 0.2 mM each dNTPs, 1.25 U Advantage[®] DNA polymerase). The assembly PCR program was performed with 25 cycles of 94°C for 30 s, 55°C for 30 s and 72°C for 90 s. Subsequently, 2 µl of the assembly mixture was diluted 10-fold in 20 µl of PCR mixture (2 µl 10× Advantage buffer, 1.5 mM MgCl₂, 0.1% Triton X-100, 0.1 mg/ml BSA, 0.2 mM each dNTPs, 3 U Advantage[®] DNA polymerase and the two outermost primers at 1 µM each) and the second PCR program was started. This consisted of a denaturation step of 94°C for 30 s, followed by 20 cycles of 94°C for 30 s, 68°C for 45 s and 72°C for 90 s and a final incubation cycle at 72°C for 10 min. The PCR product was analyzed on 0.8% agarose gel and then purified with a PCR-Purification Kit (Qiagen) and then cloned into pGEM-T vector. Several colonies were picked and their plasmids were isolated for restriction and sequencing analysis using oligonucleotides P1, P5, P11, P17, P23, P29 and P64. Three clones (K76 sensitive, K76T resistant and K76I resistant) were corrected to the desired sequence using a modified overlap extension PCR method.

2.2.5 Transformation of *Pichia pastoris* and confirmation of *pfert* integration

The synthetic genes were cloned into the *P. pastoris* pPICZA vector using the *EcoR* I and *Not* I sites of the polylinker region. After digestion of 20 µg plasmids with *Sac* I, the

Chapter 2 Expression of Substituted PfCRT

linearized constructs were transformed into the *P. pastoris* KM71 strain by electroporation (pulse conditions were 1.5 kV at 400 Ω and 2 μ F). The expressed PfCRT colonies were selected on plates containing 1 mg/ml Zeocin.

The yeast genomic DNA was prepared as follows: colonies of each construct were grown in 5 ml YPD medium overnight. The cell pellet was dissolved in 280 μ l TE Buffer (100 mM Tris pH 8.0, 100 mM EDTA), 300 μ l distilled water and 3 μ l β -mercaptoethanol. The mixture was incubated at 30°C for 45 min, and then centrifuged at top speed in a microcentrifuge for 2-3 sec. The pellet was resuspended in 500 μ l S Buffer (1.0 M Sorbitol, 10 mM PIPES, pH 6.5) and centrifuged again. The supernatant was discarded. The cell pellet was resuspended in 500 μ l S Buffer containing 1 mg/ml Zymolyase 20T. The mixture was incubated at 30°C for 1 hr and then the supernatant was discarded by centrifugation. The cell pellet was suspended in 200 μ l TE containing 0.1% SDS and 2 μ g Proteinase K. This was incubated at 37°C for 3 hr with occasional mixing, and subsequently incubated at 65°C for 20 min. Then the mixture was extracted with 200 μ l of 1 M Tris saturated phenol:chloroform (1:1). After centrifuging, the upper aqueous layer was extracted with 200 μ l chloroform. The upper layer was then added to 500 μ l 95% ethanol and incubated at room temperature for 10 min. Then the DNA was obtained after 20 min centrifugation at 15,000 g. The DNA was resuspended in 200 μ l TE Buffer containing 150 mM NaCl and 1 μ g Ribonuclease A and then incubated at 37°C for 1 hr. The resulting mixture was extracted with phenol:chloroform (1:1), and chloroform. Finally, 2.5 volumes of 95% ethanol was added to the genomic DNA supernatant and incubated at room temperature for 10 min. The genomic DNA (100 μ g) was obtained after centrifugation at 15,000 g for 20 min at 4°C and resuspended in 50 μ l distilled water.

Chapter 2 Expression of Substituted PfCRT

Twenty nanograms of genomic DNA and 0.4 μ M each of 5'AOX and 3'AOX primers were added to 25 μ l PCR mixture containing 2.5 μ l 10 \times PCR buffer, 1.5 mM MgCl₂, 0.2 mM dNTPs, and 0.5 U DNA polymerase. The PCR program consisted of a denaturation step of 94°C for 3 min, followed by 30 cycles of 94°C for 1 min, 50°C for 1 min, and 58°C for 1.5 min and a final incubation cycle at 58°C for 7 min. The PCR product was analyzed on 0.8% agarose gel.

2.2.6 Growth of *Pichia pastoris*

Several colonies of each construct were selected for expression trials in a 500 ml shake flask containing 100 ml MGYH medium (1.34% w/v yeast nitrogen base without amino acid, 1% v/v glycerol, 0.4 mg/liter biotin and 40 mg/liter histidine) and incubated at 30°C with shaking at 250 rpm to an OD₆₀₀ over 2.0 (28 hr), then the cells were centrifuged at 2,500 g for 10 min and the cell pellets were resuspended in 20 ml MMH medium (1.34% w/v yeast nitrogen base without amino acid, 0.5% v/v methanol, 0.4 mg/liter biotin and 40 mg/liter histidine) in 250 ml baffled shake flasks covered with cheesecloth. Incubation was continued for 72 hr with further additions of methanol (0.5% v/v) at 24 hr and 48 hr. Cells were finally collected by centrifugation at 2,500 g for 5 min at 4°C and stored at -80°C for further use.

2.2.7 Preparation of microsomes from *Pichia pastoris*

P. pastoris microsomes were prepared according to established methods with some modification (Lerner-Marmarosh et al., 1999). Yeast was harvested and resuspended in ice-cold yeast homogenization buffer (0.33 M sucrose, 300 mM Tris-Cl, pH 7.4, 1 mM

Chapter 2 Expression of Substituted PfCRT

EDTA, 1 mM EGTA, 2 mM DTT and protease inhibitors) at a concentration of 0.5 g wet weight of cells per ml. Protease inhibitor cocktail and 1 mM PMSF were added. After adding 1.5 g glass beads (0.45 – 0.5 mm diameter) per gram of yeast cell, the cells were mechanically disrupted 12 times, for 1 min each, under liquid CO₂ cooling conditions in a Braun homogenizer (type 853033) or disrupted by *French press*. The homogenate was centrifuged at 3,500 g for 30 min at 4°C, and the pellet was discarded, and the supernatant was centrifuged at 14,000 g for 45 min at 4°C. These steps removed unbroken cells, nuclei, and mitochondrial fractions, which contained little PfCRT. The supernatant was ultracentrifuged at 200,000 g for 90 min at 4°C and the pellet containing the microsomes was resuspended in buffer A (50 mM Tris-Cl, pH 7.4, 10% v/v glycerol containing protease inhibitor cocktail and 1 mM PMSF) to the same volume as before the 200,000 g centrifugation step. The microsome suspension was stored at -80°C for further use.

2.2.8 Detection of expressed PfCRT with Western blot

Protein (10 or 20 µg of microsomes) was electroblotted onto PVDF Immobilon P membrane (MilliPore) after separation by SDS-PAGE gels according to the procedure described by Towbin *et al.* (Towbin et al., 1979). After electroblotting, the membrane was rinsed in methanol for 30 s and air dried for 30 min. The blocking step was started by incubating for 1 hr at room temperature in TTBS (10 mM Tris-HCl, pH 7.5, 150 mM NaCl, and 0.5% Tween 20) containing 5% powdered skim milk. The membrane was incubated with the primary antibody (e.g. anti-his or anti-PfCRT (1:3,000)) in TTBS at 4°C overnight, washed with TTBS 3 times for 10 min each and then incubated with horseradish peroxidase-conjugated secondary goat anti-rabbit antibody (1:2,500) in

TTBS for 1 hr at room temperature, followed by washing and detection with the SuperSignal Substrate Western Blotting kit (Pierce). The chemiluminescence signal was analyzed by a LumiImager (Roche). Primary antibody against PfCRT was a generous gift of Tom Wellems.

2.2.9 Solubilization of PfCRT and purification by Ni²⁺-NTA agarose

PfCRT is a membrane protein and its solubilization requires the use of detergents (Kohler et al., 1997). Various detergents were evaluated for their efficiency to solubilize PfCRT from microsomes. Microsomes (100 µg) were solubilized in buffer A supplemented with 1% (w/v) CHAPS, n-dodecyl-β-D-maltoside (DDM), n-octyl-β-D-glucopyranoside (OG) and Triton X-100. The suspensions were mixed and incubated on ice for 30 min. The insoluble material was pelleted by centrifugation (100,000 g) for 20 min at 4°C. The soluble and insoluble fractions were analyzed by western blotting.

After determining which detergent was the best, the microsome pellet was resuspended in buffer A containing 0.6% W/V DDM plus protease inhibitors as above on ice. The suspension was mixed by inversion and incubated at 4°C for 30 min on a rotator. It was then centrifuged at 100,000 g for 30 min. The supernatant was kept for purification.

One milliliter column of Ni²⁺-NTA agarose resin (Qiagen) was pre-equilibrated in buffer A and about 100 mg of solubilized microsomal protein was added to the column. Then the column was washed with 50 ml of the buffer A containing 0.1% DDM. PfCRT was eluted with a linear imidazole gradient from 0 to 0.5 M made in the elution buffer (buffer

A containing 0.1% DDM and 0.5 M imidazole). For each fraction, 1 ml of sample was collected. The degree of purity of the resulting PfCRT was verified by 12% SDS-PAGE.

2.3 Results

2.3.1 Construction of cysteine-less and single cysteine *pfcr*t gene mutants

DNA fragments of cysteine-less *pfcr*t with a Dd2 genetic background were constructed and the full-length DNA sequence was confirmed (Figure 2-3). Then it was subcloned into yeast expression vector pPICZA at the *Eco*R I and *Not* I sites. The full-length DNA sequence of the constructed plasmids (pPICZA-PfCRT-Dd2-Cys-less) with the desired *pfcr*t mutations was confirmed. Thirty-one single cysteine-encoded *pfcr*t fragments within TMD1 and TMD4 were constructed with pPICZA-PfCRT-Dd2-Cys-less as template, one at a time using site-directed mutagenesis (Table 2-5). Full-length DNA sequences of these constructed plasmids were confirmed. After transformation to yeast, genomic DNA of these constructs was prepared. PCR was carried out with primers 5'AOX and 3'AOX. The full-length DNA sequences of these PCR products were determined and the constructs were confirmed to be correct.

Chapter 2 Expression of Substituted PfCRT

Table 2-5 Plasmids of single cysteine mutants

No.	Plasmid	Shortened name	No.	Plasmid	Shortened name
1	Plasmid-Dd2-Cys-less-I59C	pI59C	17	Plasmid-Dd2-Cys-less-E75C	pE75C
2	Plasmid-Dd2-Cys-less-F60C	pF60C	18	Plasmid-Dd2-Cys-less-T76C	pT76C
3	Plasmid-Dd2-Cys-less- I 61C	pI 61C	19	Plasmid-Dd2-Cys-less-I77C	pI77C
4	Plasmid-Dd2-Cys-less-Y 62C	pY62C	20	Plasmid-Dd2-Cys-less-F78C	pF78C
5	Plasmid-Dd2-Cys-less-I63C	pI63C	21	Plasmid-Dd2-Cys-less-A79C	pA79C
6	Plasmid-Dd2-Cys-less-L64C	pL64C	22	Plasmid-Dd2-Cys-less-F158C	pF158C
7	Plasmid-Dd2-Cys-less-S65C	pS65C	23	Plasmid-Dd2-Cys-less- V159C	pV159C
8	Plasmid-Dd2-Cys-less-I66C	pI66C	24	Plasmid-Dd2-Cys-less-L160C	pL160C
9	Plasmid-Dd2-Cys-less-I67C	pI67C	25	Plasmid-Dd2-Cys-less-Q161C	pQ161C
10	Plasmid-Dd2-Cys-less-C68C	pC68C	26	Plasmid-Dd2-Cys-less-L162C	pL162C
11	Plasmid-Dd2-Cys-less-L69C	pL69C	27	Plasmid-Dd2-Cys-less-S163C	pS163C
12	Plasmid-Dd2-Cys-less-S70C	pS70C	28	Plasmid-Dd2-Cys-less-I164C	pI164C
13	Plasmid-Dd2-Cys-less-V71C	pV71C	29	Plasmid-Dd2-Cys-less-P165C	p P165C
14	Plasmid-Dd2-Cys-less-A72C	pA72C	30	Plasmid-Dd2-Cys-less-I166C	pI166C
15	Plasmid-Dd2-Cys-less-V73C	pV73C	31	Plasmid-Dd2-Cys-less-N167C	pN167C
16	Plasmid-Dd2-Cys-less-I74C	pI74C			

2.3.2 Expression of PfCRT derivatives in *P. pastoris*

For heterologous protein expression, *pfCRT* derivatives cloned into pPICZA plasmids were introduced into *P. pastoris* by electroporation, which allows incorporation of linearized *pfCRT* genes into the yeast genome. Several clones from each construct were picked from growth plates containing 800 µg/ml Zeocin. These clones were cultured in shake flasks and the heterologous expression was induced with methanol. The production of a PfCRT derivative was tested by western blot analysis using anti-his polyclonal antibody and a band of about 45 kDa was detected. Twenty-nine out of thirty-two derivatives were found to express various levels of PfCRT, while Dd2-Cys-less-F158C, Dd2-Cys-less-L160C and Dd2-Cys-less-I166C *pfCRT* did not. The clones expressing PfCRT at the highest level were considered with high copy number of PfCRT and chosen for this study. Typical western blot results using anti-his antibody are shown in Figure 2-4. No signal was present in the control containing vector alone (pPICZA). This demonstrated that the redesigned *pfCRT* could be successfully expressed in *P. pastoris*. Dd2-Cys-less-F158C, Dd2-Cys-less-L160C and Dd2-Cys-less-I166C *pfCRT* transformed mutants failed to express.

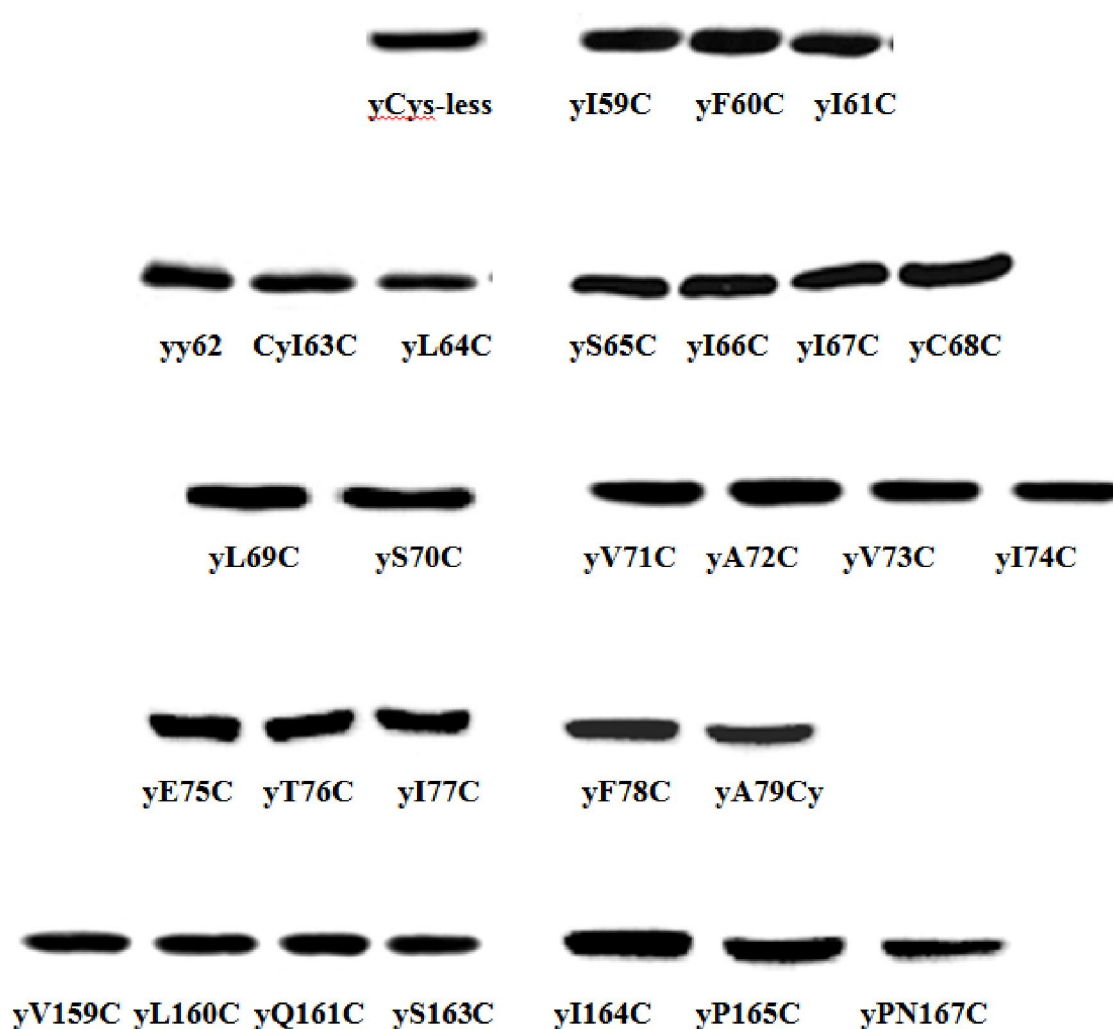


Figure 2-4 The expression of PfCRT derivatives demonstrated by western blot. PfCRT derivatives in microsomes (15 μ g) of *P. pastoris* were detected by western blot using anti-his polyclonal antibody.

The expression level was detected by western blot at several time points from 0 to 72 hr postinduction with methanol. PfCRT of Yeast-Dd2-Cys-less was expressed at 4 hr after methanol induction. The expression level reached its maximum after 24 hr and remained constant until the cells were harvested after 48 hr. When the PfCRT western blot signal (blu) was normalized to microsomes protein amount as determined using Bradford reagent, it was found that the expression levels of PfCRT in these microsomes were almost the same.

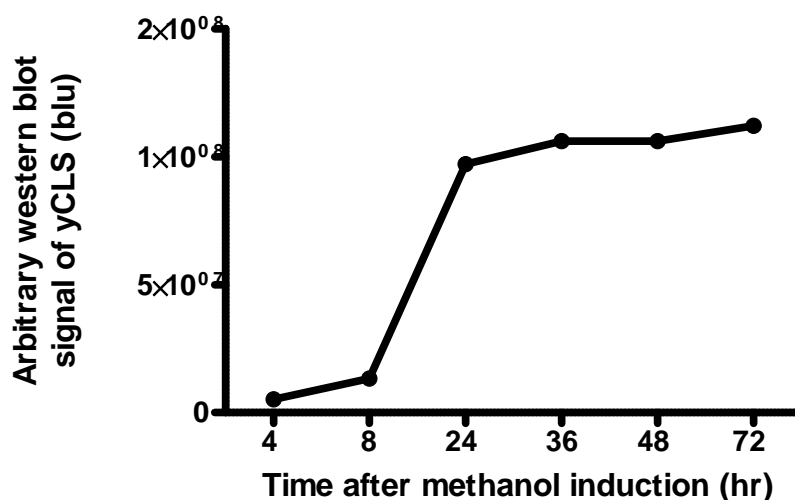


Figure 2-5 Time course of PfCRT expression in Yeast-Dd2-Cys-less Microsomes (10 μ g) were used for Western blot detection of the expression levels. The cell line was Yeast-Dd2-Cys-less. Samples were collected at 8, 24, 36, 48, and 72 hr after methanol induction.

2.3.3 Microsome preparation and purification of PfCRT

Inducible expression of redesigned *pfCRT* was mainly located on the membrane of *P. pastoris*. After initiation of the methanol feed to induce redesigned *pfCRT* expression, small samples were taken at various intervals for analysis of proteins. Cells were collected and broken by glass mill and *French press*, a rapid membrane preparation was made, and PfCRT was purified as described under “Materials and Methods” (Refer to Section 2.2). SDS-PAGE gel electrophoresis and Western blotting were performed to verify the expression of PfCRT.

2.4 Discussion

Elucidation of the structure and function of PfCRT is essential for further understanding the molecular mechanism of CQR. The protein resides in a subcellular membrane within

Chapter 2 Expression of Substituted PfCRT

an intracellular parasite, so experimental study of PfCRT transport function requires transport of substrates cross three membranes in a coordinated fashion. As it is extremely difficult to experimentally manipulate *in vivo*, an *in vitro* system is necessary.

The technology required for fabricating membrane vesicles of various types and for purifying and reconstituting polytopic integral membrane proteins has been well developed for *Pichia*. *P. pastoris* is a highly successful system for the production of a wide variety of recombinant proteins. It is capable of many of the post-translational modifications performed by higher eukaryotic cells such as proteolytic processing, folding, disulfide bond formation and glycosylation (Buckholz and Gleeson, 1991; Romanos et al., 1992). So it is a better option than the bacterial system for expression of membrane proteins. Thus heterologous expression of PfCRT in *Pichia* would assist in the further analysis of PfCRT transport function.

Our laboratory and Rope's group have successfully expressed PfCRT in *Pichia* (Tan et al., 2006; Zhang et al., 2002) and functional studies have been carried out. Using this expression system, this project aimed to employ SCAM to elucidate the structure of PfCRT and understand the mechanism of CQR.

Using site-directed mutagenesis, Cys-less *pfCRT*, twenty-one cysteine substituted *pfCRTs* within TMD1 and ten within TMD4 were constituted. PfCRT of Cys-less and single cysteine mutants within TMD1 were all expressed. But only seven out of ten within TMD4 were expressed. In this project, failed expression of PfCRT may have been a disadvantage, but it was still suitable for study of the notable position (position 163) within TMD4.

Chapter 2 Expression of Substituted PfCRT

The apparent molecular weight of PfCRT determined by SDS-PAGE was about 45 kDa, which is smaller than the calculated (49.5 kDa) value. This discrepancy may be explained by the known fact that membrane proteins may bind to SDS at a different ratio compared to other soluble proteins or may have hydrophobic stretches that do not completely unfold. These characteristics are reflected in a change in the apparent molecular mass in SDS-PAGE gels.

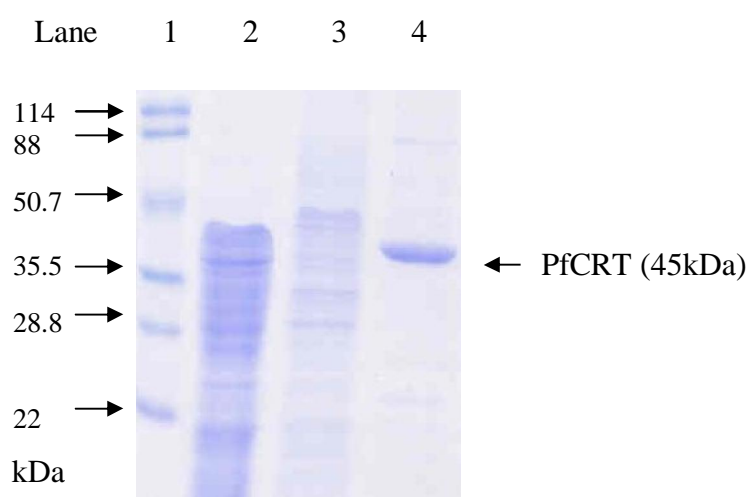


Figure 2-6 SDS-PAGE of purified PfCRTs

Microsomes PfCRTs was subjected to Ni²⁺-NTA purification. Samples were separated by SDS-PAGE and stained with Coomassie blue. Lane 1, marker; lane 2, microsomes; lane 3, flow through fraction; lane 4, purified PfCRT (3 µg).

To facilitate subsequent purification of PfCRT, a 6-histidine tag was engineered into the C-terminal of PfCRT. It was reported that the presence of the 6-histidine tag does not affect the activity of the transporter (Loo and Clarke, 1995b). Although the expression level was low (approximately 1-2% of the total amount of microsomes), the PfCRT protein could be purified to apparent homogeneity by a single chromatography step on Ni²⁺-NTA agarose.

Chapter 2 Expression of Substituted PfCRT

Purification of membrane proteins requires a detergent for solubilization. DDM is a mild non-ionic detergent. Not only can it almost completely solubilize microsomes, it also has the advantage of not inactivating most proteins as observed by others (Putman et al., 1999). Purified PfCRT will be used and reconstituted into proteoliposomes for further studies.

Chapter 3

Cysteine Scanning of Transmembrane Domain 1 of PfCRT

Abstract

The microsomes isolated from each of the PfCRT-producing *P. pastoris* strains were used for CQ transport activity assay. Dd2-Cys-less PfCRT could accumulate $^3\text{H-CQ}$ in a concentration-dependent manner. The $^3\text{H-CQ}$ transport activity was specific. There were significantly different CQ accumulation activities among these mutants. This suggests that cysteine substitution of amino acids affects the function *via* the amino acid composition of the TMD1 helix.

Modified by MTSES, Dd2-Cys-less-T76C PfCRT microsomes can accumulate more CQ when the concentration of MTSES increases. MTSET and MTSEA led to a decrease of specific CQ accumulation as the concentrations of these two MTS reagents increased. This suggests that the charged 76th amino acid affects CQ accumulation.

In scanning experiments on the sensitivity of single cysteine substitution mutants to MTSES reagent, the modifications in position 62, 71 and 73 in TMD1 displayed lower relative activity.

Substrate (CQ) protection from MTS reagent modification was carried out in the presence of non-radiolabeled CQ. In assaying these, only the 76th showed protection effects. This result strongly suggests that the 76th is a binding site of CQ in PfCRT.

3.1 Introduction

3.1.1 Conversion of lysine 76 to threonine in TMD1 confers CQR phenotype

Chloroquine is the most successful antimalarial drug ever discovered. Chloroquine is held within the parasite's internal DV, an acidic organelle in which chloroquine accumulates to high concentrations and exerts its toxic effect. The suggestion originally given by Yayon and confirmed by Bray by isolating DVs from the parasite (Yayon, 1985; Yayon et al., 1985). But how CQ accumulates and exerts its toxic effect is subject to ongoing debate.

Twenty point mutations within TMD1 have been found in the *pfcr* gene to date from CQR field isolates or laboratory clones through drug selection.(Cooper et al., 2005; Walliker et al., 2005; Wellems and Plowe, 2001). Related research has shown that substitution of lysine (K) to Threonine (T) for at position 76 (K76T) is the most pivotal change of CQR parasites (Djimde et al., 2001a; Fidock et al., 2000b). The 76T and other mutations in *pfcr* have been employed as molecular markers for predicting CQR in field surveys, although CQR is not always linked to mutant *pfcr* alleles in field isolates due to host immunity and other factors (Djimde et al., 2001a; Djimde et al., 2001b; Tinto et al., 2008);(Djimde et al., 2003),

Mutations in *pfcr* that lead to the CQR phenotype were provided by *in vitro* drug selection (Cooper et al., 2002) and allelic exchange studies (Sidhu et al., 2002). When selected by lethal doses of CQ, a susceptible parasite (106/1) carrying six mutations in *pfcr* (not 76T) commonly found in Southeast Asian CQR parasites became CQR. Replacement of the wild type *pfcr* allele in the susceptible progeny GC03 of the

HB3xDd2 cross (Wellems et al., 1990) with up to eight *pfcr*t alleles from CQR parasites originating from Asia, Africa and South America consistently produced the CQR phenotype and reduced verapamil reversibility that is always associated with CQR and substitution at the 76 PfCRT position (Sidhu et al., 2002).

3.1.2 PfCRT is a putative transporter

PfCRT has been predicted to have ten transmembrane domains and is localized to the DV membrane (Fidock et al., 2000b). By bioinformatics analyses, Martin and Kirk suggested that PfCRT belongs to a drug/metabolite transporter superfamily (Martin and Kirk, 2004; Tran and Saier, 2004). Thus it can be assumed that the N- and C-termini of PfCRT are predicted to be located on the parasite's cytoplasmic side of the DV membrane (Martin and Kirk, 2004). PfCRT was also predicted to be a dimer within the DV membrane, with TMDs 1, 2, 3, 6, 7 and 8, functioning mainly in substrate discrimination and recognition; TMDs 4 and 9 in substrate binding and translocation; and TMDs 5 and 10 in the formation and/or stabilization of the homodimeric structure (Martin and Kirk, 2004; Tran and Saier, 2004).

Comparing several susceptible and CQR parasites (Sanchez et al., 2004; Sanchez et al., 2003), CQR parasites have trans-stimulated CQ accumulation inside the DV, a phenomenon that is energy-dependent and not due to simple passive diffusion through channels or pores. This CQ stimulation phenomenon in CQR parasites with *pfcr*t CQR alleles suggested that *pfcr*t is directly or indirectly involved in a transporter-mediated CQ efflux system in CQR parasites (Sanchez et al., 2004; Sanchez et al., 2003).

3.1.3 Characterization of PfCRT by heterologous expression system

Heterologous expression of PfCRT and *in vitro* experiments provide supporting evidence that PfCRT is a transporter (Tan et al., 2006). Expression of PfCRT in yeast results in an increased proton (H^+) gradient across the vesicular membrane with reduced pH inside, which is thought to be due to either the effect of PfCRT on chloride (Cl^-) transport or ATPase activity (Zhang et al., 2002). PfCRT was also found to bind specifically to CQ at physiological concentrations, although no significant difference is observed in binding affinity of CQ to PfCRT from wild type (CQS) and mutant (CQR) parasites (Zhang et al., 2004).

In contrast to observations in yeast, no differences in Cl^- conductance between control and PfCRT-expressing oocytes were observed (Nessler et al., 2004). *Xenopus laevis* oocytes expressing PfCRT show a reduced intracellular membrane potential and an alkaline pH relative to controls, which are attributed to the activation of a nonselective cation transporter and an endogenous Na^+-H^+ exchanger (NHE). Because these two transmembrane pathways are independent, they do not support the role of PfCRT as a direct CQ transporter. From these studies, it was proposed that PfCRT expression results in activation of the endogenous transporter systems: H^+ -ATPase in yeast and cation transporter and NHE in oocytes.

When PfCRT is expressed in the slime mold *Dictyostelium discoideum*, small reductions in pH and significantly reduction of verapamil-reversible intravesicular CQ accumulation in K76T CQR mutants is observed relative to control and wild type PfCRT cells (Naude et al., 2005). This reduced CQ accumulation is most likely due to a PfCRT-mediated

energy-dependent efflux mechanism rather than to the small intravesicular changes in pH and CQ uptake.

3.1.4 Use of microsomes in CQ transport analysis of PfCRT

Genetic cross experiment and field studies (Fidock et al., 2000d) have been used to elucidate CQ resistance associated with PfCRT. To study CQ accumulation in the parasite DV would be ideal but this is complicated by the presence of other membranes, i.e. red blood cell membrane, parasite plasma membrane and parasitophorous vacuole membrane, in the native system. Membrane preparations from parasitized red blood cells and purified preparations of specific organelles, particularly the DVs, have been employed to analyze CQ accumulation (Herwaldt et al., 1990; Saliba et al., 1998). Although insights can be gained from studies of purified digestive DVs, CQ transport across the DV membrane is complicated by the existence of several other proteins (e.g. PfMDR1 and CG2), which were previously regarded as responsible for CQ uptake (Ridley, 1998; Riordan et al., 1985). Therefore, a more useful approach is to conduct PfCRT-mediated CQ transport studies using membrane vesicles isolated from PfCRT expressed in a heterogeneous system. Membrane vesicles offer great advantages for finding PfCRT-mediated CQ accumulation and its ability to control the intra- and extra-vesicular medium.

Studies of membrane protein function using heterologous expression systems have been documented, for example, P-glycoprotein and LmrP (Fritz et al., 1999; Putman et al., 2001). In the current study, PfCRT was expressed in the yeast *P. pastoris* and found to be

Chapter 3 Cys-Scanning of TMD1

localized to the membrane fractions. In this chapter, isolation of membrane vesicle preparations from these yeast cells to study ^3H -CQ accumulation is described.

3.2 Materials and Methods

3.2.1 Materials

Protein G-Agarose was from Santa Cruz. $^3\text{H-CQ}$ (specific activity: 5 Ci/mmol) was purchased from American Radiolabelled Chemicals Inc. (2-(Trimethylammonium)ethyl) methanethiosulfonate bromide (MTSET), (2-aminoethyl) methanethiosulfonate hydrobromide (MTSEA) and sodium (2-sulfonatoethyl) methanethiosulfonate (MTSES), were purchased from Toronto Research Chemicals (North York, Ontario, Canada). Dodecyl- β -D-maltoside (DDM) was from Amresco.

3.2.2 Culture of *P. pastoris* cells and preparation of microsomes from *P. pastoris*

Frozen stocks of the cell lines (Table 2-1) were streaked on YPD agar plates containing 100 $\mu\text{g/ml}$ Zeocin. One colony from each cell line was grown in 100 ml of MGYH medium. The details are described in Section 2.2.6. After 24 hr of induction with methanol, cells were harvested by centrifugation at 3,500 g for 5 min at 4°C. The microsomes were prepared from *P. pastoris* according to Section 2.2.7. Finally, the microsomes were resuspended in transport buffer (0.25 M sucrose, 0.01 M Tris-HCl, pH 7.4) and used for $^3\text{H-CQ}$ uptake assay.

3.2.3 Determination of the orientation of PfCRT in the membrane of microsomes

The orientation of PfCRT in the microsomes was determined by using antibodies raised against the C-terminal 6-histidine tag of PfCRT. Microsomes (100 µg) were treated with 1% DDM or untreated for 1 hr at 4°C. Subsequently, the microsomes were incubated for 2 hr at 4°C with 200 ng anti-his polyclonal antibody. Twenty microliters of Protein G-Agarose suspension was added and the mixture was incubated at 4°C on a rocker platform overnight. Microsomes were then collected by centrifugation at 10,000 g for 30 sec at 4°C. After 4 washes with PBS containing 0.5% BSA, microsomes were separated by SDS-PAGE. The proteins were blotted onto PVDF membranes and the amount of bound antibody was determined by western blotting using anti-PfCRT polyclonal antibody and densitometry.

3.2.4 Assay of the accumulation of ³H-CQ in microsomes

³H-CQ uptake in microsomes was measured by a modified method based on Prabhu and Basivireddy (Basivireddy and Balasubramanian, 2003; Prabhu and Balasubramanian, 2003). ³H-CQ may be taken up by PfCRT-containing microsomes. For susceptible mutants of PfCRT, passage of the drug is obstructed and low levels of CQ would bind and be transported into the microsomes and *vice versa* for the CQR mutants. By detecting the level of radioactivity accumulated in the microsomes, CQ transport activities of different PfCRT mutants could be assessed. The assay was performed on PfCRT-harboring microsomes, however not only PfCRT reacts with CQ. Accumulation of ³H-CQ as an effect of PfCRT was therefore deduced by an indirect approach, in which the count of non-specific binding (due to non-specific binding sites of various

microsomal structures) was subtracted from the count of total binding (due to binding on both PfCRT and non-specific sites). All counts were done in triplicate.

To determine the total count, 50 µg of microsomes in 10 mM Tris-Cl pH 7.4, 0.25 M sucrose was mixed with 3 mM ATP and 154 nM [³H]-CQ. After incubation at 37°C for 5 min, 200-fold cold CQ was added to quench the reaction. PEG-8000 (12.5%) was added to precipitate the microsomes which were then spun down and mixed with cold buffer with 200-fold CQ. The mixture was spun again and immersed in 5 ml scintillation buffer. Radioactive signals were counted after overnight rocking.

To determine the non-specific count, 50 µg of microsomes was mixed with 3 mM ATP and 200-fold cold CQ. After incubation at 37°C for 15 min, 154 nM ³H-CQ was added and the mixture was incubated at 37°C for 5 min. The reaction was quenched and subsequent steps were the same as those for the total count.

All experimental points were determined at least in triplicate. Standard error of means was calculated where possible, and they are indicated as error bars in the figures. Binding data was fitted by non-linear regression in Prism 5.0 software using the one-site hyperbola binding model ($Y = (V_{max} \cdot X) / (K_m + X)$).

3.2.5 Treatment with MTS reagents

To identify and characterize the effects of single-cysteine PfCRT mutants by MTS-linked probes, MTS powders were freshly dissolved in water just before starting the next step (Wang et al., 2006; Ye and Maloney, 2002). The concentration of the MTS reagents were 10-fold of the final concentration. The proper volume of MTS solution was added to

prepared microsomes. The reaction concentration of MTS varied from 10 μ M to 40 mM. The further steps were carried out according to the procedure of “PEG precipitation for CQ accumulation” (see Section 3.2.4). Specifically, MTS reagents were incubated with the desired microsomes in working buffer (0.25 M Sucrose, 5 mM MgCl₂, 10 mM Tris-Cl, pH 7.4, 1.5 μ l ATP) at 37°C for 10 min. MTS reagent was freshly prepared in water and used within 1-2 min. Reaction buffer (0.25 M Sucrose, 5 mM MgCl₂, 10 mM Tris-Cl, pH 7.4, 1.5 μ l ATP, 125 nM ³H-CQ) was incubated at 37°C for 5 min. Cold CQ of 200-fold was added to stop reactions. In this procedure, for total counting, microsomes in working buffer were incubated at 37°C for 10 min. Reaction buffer was added at 37°C for 5 min. Cold CQ of 200-fold was added to stop the reactions. For non-specific counting, microsomes were mixed with 200-fold cold CQ at 37°C for 10 min. Reaction buffer was added at 37°C for 5 min.

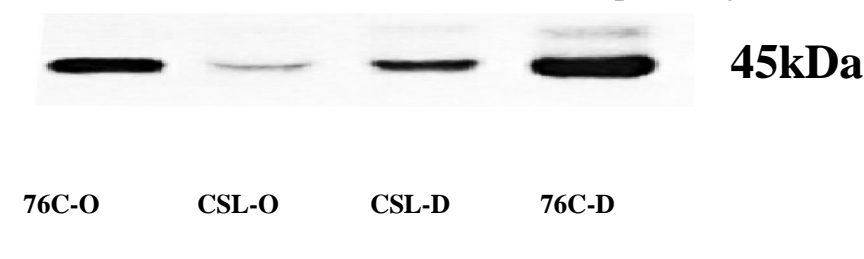
When protection by CQ was studied, the incubation with MTS reagents was carried out in the presence of desired concentrations of non-radiolabeled CQ. Specifically, non-radiolabeled CQ was incubated with microsomes in working buffer (0.25 M Sucrose, 5 mM MgCl₂, 10 mM Tris-Cl, pH 7.4, 1.5 μ l ATP) at 37°C for 10 min. PEG precipitation (see Section 3.2.4) was performed and the precipitate was washed twice with working buffer at room temperature. Then the PEG precipitates were re-suspended. Afterwards the procedure was the same as that of non-protection.

Specific CQ accumulation was calculated by subtracting the CPM counts obtained with 200-fold excess unlabeled CQ from those obtained with ³H-CQ alone. All experiments were carried out at least in triplicate. Standard errors of means were calculated where possible, and they are indicated as error bars in the figures.

3.3 Results

3.3.1 Determination of the orientation of PfCRT across microsomes

To determine the orientation of PfCRT across microsomes, a 6-histidine tag was introduced to the C-terminal of mutated PfCRT in the procedure of site-directed mutagenesis. Microsomes were incubated with anti-his antibodies in the presence of 0 or 1% DDM. At 1% concentration, DDM completely solubilized the microsomes, allowing all PfCRT proteins to bind to the anti-his antibodies (Figure 3-1, lanes 76C-O and CSL-O). In the absence of detergent, only PfCRT in microsomes with the 6-histidine tag present on the external sides could bind to the anti-his antibodies (lanes 76C-D and CSL-D). After comparison of densitometry, it was found that about half of the PfCRTs with a 6-histidine tag were present on the external surface of the microsomes. Thus, PfCRT protein adopts a partially “in” and partially “out” orientation in the microsomes.



Densitometry of 76C-O is 32% of 76C-D;
Densitometry of CSL-O is 45% of CSL-D

Figure 3-1 Western blot of orientation of PfCRT in microsomes

Orientation of PfCRT in microsomes was determined by incubation PfCRT microsomes with anti-his polyclonal antibody in the presence of 0% DDM (76C-O from yT76C and CSL-O from yCys-less), or 1% DDM (76C-D from yT76C and CSL-D from yCys-less). Amount of bound antibody was determined by western blotting using anti-PfCRT polyclonal antibody and densitometry.

3.3.2 PfCRT microsomes transport CQ in a saturable manner

The transport of CQ by PfCRT has been demonstrated by our lab (Tan et al., 2006). To further investigate the role of PfCRT in mediating CQ transport by SCAM, the transport activities of mutated PfCRT needed to be determined. Three mutagenic PfCRTs were chosen to carry out saturation assays (Table 3-1). The microsomes isolated from each *P. pastoris* were used to determine the transport activity. Figure 3-2 shows that Dd2-Cys-less PfCRT-containing microsomes could accumulate $^3\text{H-CQ}$ in a concentration-dependent manner. The $^3\text{H-CQ}$ transport activity was specific because it could be competed for by excess unlabeled CQ. The specific accumulation of $^3\text{H-CQ}$ was saturable at approximately 150 nM of $^3\text{H-CQ}$ (Figure 3-2). Non-linear regression analysis using the one-site hyperbola (Michaelis-Menten) model of $Y = (V_{\max} \cdot X)/(K_m + X)$ yields a V_{\max} of 23.82 ± 2.1 pmol/mg microsomes/min and a K_m of 97.65 nM. The same experiments were carried out for other mutated PfCRTs and the V_{\max} values for the Dd2-Cys-less-I59C mutant (11.19 ± 1.6) and Dd2-Cys-less-T76C PfCRT (18.63 ± 1.9) were

found (Table 3-1). This showed that there were significant differences in CQ accumulation activity among these mutants.

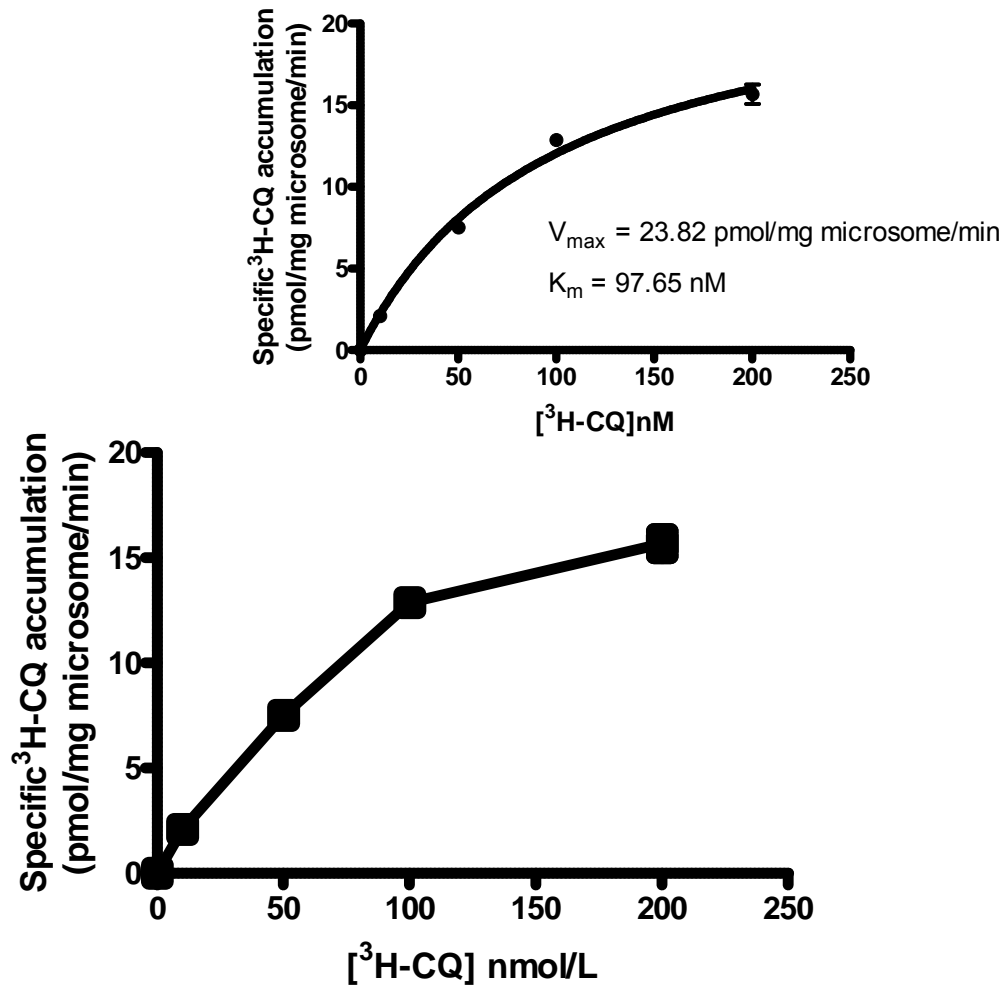


Figure 3-2 Dependence of $^3\text{H-CQ}$ uptake on $^3\text{H-CQ}$ concentration

$^3\text{H-CQ}$ uptake into Dd2-Cys-less microsomes ($50\mu\text{g}$) was measured using indicated $^3\text{H-CQ}$ concentrations. Incubation time was 1 minute. Specific $^3\text{H-CQ}$ uptake (dot) was calculated by subtracting nonspecific $^3\text{H-CQ}$ count from total $^3\text{H-CQ}$ count (lower). Non-linear regression analysis using Michaelis-Menten model $Y = (V_{\max} \cdot X) / (K_m + X)$ is shown in the inset. Data points represent means \pm S.E. ($n=3$).

Table 3-1 Summary of V_{\max} values of microsomes containing Dd2-Cys-less, Dd2-Cys-less-I59C and Dd2-Cys-less-T76C .

Mutants	V_{\max}	
	Mean	S.E.
Dd2-Cys-less	23.82	2.1
Dd2-Cys-less-I59C	11.19	1.6
Dd2-Cys-less-T76C	18.63	1.9

3.3.3 Dependence of $^3\text{H-CQ}$ uptake on microsome concentration and incubation time

To determine the working concentration of mutagenic mutant PfCRT in the reaction system, the $^3\text{H-CQ}$ accumulation activity was characterized with microsomes containing Dd2-Cys-less PfCRT. The effect of microsome concentration on CQ accumulation was studied by varying the amount of membrane protein per assay. As the amount of protein increased, the specific accumulation increased (Figure 3-3). The accumulation activity reached almost saturation when 20 μg of microsomes was used.

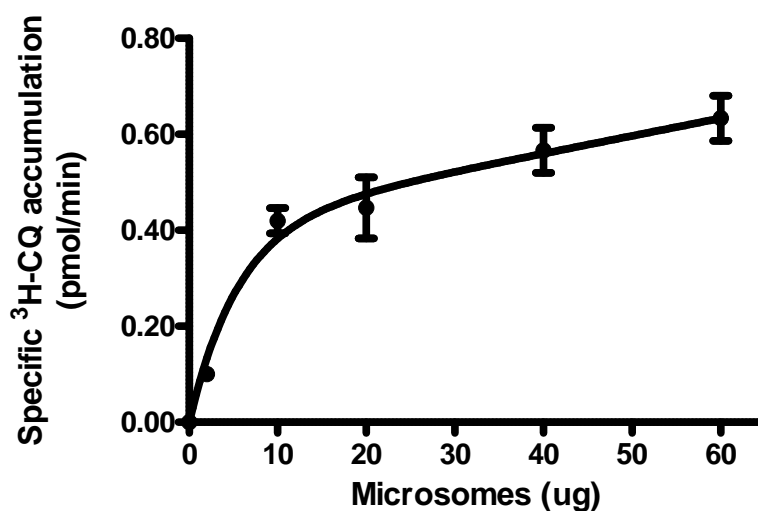


Figure 3-3 Dependence of ³H-CQ uptake on concentration of microsomes
Measurements were performed in triplicate. Samples containing 5-60 μg of microsomes containing Dd2-Cys-less PfCRT were incubated with 150 nM ³H-CQ for 1 minute. Data points represent means \pm S.E. (n=3).

To determine the time course of CQ transport of PfCRT mutants in the reaction system, the ³H-CQ accumulation activity was characterized with microsomes containing Dd2-Cys-less PfCRT. The initial accumulation within the first minute was linearly proportional to incubation time. The initial accumulation rate was estimated to be 20.20 ± 0.92 pmol CQ/mg microsomes/min. It almost reached saturation within 60 sec and the level remained the same for a period of 60 min (see inset of Figure 3-4).

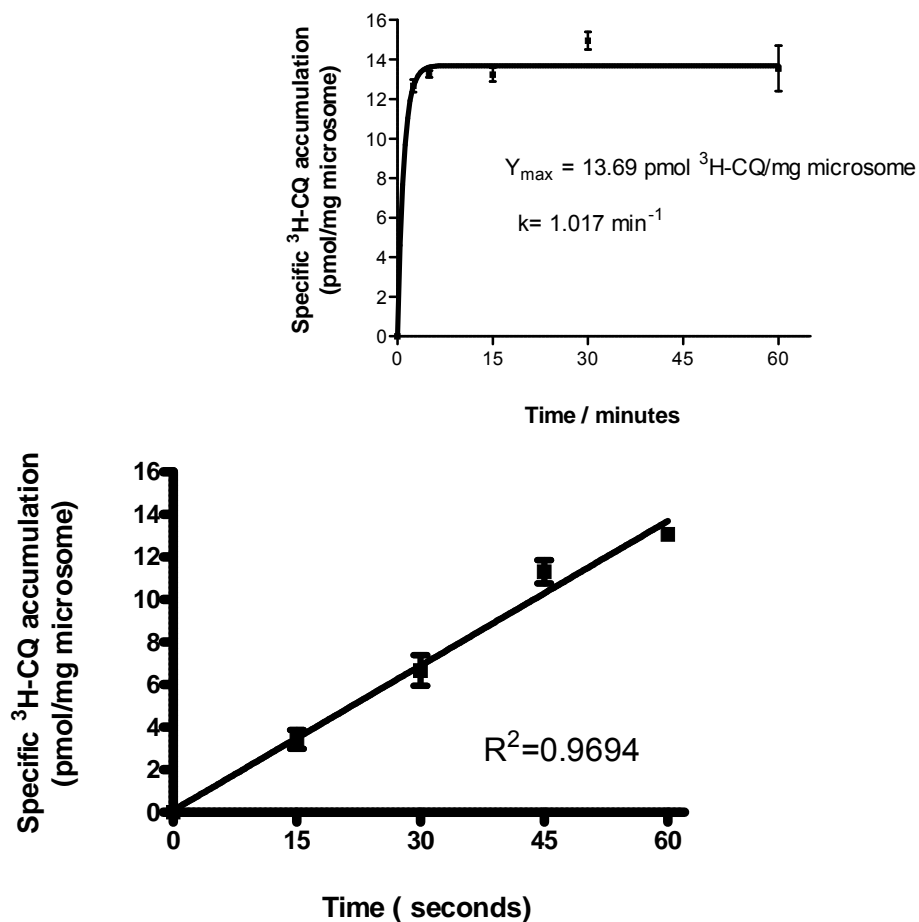


Figure 3-4 Time course of $^3\text{H-CQ}$ accumulation in microsomes of mutated PfCRT
Microsomes (50 μg) were incubated with 150 nM $^3\text{H-CQ}$. Specific $^3\text{H-CQ}$ accumulation activities were measured in triplicate for 3 independent experiments and expressed in pmol/mg microsomes. Data points represent means \pm S.E. (n=3).

3.3.4 The specific $^3\text{H-CQ}$ accumulation activity of single cysteine-substituted mutants

The specific $^3\text{H-CQ}$ accumulation activity of the Dd2-Cys-less parent and twenty-one single cysteine-containing mutants within TMD1 were analyzed (Figure 3-5). All of the mutants show different accumulation of CQ. These discrepancies of specific activity ranged from about 7 to 15 pmol/mg microsomes/min.

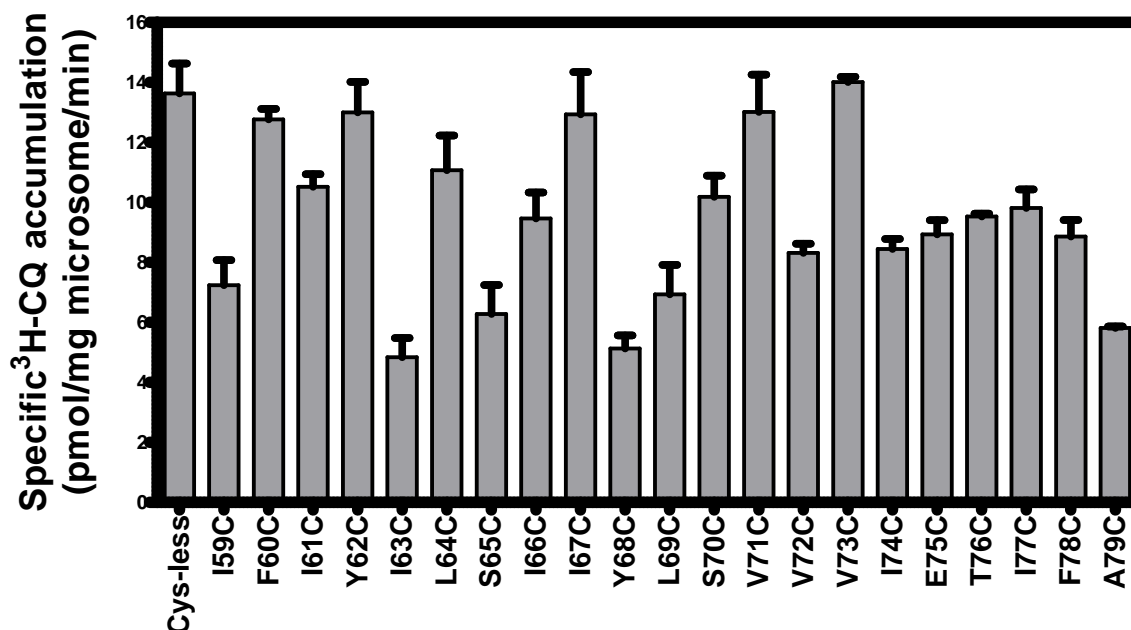


Figure 3-5 The Specific ³H-CQ accumulation of Pfert of Dd2-Cys-less parent and 21 single cysteine recovery mutants within TMD1

Microsomes (50 μ g) were incubated with 150 nM ³H-CQ. Specific ³H-CQ accumulation activities were measured in triplicate for 3 independent experiments and expressed in pmol/mg microsomes. Data points represent means \pm S.E. (n=3).

3.3.5 MTS concentration-dependence modification

To determine the optimal reaction conditions, MTS reagent concentration-dependence assays were carried out. Varied concentrations of MTSES, MTSET and MTSEA were used. The ability of CQ accumulation of microsomes containing PfCRT of Dd2-Cys-less-T76C and Dd2-Cys-less was indicated as the specific accumulation ability (pmol/mg microsomes/min). The concentrations of MTSES, MTSET and MTSEA ranged from 0-12 mM, 0-3 mM and 0-1.2 mM respectively. After modification by MTSES, MTSET and MTSEA the specific ³H-CQ accumulation of each PfCRT was saturable at approximately at 8 mM, 1.5 mM and 0.6 mM respectively (Figure 3-6, Figure 3-7 and Figure 3-8). Modified by MTSES, the ability of CQ accumulation of Dd2-Cys-less-T76C PfCRT-

containing microsomes increased as the concentration of MTSES increased. Meanwhile, MTSET and MTSEA led to a decrease of specific CQ accumulation as the concentration of these two MTS reagents increased. This suggests that high concentration MTSES can enhance the ability of CQ accumulation of Dd2-Cys-less-T76C PfCRT, and MTSET and MTSEA have adverse effects. In the meantime, Dd2-Cys-less PfCRT did not show a significant decrease or increase of specific CQ accumulation as the concentration of these three MTS reagents increased.

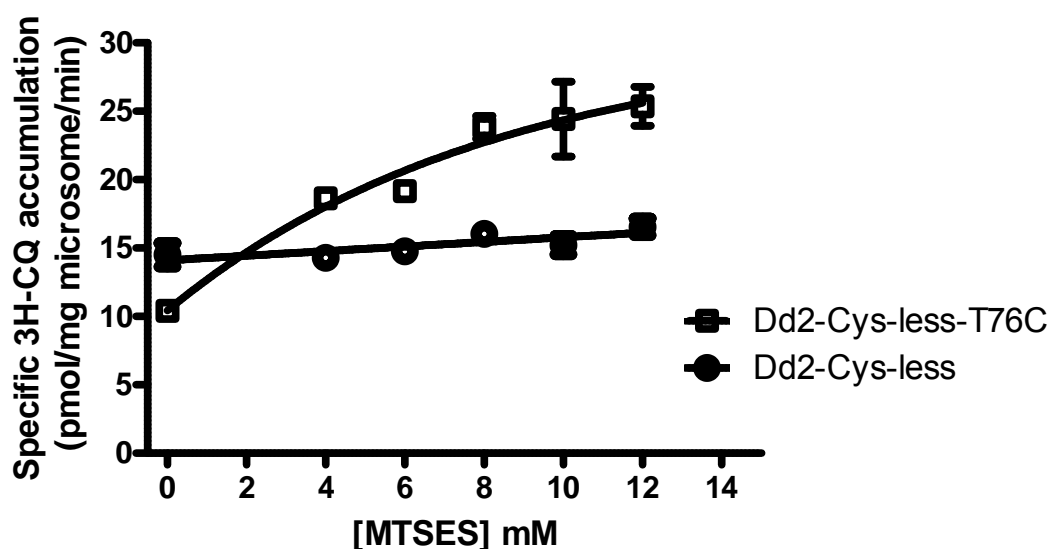


Figure 3-6 MTSES concentration dependence of the ability of CQ accumulation of microsomes containing mutagenic PfCRT

Microsomes (50 μ g) were incubated with 150 nM 3 H-CQ. Specific 3 H-CQ accumulation activities were measured in triplicate for 3 independent experiments and expressed in pmol/mg microsomes. The ability of CQ accumulation of microsomes containing mutagenic PfCRT (Dd2-Cys-less-T76C and Dd2-Cys-less) is indicated as the specific accumulation ability (pmol/mg microsomes/min). MTSES concentration ranges from 0-12 nM. Data points represent means \pm S.E. (n=3).

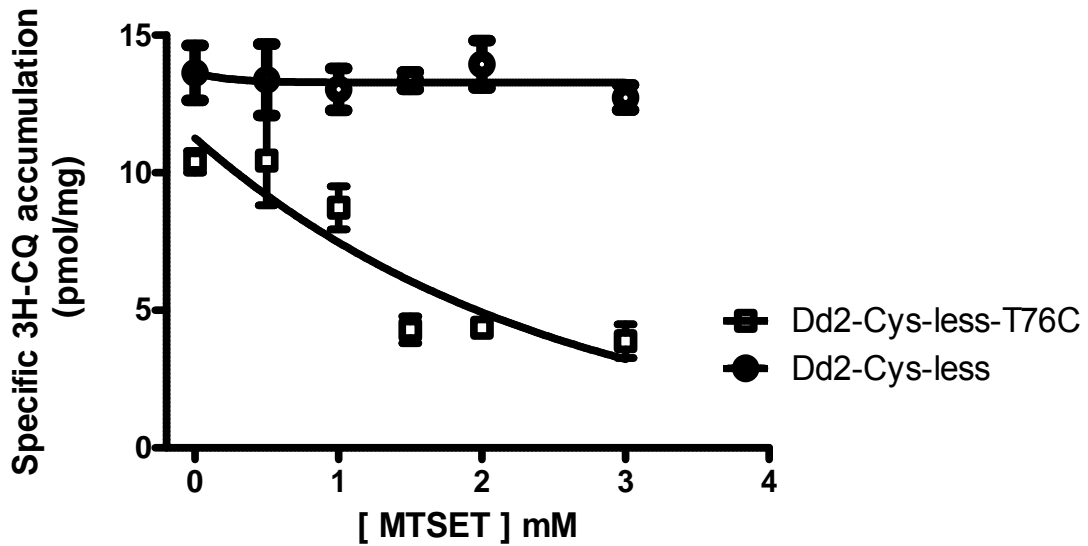


Figure 3-7 MTSET concentration dependence of the ability of CQ accumulation of microsomes containing mutagenic PfCRT

Microsomes (50 μ g) were incubated with 150 nM ^3H -CQ. Specific ^3H -CQ accumulation activities were measured in triplicate for 3 independent experiments and expressed in pmol/mg microsomes. The ability of CQ accumulation of microsomes containing mutagenic PfCRT (Dd2-Cys-less-T76C and Dd2-Cys-less) is indicated as the specific accumulation ability (pmol/mg microsomes/ min). MTSET concentration ranges from 0-3 nM. Data points represent means \pm S.E. (n=3).

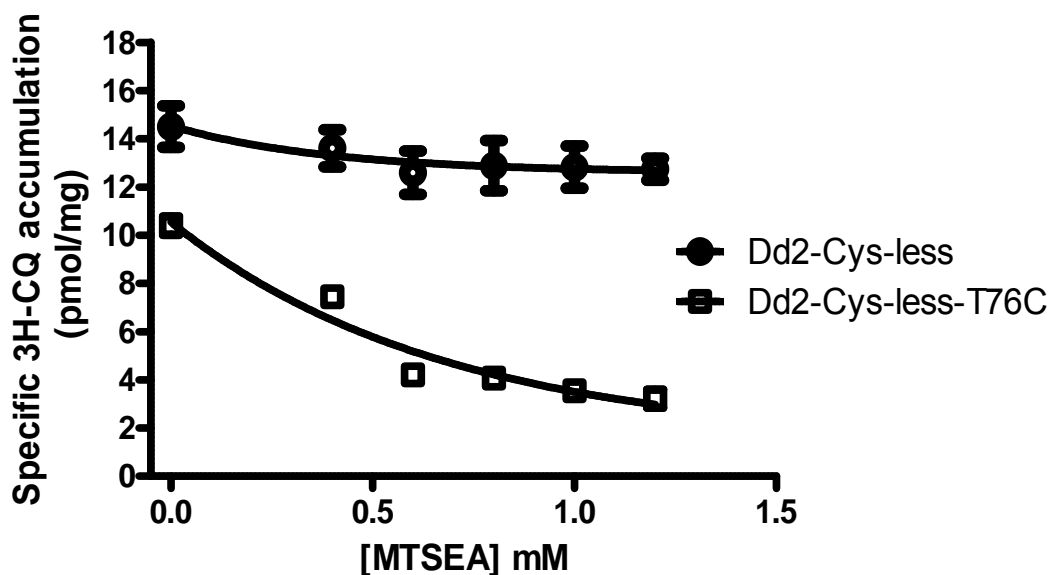


Figure 3-8 MTSEA concentration dependence of the ability of CQ accumulation of microsomes containing mutagenic PfCRT
 Microsomes (50 μ g) were incubated with 150 nM 3 H-CQ. Specific 3 H-CQ accumulation activities were measured in triplicate for 3 independent experiments and expressed in pmol/mg microsomes. The ability of CQ accumulation of microsomes containing mutagenic PfCRT (Dd2-Cys-less-T76C and Dd2-Cys-less) is indicated as the specific accumulation ability (pmol/mg microsomes/ min). MTSEA concentration ranges from 0-1.2 mM. Data points represent means \pm S.E. (n=3).

3.3.6 The sensitivity of single cysteine-substituted mutants to MTSES

To scan TMD1 residues, single cysteine-substitution mutants located between 59 and 79 were studied. Their ability to accumulate CQ after exposure to MTS reagents are show in Figure 3-9, Figure 3-10 and Figure 3-11.

MTSES is a negatively charged reagent that reacts very rapidly and specifically with cysteine groups. When MTSES is incubated with microsomes, the modification should be thoroughly complete (Refer to Section 3.2.4). The relative activity of single cysteine-substituted mutants is represented as percent of specific CQ accumulation of untreated MTSES (no MTSES modification) (Figure 3-9).

Among these mutants, Dd2-Cys-less-T76C displayed a higher relative activity (SD >125% of the mean) and Dd2-Cys-less-I67C, Dd2-Cys-less-V71C and Dd2-Cys-less-V73C displayed a lower relative activity (SD <25% of the mean). Dd2-Cys-less displayed approximately the same activity as untreated with MTSES.

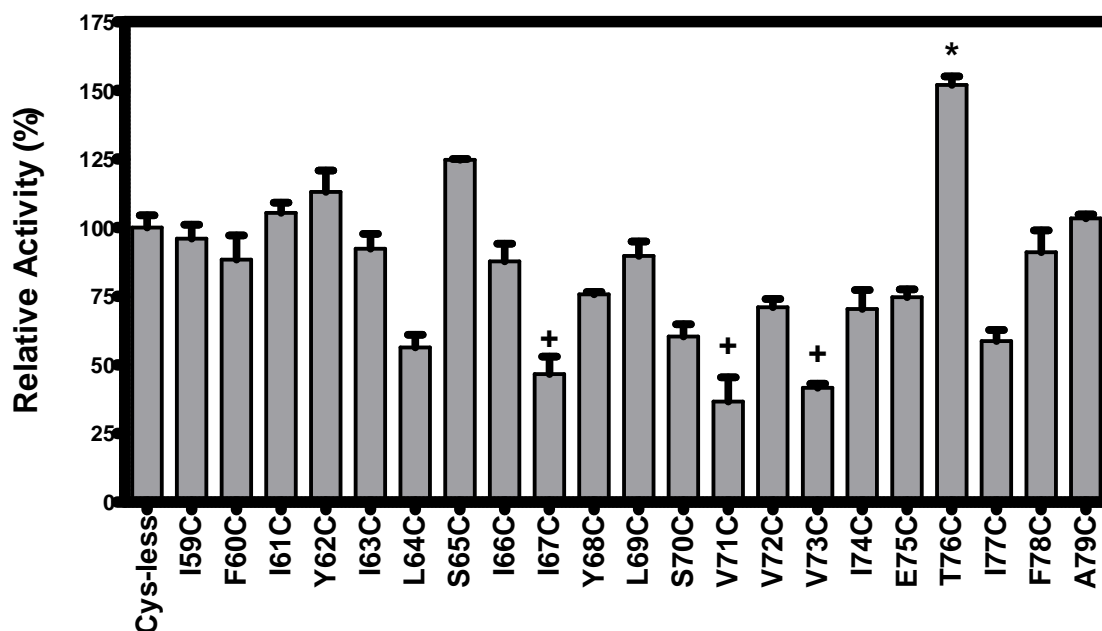


Figure 3-9 Sensitivity of single cysteine substitution mutants to MTSES

Incubate MTSES (10mM) solution with prepared microsomes (50 μ g) for 10 min. The relative activity of single cysteine-substitution mutants is expressed as percent of specific CQ accumulation ability of untreated MTSES (no MTSES reagent). + indicates the related activity SD <25% of the mean; * indicates the related activity SD >125% of the mean. Data are means \pm S.E. (n=3).

3.3.7 The sensitivity of single cysteine substitution mutants to MTSET

MTSET is a positively-charged reagent that reacts very rapidly and specifically with cysteine groups as MTSES. Among these mutants, Dd2-Cys-less-I67C and Dd2-Cys-

less- V73C and Dd2-Cys-less- I76C displayed a lower relative activity (SD <50% of the mean) and Dd2-Cys-less displayed approximately the same activity as untreated with MTSET.

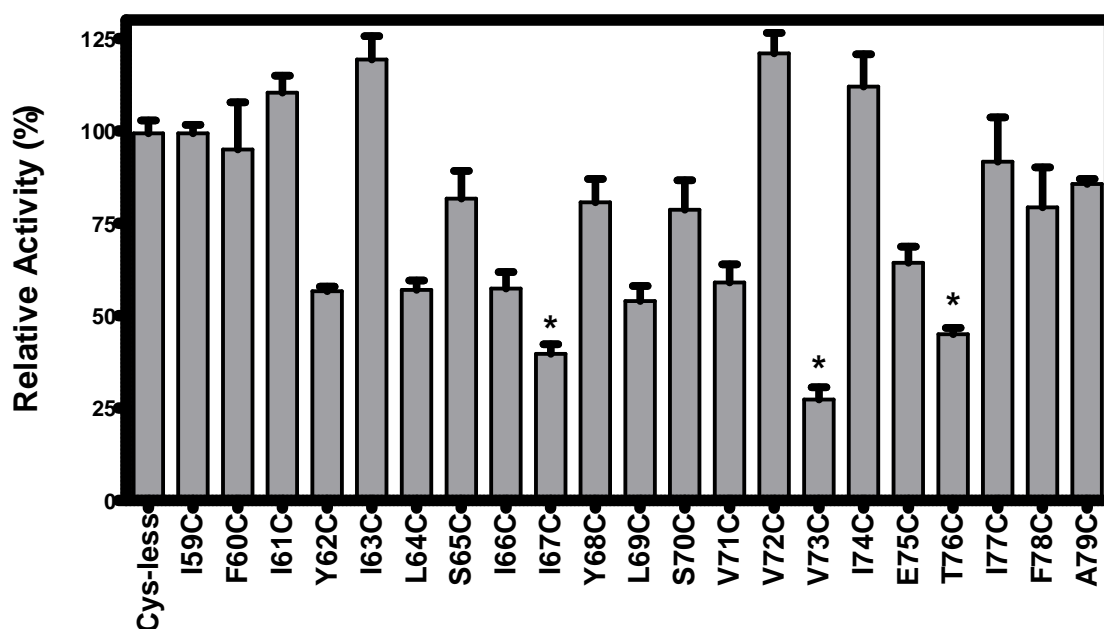


Figure 3-10 Sensitivity of single cysteine substitution mutants to MTSET
Incubate MTSET (2mM) solution in prepared microsomes (50 μ g) for 10 min. The relative activity of single cysteine-substitution mutants is expressed as percent of specific CQ accumulation ability of untreated MTSET (no MTSET reagent). + indicates the related activity SD <50% of the mean. Data are means \pm S.E. (n=3).

3.3.8 The sensitivity of single cysteine substitution mutants to MTSEA

MTSEA is a positively-charged reagent that reacts very rapidly and specifically with cysteine groups as MTSES and MTSET. Among these mutants, Dd2-Cys-less- Y62C and Dd2-Cys-less- V73C and Dd2-Cys-less- I76C displayed a lower relative activity (SD

<25% of the mean). Dd2-Cys-less displayed approximately the same activity as untreated with MTSET.

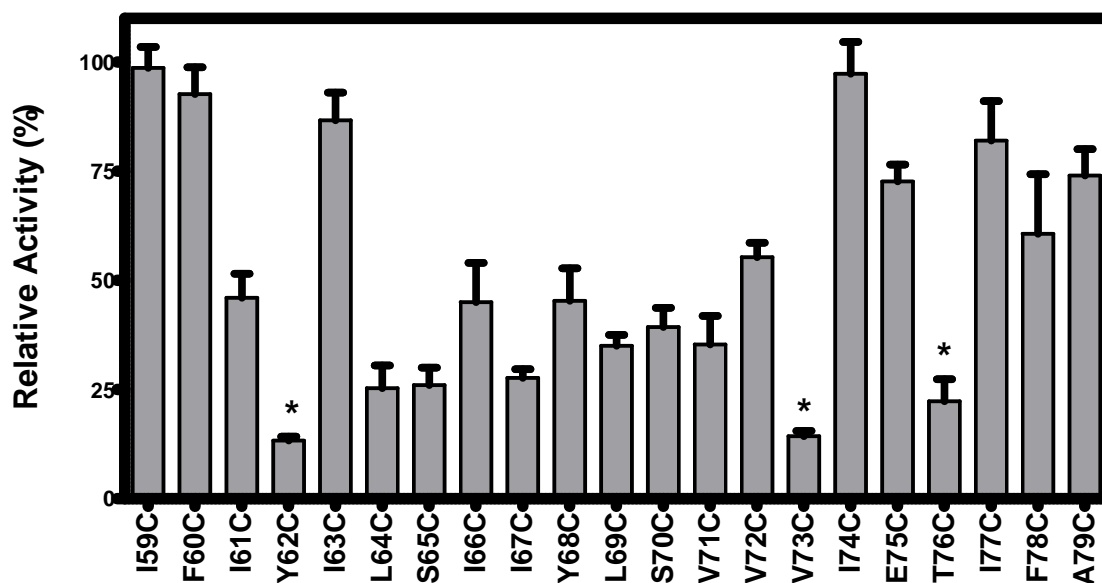


Figure 3-11 Sensitivity of single cysteine substitution mutants to MTSEA

Incubate MTSEA (0.5mM) solution in prepared microsomes (50 μ g) for 10 min. The relative activity of single cysteine-substitution mutants is expressed as percent of specific CQ accumulation ability of untreated MTSEA (no MTSEA reagent). * indicates the related activity SD <25% of the mean. Data are means \pm S.E. (n=3).

3.3.9 CQ protection of MTSES modification

The permeation pathway may be defined as the collection of residues exposed to the hydrophilic environment in the inward- and outward-facing conformations of the transporter (Yan and Maloney, 1993), and cysteine-scanning mutagenesis has been used to develop two operational tools useful in characterizing such positions (Fu et al., 2001; Yan and Maloney, 1993). Cysteine substitutions in such residues may provide informative targets for hydrophilic, thiol-directed probes able to enter the pathway and

this can occur, in principle, for probes entering from either end of the pathway (Fu et al., 2001; Yan and Maloney, 1993). It can be anticipated that if substrate is present, probe modification may be affected.

To study substrate (CQ) protection of MTSES modification, incubation of microsomes with MTSES reagents was carried out in the presence of non-radiolabeled CQ (Refer to Section 3.2.5). In this experiment, Dd2-Cys-less-T76C, which displayed a higher relative activity (SD >125% of the mean) and Dd2-Cys-less-I67C, Dd2-Cys-less-V71C and Dd2-Cys-less-V73C, which displayed a lower relative activity (SD <25% of the mean), were chosen for further studies (see section 3.3.6 and Figure 3-9).

Non-radiolabeled CQ (0-250 nM) was incubated with microsomes in working buffer (0.25 M Sucrose, 5 mM MgCl₂, 10 mM Tris-Cl, pH 7.4, 1.5 µl ATP) at 37°C for 10 min. PEG precipitation was performed (see Section 3.2.4) and the precipitate washed twice with working buffer at room temperature. The PEG precipitate was re-suspended. Afterwards, the procedure was the same as that of non-protection.

To determine the protective concentration of non-radiolabeled CQ, microsomes of Dd2-Cys-less were chosen to carry out protection assays in the absence of MTSES. The results showed that 1 nM non-radiolabeled CQ pre-incubation had no effect on ³H-CQ accumulation activity. This concentration of non-radiolabeled CQ then was chosen to perform further CQ protection assays (Figure 3-12). The relative activity of single cysteine-substitution mutants is expressed as percent of specific CQ accumulation ability of untreated MTSES (no MTSES modification). Figure 3-13 shows that CQ pre-incubation weakened the effect of MTSES on Dd2-Cys-less-T76C CQ accumulation

ability. Meanwhile, Dd2-Cys-less-I67C, Dd2-Cys-less-V71C and Dd2-Cys-less-V73C were not affected. This suggests that CQ prevents PfCRT from a modification of MTSES.

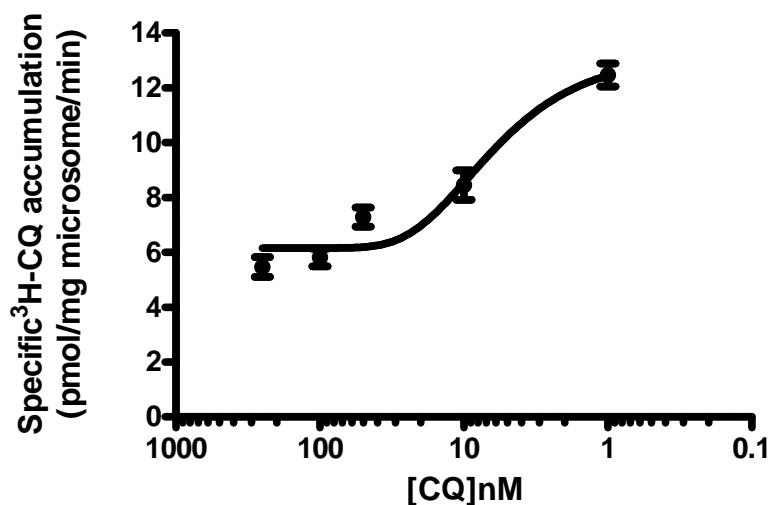


Figure 3-12 Specific ³H-CQ accumulation by microsomes of Dd2-Cys-less with pre-incubation of non-radiolabeled CQ

Incubate non-radiolabeled CQ (0-250 nM) with microsomes (50 μ g) of Dd2-Cys-less in working buffer at 37 °C for 10 min. Perform PEG precipitation and wash the precipitates two times with working buffer at room temperature. Re-suspend the PEG precipitates. Afterwards procedure is the same as that of non-protection. Data points represent means \pm S.E. (n=3).

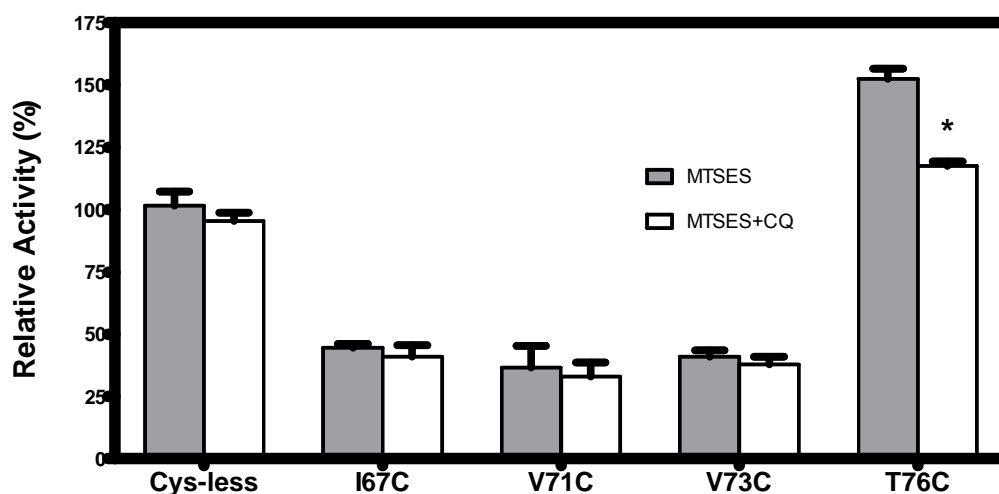


Figure 3-13 CQ protection to MTSES modification

Microsomes (50 μ g) of Dd2-Cys-less-T76C, Dd2-Cys-less-I67C, Dd2-Cys-less-V71C and Dd2-Cys-less-V73C incubate with non-radiolabeled CQ (1nM) at 37°C for 10 min. Re-suspend the PEG precipitates and incubate with MTSES (10mM). Afterwards procedure is the same as that of non-protection (see Section 3.2.4).

*, significant difference (P<0.05) compared to non-protection (in absence of non-radiolabeled CQ). Data are means \pm S.E. (n=3).

3.3.10 CQ protection of MTSET modification

The assay of CQ protection of MTSET modification was carried out in the presence of non-radiolabeled CQ. In this experiment, Dd2-Cys-less-I67C and Dd2-Cys-less-V73C and Dd2-Cys-less-I76C, which displayed a lower relative activity (SD <25% of the mean), were chosen for further studies (see section 3.3.6 and Figure 3-10).

The method was the same as described in Section 3.3.9. Figure 3-14 shows that CQ pre-incubation weakened the effect of MTSET on Dd2-Cys-less-T76C CQ accumulation ability. Meanwhile, Dd2-Cys-less-I67C and Dd2-Cys-less-V73C were not affected. This suggests that CQ prevents PfCRT from modification by MTSET.

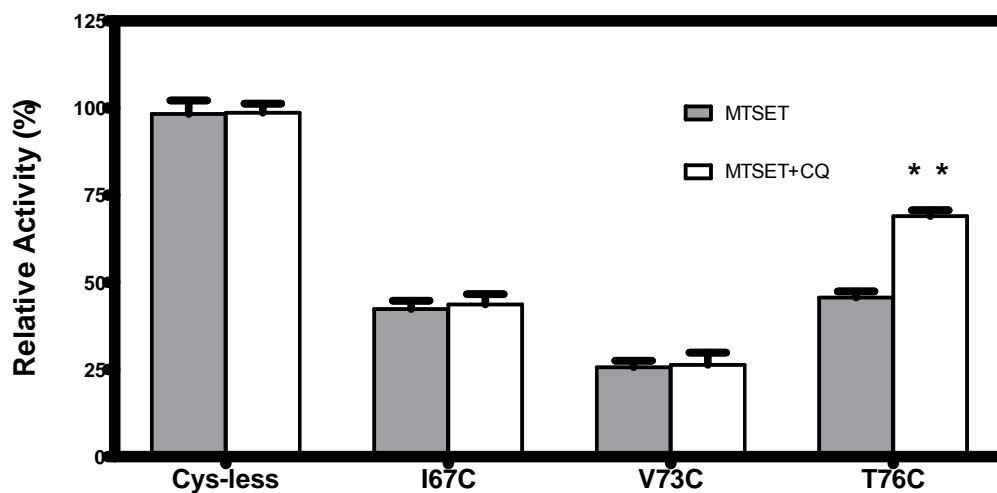


Figure 3-14 CQ protection to MTSET modification

Microsomes (50 μ g) of Dd2-Cys-less-I67C and Dd2-Cys-less-V73C and Dd2-Cys-less-I76C incubate with non-radiolabeled CQ (1nM) at 37 °C for 10 min. Re-suspend the PEG precipitates and incubate with MTSET (2mM). Afterwards procedure is the same as that of non-protection (see Section 3.2.4). **, significant difference ($P < 0.001$) compared to non-protection (in absence of non-radiolabeled CQ). Data are means \pm S.E. (n=3).

3.3.11 CQ protection of MTSEA modification

The assay of CQ protection of MTSET modification was carried out in the presence of non-radiolabeled CQ. In this experiment, Dd2-Cys-less-Y62C and Dd2-Cys-less-I76C, which displayed a lower relative activity (SD <25% of the mean), were chosen for further studies (see section 3.3.6 and Figure 3-10).

The method was the same as described in Section 3.3.9. Figure 3-15 shows that CQ pre-incubation weakened the effect of MTSES on Dd2-Cys-less-T76C CQ accumulation ability. Meanwhile, Dd2-Cys-less-Y62C was not affected. This suggests that CQ prevents PfCRT from modification by MTSEA.

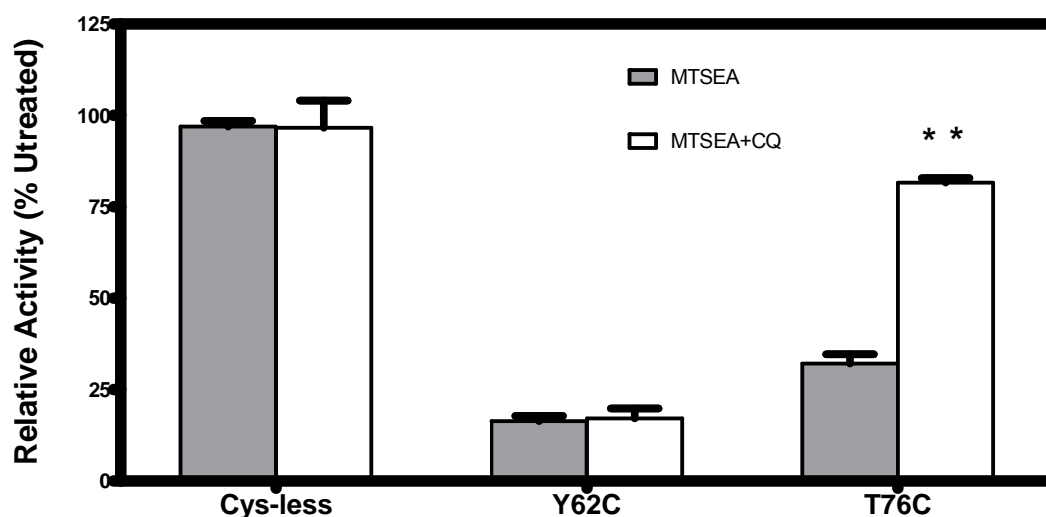


Figure 3-15 CQ protection to MTSEA modification

Microsomes (50 μ g) of Dd2-Cys-less-Y62C and Dd2-Cys-less-I76C incubate with non-radiolabeled CQ (1nM) at 37°C for 10 min. Re-suspend the PEG precipitates and incubate with MTSEA (0.5mM). Afterwards procedure is the same as that of non-protection (see Section 3.2.4).

** , significant difference ($P < 0.001$) compared to non-protection (in absence of non-radiolabeled CQ). Data are means \pm S.E. (n=3).

3.4 Discussion

It is suggested that PfCRT is directly or indirectly involved in a transporter-mediated CQ efflux system in CQR parasites (Sanchez et al., 2004; Sanchez et al., 2003). PfCRT has been predicted to have ten transmembrane domains and is localized to the DV membrane (Fidock et al., 2000b). Bioinformatics analyses suggest that PfCRT belongs to a drug/metabolite transporter superfamily (Martin and Kirk, 2004; Tran and Saier, 2004). It is predicated that the N- and C-termini of PfCRT are located on the cytoplasmic side of the DV membrane in the parasite (Martin and Kirk, 2004). PfCRT was also predicted to be a dimer within the DV membrane, with TMDs 1, 2, 3, 6, 7 and 8, functioning mainly in substrate discrimination and recognition; TMDs 4 and 9 in substrate binding and translocation; and TMDs 5 and 10 in the formation and/or stabilization of the homodimeric structure (Martin and Kirk, 2004; Tran and Saier, 2004). Within the ten putative TMDs, positively-charged residues (Lysine or Arginine) were predicted to lie in the extra-membrane segments or in the termini regions.

Substitution of Threonine (T) for Lysine (K) at position 76 (K76T) is the most pivotal change in CQR parasites (Djimde et al., 2001a; Fidock et al., 2000b). Using SCAM, it is possible to find the detailed functional and structural information about TMD1, within which 76 is localized. Twenty-one cysteine-substituted PfCRTs within TMD1 were constituted and the PfCRT of Cys-less and recoveries within TMD1 were all expressed.

The orientation of PfCRT in different microsomes was almost the same (50% ISOV). Thus comparing the transport activity of CQ in different microsomes can be interpreted only by PfCRT action, not by its orientation.

The microsomes isolated from each *P. pastoris* were used to determine the transport activities. Dd2-Cys-less PfCRT could accumulate $^3\text{H-CQ}$ in a concentration-dependent manner. The $^3\text{H-CQ}$ transport activity was specific because it could be competed for by excess un-radiolabeled CQ (Figure 3-2, Figure 3-3 and Figure 3-4). We found that there were significantly different CQ accumulation activities among these mutants (Figure 3-5). This suggests that CQ might interact with the internal (intra-DV) lumen of PfCRT, supporting the hypothesis that CQR parasites result from the presence of PfCRT-mediated CQ transport out of the DV. Differently reconstituted PfCRTs may contribute to the variation of CQ accumulation. This suggests that cysteine substitution for obligate amino acids affects function via the amino acid composition of the TMD1 helix.

SCAM and charged MTS reagents, MTSES, MTSET and MTSEA have been successfully applied to the structural and functional elucidation of channels and transporters (Akabas and Karlin, 1995; Akabas et al., 1994; Akabas et al., 1992). Because these reagents introduce a positive or negative charge at the position of a previously neutral cysteine residue, they frequently cause a functional change in channel or transporter protein that then can be measured (Akabas et al., 1992).

Modified by MTSES, Dd2-Cys-less-T76C PfCRT microsomes accumulated more CQ when the concentration of MTSES increased (Figure 3-6). Meanwhile, MTSET and MTSEA led to a decrease of specific CQ accumulation as the concentration of these two MTS reagents increased (Figure 3-7 and Figure 3-8). This suggests that high

concentrations of MTSES can improve the ability of CQ accumulation of Dd2-Cys-less-T76C PfCRT and MTSET and MTSEA have adverse effects. In the meantime, Dd2-Cys-less PfCRT did not show a significant decrease or increase of specific CQ accumulation as the concentration of these three MTS reagents increased. This suggests that a charged 76th amino acid affects CQ accumulation (Pochini et al., 2004; Ye et al., 2008). According to the reduced positivity model (Warhurst, 2001) (Figure 3-16), position 76 positively-charged CQ-susceptibles repel CQ from the PfCRT pathway. Neutralized 76 (76T) CQR allows CQ to enter the PfCRT channel and expel CQ.

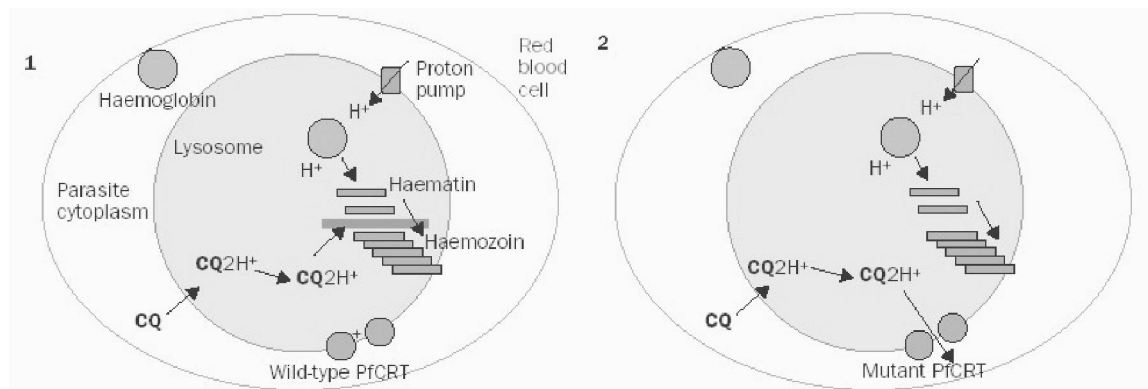


Figure 3-16 Role of PfCRT in chloroquine resistance in *P. falciparum*

Intraerythrocytic malaria parasites digest hemoglobin in their lysosomes. Chloroquine (CQ) diffuses in as base and is trapped by protonation (CQ2H⁺) due to the acidic environment of lysosome. Drug cannot escape through positively charged pore (PfCRT) leading to cytoplasm. CQ binds hematin in lysosome and prevents detoxification to hemozoin, leading to death of parasite. Mutated PfCRT of chloroquine-resistant parasite loses positively charged group, which allows CQ to enter cytoplasm, and hematin detoxification continues unaffected. (Warhurst et al., 2002)

Our study accords experimentally with this hypothesis. The results can be interpreted as 76 negatively charged by MTSES facilitates CQ binding to PfCRT, thus increasing the CQ accumulation in microsomes. When modified by MTSET and MTSEA, positively charged 76 impedes the CQ binding and so CQ accumulation.

Chapter 3 Cys-Scanning of TMD1

In scanning experiments on the sensitivity of single cysteine substitution mutants to MTSES reagent (Figure 3-9, Figure 3-10 and Figure 3-11), 62, 71 and 73 displayed a lower relative activity (SD <25% of the mean). These three amino acids somewhat face the same lumen of the helix (Figure 3-17). Thus they may have higher accessibility to be modified and impede CQ transport. Position 67, which is opposite to 76 within the helix, demonstrated higher accessibility to MTS. This may be due to a special pathway for MTS to get access to it (Akabas et al., 1992; Altenbach et al., 1990; Frillingos and Kaback, 1997). This hypothesis needs more evidence to be verified. We noted that only negatively charged 76 demonstrated a higher CQ accumulation, so a different interpretation is needed for the 76th amino acid residue.

Substrate (CQ) protection of MTS reagent modification was carried out in the presence of non-radiolabeled CQ. In these assay, only 76 showed protection effects. This result strongly suggests that 76 is a binding site of CQ in PfCRT, More kinetic tests are needed to verify this hypothesis.

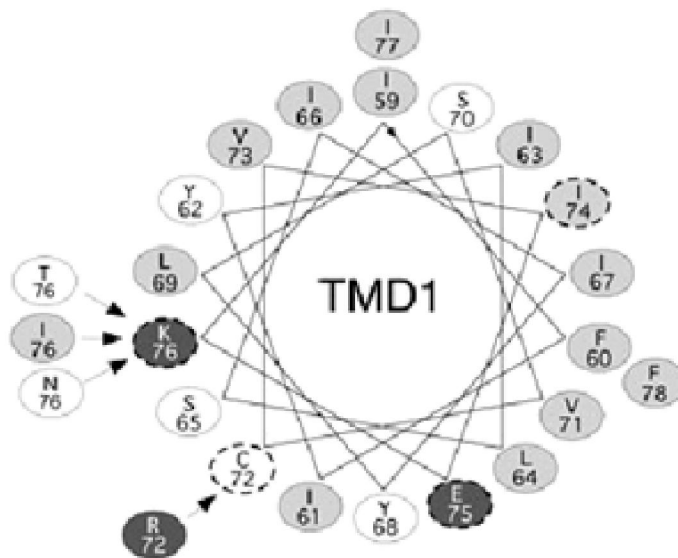
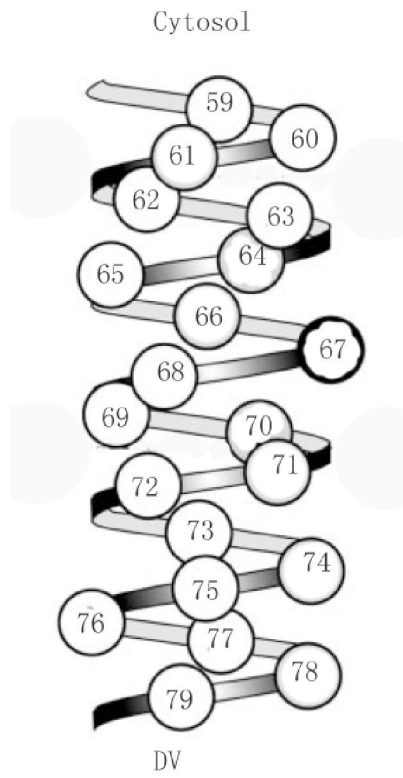


Figure 3-17 Integrated view of TMD1 of PfCRT

Chapter 4

Reconstitution of Proteoliposomes and cysteine Scanning of Transmembrane Domain 1 of PfCRT

Abstract

Reconstituted proteoliposomes were used in this project to study the PfCRT. Dd2-Cys-less-Y62C, Dd2-Cys-less-I67C, Dd2-Cys-less-V71C, Dd2-Cys-less-V73C and Dd2-Cys-less-T76C were chosen. All of them were purified with Ni²⁺-NTA agarose gel.

Dd2-Cys-less reconstituted proteoliposomes could accumulate ³H-CQ in a concentration-dependent manner. The ³H-CQ transport activity was specific. This suggests that Dd2-Cys-less reconstituted proteoliposomes have significant specific CQ accumulation activity. MTSES and MTSET were chosen for proteoliposomes studies. After modification by MTSES, Dd2-Cys-less-T76C demonstrated a higher relative activity and Dd2-Cys-less-I67C and Dd2-Cys-less-V73C displayed a lower relative activity. After modification by MTSET, only Cys-less-I67C and Dd2-Cys-less-V73C displayed a lower relative activity. These results suggest that 76, 73 and 67 are accessible to MTS.

In the CQ protection assay, CQ prevented 76 from modification of MTSES and the 76th amino acid of PfCRT may be involved in the site where MTSET modification takes place.

4.1 Introduction

4.1.1 Reasons for reconstitution of proteoliposomes

The cell plasmalemma is a biological membrane. It contains a wide variety of biological molecules, primarily proteins and lipids, which are involved in a variety of cellular processes. Although there are some advantages, including the fact that the transport protein is in its natural state, and intact cells have a complete system to support transport, there are disadvantages of the uptake assay in intact cells or membrane vesicles. Membrane proteins have relatively low expression levels in native tissue so that they are not accessible for detailed structural and biochemical analysis (Bathori et al., 1993; Palmieri et al., 1993). Although heterologous expression systems have been used to overcome this shortfall, live cells have a metabolic mechanism to modify or degrade substrates and this will affect the subsequent measurement. As well as target transport proteins, membrane vesicles still contain other irrelevant membrane proteins, such as pores or enzymes that might affect transport assays. Therefore, while membrane proteins are studied in either whole cells or membrane vesicles, other proteins and cellular components or processes may complicate the data interpretation. One approach to resolve this complexity is to purify an individual membrane protein and study its properties individually (Bevans et al., 1998; Dean et al., 1999; Jaburek and Garlid, 2003; Martin et al., 2004; Sentjurc et al., 1999; Wadia and Dowdy, 2002).

Reconstitution of membrane-bound enzymes and transport proteins with an artificial phospholipid bilayer (liposome) is one of the most useful techniques to study the

Chapter 4 Proteoliposomes and Cys-scanning TMD1

functional aspects of these proteins. Purified transporters can be reconstituted into liposomes by dilution of a ternary mixture containing proteins, lipids, and detergents. Or researchers can use BioBeads (Bio-Rad, Hercules, USA) to absorb and remove detergents (Racker, 1979; Silvius, 1992). Once the free detergent concentration in the mixture is lower than the critical micellar concentration, detergent is recruited from the bound detergent pool, and the association of proteins and lipids is initiated. The reconstituted proteoliposomes contain a single type of transporter facing both sides of the lipid membrane and can be assayed for transport activity. There are many successful examples of membrane proteins that have been purified and reconstituted into proteoliposomes for functional characterization (Grinius et al., 2002; Grinius and Goldberg, 1994; Margolles et al., 1999; Putman et al., 1999; Shapiro et al., 1997; Yerushalmi et al., 1995; Zgurskaya and Nikaido, 1999).

4.1.2 Characteristics of liposomes

Liposomes are small, spherical vesicles which consist of amphiphilic lipids, enclosing an aqueous core. The lipids are predominantly phospholipids which form bilayers similar to those found in biomembranes. They are composed of cholesterol and phospholipids, for example, phosphatidylcholine, phosphatidylethanolamine and phosphatidylserine. These phospholipids possess a hydrophobic tail structure and a hydrophilic head component. Depending on the processing conditions and the chemical composition, liposomes are formed with one or several concentric bilayers. Liposomes are often distinguished according to their number of lamellae and size. Small unilamellar vesicles (SUV), large unilamellar vesicles (LUV) and large multilamellar vesicles (MLV) or multivesicular vesicles (MVV) are differentiated (Figure 4-1). SUVs show a diameter of 20 to

Chapter 4 Proteoliposomes and Cys-scanning TMD1

approximately 100 nm. LUVs, MLVs, and MVVs range in size from a few hundred nanometers to several microns. The thickness of the membrane (phospholipid bilayer) measures approximately 5 to 6 nm.

SUVs are produced by disruption of MLV suspensions using sonic energy (sonication). MLV suspensions are disrupted either by several freeze-thaw cycles or by extrusion through a large pore size (typically 400 nm) to yield LUVs with a mean diameter of 100 nm to 400 nm. LUVs contain only a double layer membrane, suitable for entrapment of aqueous materials. Therefore, LUVs are probably the best system for studying membrane protein function.

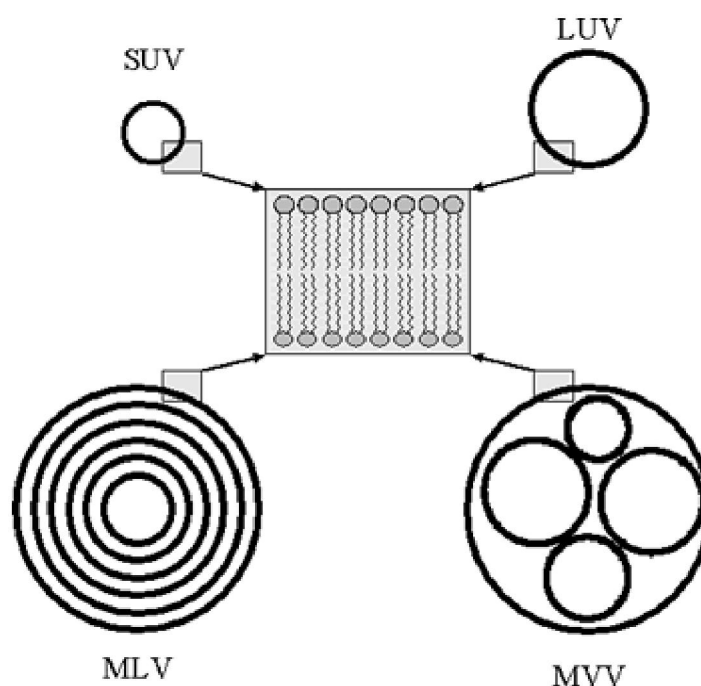


Figure 4-1 Schematic illustration of liposomes of different size and number of lamellae
SUV: Small unilamellar vesicles; LUV: Large unilamellar vesicles; MLV: Multilamellar vesicles;
MVV: Multivesicular vesicles.

Chapter 4 Proteoliposomes and Cys-scanning TMD1

Our lab has established a proteoliposomes constitution system used for transporter studies (Tan et al., 2006). To reconstitute proteoliposomes, *E. coli* total lipids and egg phosphatidylcholine (EPC) were employed to reconstitute purified PfCRT and the proteoliposomes derived were used to study the functions of PfCRT. This system can help to differentiate between direct effects mediated by PfCRT itself or through other molecular partners. The *E. coli* total lipids contain phosphatidylethanolamine, phosphatidylglycerol, cardiolipin, phosphatidylserine, and some other lipids. Egg PC (EPC, Egg phosphatidylcholine) together with *E. coli* total lipids was successfully used for reconstitution. The successful formation of proteoliposomes was demonstrated by direct visualization of the proteoliposomes using light microscopy. The majority of proteoliposomes were LUVs. All three proteoliposomes contained mainly unilamellar vesicles with a small population of oligolamellar liposomal structures. The highest specific CQ transport activity was detected at a lipid-to-protein ratio of 150. The reconstitution efficiency was approximately 30% and approximately 50% of the reconstituted PfCRT faced inward. Therefore, 15% of the protein in the proteoliposomes consists of PfCRT in a transport-competent orientation (Tan et al., 2006).

4.1.3 Application of proteoliposome reconstitution in basic research

The reconstituted proteoliposomes contain a single type of transporter facing both sides of the lipid membrane and can be assayed for transport activity. Transport activity can be measured more convincingly and conclusively in a reconstituted system than in microsomes. Reconstitution studies may display the minimal requirements for the function of a membrane protein.

Chapter 4 Proteoliposomes and Cys-scanning TMD1

For example, Xie et al purified and reconstituted nucleoside transporter NupG into liposomes and observed nucleoside transport in proteoliposomes (Xie et al., 2004). Juge co-reconstituted vesicular glutamate transporter VGLUT1 and bacterial F-ATPase into liposomes and found that ATP induced L-glutamate uptake in proteoliposomes (Juge et al., 2006). Bowsher reconstituted amyloplast envelope membrane proteins from spring wheat and assayed ADP, AMP, and ADP-glucose transport in these proteoliposomes (Bowsher et al., 2007). Eytan et al reconstituted P-glycoprotein from cultured multidrug-resistant Chinese hamster ovary cells and observed ATP-driven, valinomycin-dependent uptake of rubidium in these proteoliposomes (Eytan et al., 1996a; Eytan et al., 1996b).

In this study, using the established reconstitution system, PfCRT proteins were purified and reconstituted in liposomes. SCAM assays were carried out to verify the results from microsomes.

4.2 Materials and Methods

4.2.1 Materials

All lipids were purchased from Avanti Polar Lipids Inc. (2-(Trimethylammonium)ethyl) methanethiosulfonate bromide (MTSET), (2-aminoethyl) methanethiosulfonate hydrobromide (MTSEA) and sodium (2-sulfonatoethyl) methanethiosulfonate (MTSES), were purchased from Toronto Research Chemicals (North York, Ontario, Canada). All other chemicals were from Sigma chemicals and were of analytical grade.

4.2.2 Preparation of liposomes

Liposomes were prepared according to the method of Tan (Tan et al., 2006). The *E. coli* total lipid extracts and egg yolk phosphatidylcholine (Avanti Polar Lipids) were dissolved in chloroform at a concentration of 10 mg/ml, and stored at -80°C. For the preparation of liposomes, the *E. coli* total lipid extract and egg yolk phosphatidylcholine in a 3:1 ratio (w/w) were evaporated to dryness using N₂ gas to produce a film, which was subsequently lyophilized for 2 hr to remove the last traces of solvent. The lipid film was resuspended in 50 mM potassium phosphate (pH 7.0) at a concentration of 20 mg/ml and then vortexed vigorously to make it dissolve completely. The lipid suspension was then subjected to more than five cycles of freezing (in liquid nitrogen) and thawing (in a 40°C water bath). At this stage, the liposomes were stored at -80°C until further use.

4.2.3 Reconstitution of PfCRT

PfCRT protein was reconstituted into liposomes according to the procedure of Tan (Tan et al., 2006). The liposomes were slowly thawed and extruded (11 times) through a 400 nm polycarbonate filter to obtain unilamellar liposomes with a relatively homogeneous size. Subsequently, the liposomes were diluted to 4 mg of lipid/ml with 50 mM potassium phosphate (pH 7.0) and saturated with detergent, which was followed by measuring the OD_{540nm}, as described by Paternostre *et al* (Paternostre et al., 1988). The purified PfCRT protein was mixed with the detergent-saturated liposomes (1 μmol of dodecyl maltoside/mg of lipid) at an appropriate ratio of protein to lipid and incubated for 30 min at room temperature under gentle agitation. The final protein-to-lipid ratio was always 1:50-1:200 (w/w), and the final glycerol concentration never exceeded 1% (v/v). The detergent was removed by adsorption onto polystyrene beads (Bio-Beads SM2, Bio-Rad) as described previously (Knol et al., 1996). Usually, Bio-Beads SM2 were added at a weight of 80 mg/ml and the samples were incubated for 1 hr at room temperature. Fresh Bio-Beads were added twice and the samples were incubated at 4°C overnight and at room temperature for 1 hr, respectively. Finally, the proteoliposomes were collected by centrifugation (200,000 g for 1 hr at 4°C), resuspended in 0.25 M sucrose and 0.01 M Tris (pH 7.4) for CQ transport activity, or in 10 mM Hepes (pH 7.0) for pHi assay. Liposomes for control experiments were prepared in the same way as proteoliposomes except for the addition of protein. The liposomes were stored at -80°C until use.

4.2.4 Assay of the accumulation of ³H-CQ in proteoliposomes

³H-CQ may be taken up by PfCRT-reconstituted proteoliposomes (Tan et al., 2006). The procedure of ³H-CQ uptake in proteoliposomes is the same as in microsomes (Refer to Section). Briefly, to determine the total count, reconstituted proteoliposomes were resuspended in reaction solution (10 mM Tris-Cl pH 7.4, 0.2 M sucrose, 3 mM ATP and 154 nM ³H-CQ). After incubation at 37°C for 5 min, 200-fold cold CQ was added to quench the reaction. After “PEG precipitation” (Refer to Section), the reaction was stopped by adding 200-fold non-radiolabeled CQ. Radioactive signals were counted after overnight rocking. To determine the non-specific count, reconstituted proteoliposomes were resuspended in reaction solution. After incubation at 37°C for 10 min, 154 nM ³H-CQ was added and subsequent steps were the same as those for total count.

All experiments were carried out at least in triplicate. Standard error of means was calculated where possible, and they are indicated as error bars in the figures. Binding data were fitted by non-linear regression in Prism 5.0 software using the one-site hyperbola binding model ($Y = (V_{max} \cdot X) / (K_m + X)$).

4.2.5 Treatment with MTS-linked reagents

The procedure of characterizing the effects of single-cysteine mutated PfCRT modified by MTS reagents in proteoliposomes was the same as in microsomes (Refer to Section 3.2.5). Briefly, MTS was added to prepared proteoliposomes. The reaction concentration of MTS varied from 10 μM to 40 mM. Further steps were carried out according to the procedure of “PEG precipitation for CQ accumulation” (Refer to Section 3.2.4). For non-specific counts, proteoliposomes were incubated with 200-fold non-radiolabeled CQ at

Chapter 4 Proteoliposomes and Cys-scanning TMD1

37°C for 10 min before $^3\text{H-CQ}$ uptake started. For total counting, 200-fold non-radiolabeled CQ was not added in this step.

When protection by CQ was studied, the incubation of $^3\text{H-CQ}$ with MTS reagents was carried out in the presence of desired concentrations of non-radiolabeled CQ. Specifically, non-radiolabeled CQ was incubated with desired proteoliposomes in working buffer (0.25 M Sucrose, 5 mM MgCl_2 , 10 mM Tris-Cl, pH 7.4, 1.5 μl ATP) at 37°C for 10 min. PEG precipitation was performed (see Section 3.2.4) and the precipitate washed twice with working buffer at room temperature. Then PEG precipitates were resuspended. Afterwards the procedure was the same as that of non-protection.

Specific CQ accumulation was calculated by subtracting the CPM counts obtained with 200-fold excess unlabeled CQ from those obtained with $^3\text{H-CQ}$ alone. All experiments were carried out at least in triplicate. Standard errors of means were calculated where possible, and they are indicated as error bars in the figures.

4.3 Results

4.3.1 Reconstitution of PfCRT

PfCRT of Dd2-Cys-less-Y62C, Dd2-Cys-less-I67C, Dd2-Cys-less-V71C, Dd2-Cys-less-V73C and Dd2-Cys-less-T76C was purified with Ni²⁺-NTA agarose gel (Refer to section 2.2.9). Analysis of SDS-PAGE gels and western blot by densitometry showed that PfCRT protein could be isolated at a high level of purity (

Figure 4-2).

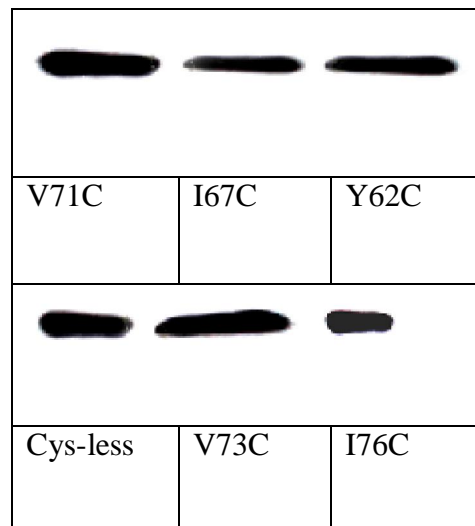


Figure 4-2 Typical western blot results of PfCRT mutants using anti-his antibody
Purified microsomes fraction of PfCRT of Dd2-Cys-less, Dd2-Cys-less-Y62C, Dd2-Cys-less-I67C, Dd2-Cys-less-V71C, Dd2-Cys-less-V73C and Dd2-Cys-less-T76C was analyzed by western blot using anti-his antibody.

Western blot analysis was carried out to measure the efficiency of reconstitution of proteoliposomes. The amount of PfCRT before and after reconstitution was compared. About 31% of PfCRT remained in the proteoliposomes after reconstitution. (Table 4-1)

Table 4-1 Reconstitution efficiency of mutagenic PfCRT proteins in reconstituted proteoliposomes

Proteoliposomes	Efficiency (%) (means±S.E., n=5)
Dd2-Cys-less	32±3
Dd2-Cys-less-Y62C	28±2
Dd2-Cys-less-I67	30±4
Dd2-Cys-less-V71C	30±1
Dd2-Cys-less-V73C	32±2
Dd2-Cys-less-T76C	31±2
Average	31±2

4.3.2 Reconstituted proteoliposomes transport CQ in a saturable manner

To determine the working concentration of reconstituted proteoliposomes in the reaction system, ³H-CQ accumulation activity was characterized with liposomes (no reconstituted PfCRT) and reconstituted Dd2-Cys-less proteoliposomes (Figure 4-3).

Chapter 4 Proteoliposomes and Cys-scanning TMD1

Figure 4-3 shows that PfCRT (Dd2-Cys-less) reconstituted proteoliposomes could accumulate $^3\text{H-CQ}$ in a concentration-dependent manner. The $^3\text{H-CQ}$ transport activity was specific because it could be competed for by excess unlabeled CQ. The specific accumulation of $^3\text{H-CQ}$ was saturable at approximately 100 nM of $^3\text{H-CQ}$ (Figure 4-3). Non-linear regression analysis using the one-site hyperbola (Michaelis-Menten) model of $Y = (V_{\max} \cdot X) / (K_m + X)$ yielded a V_{\max} of 117.5 ± 2.1 pmol/mg proteoliposomes/min and a K_m of 59.27 nM. Non-reconstituted liposomes had a low uptake and were saturable at approximately 10 nM of $^3\text{H-CQ}$ (Figure 4-3). This suggests that PfCRT (Dd2-Cys-less) reconstituted proteoliposomes have significant specific CQ accumulation activity.

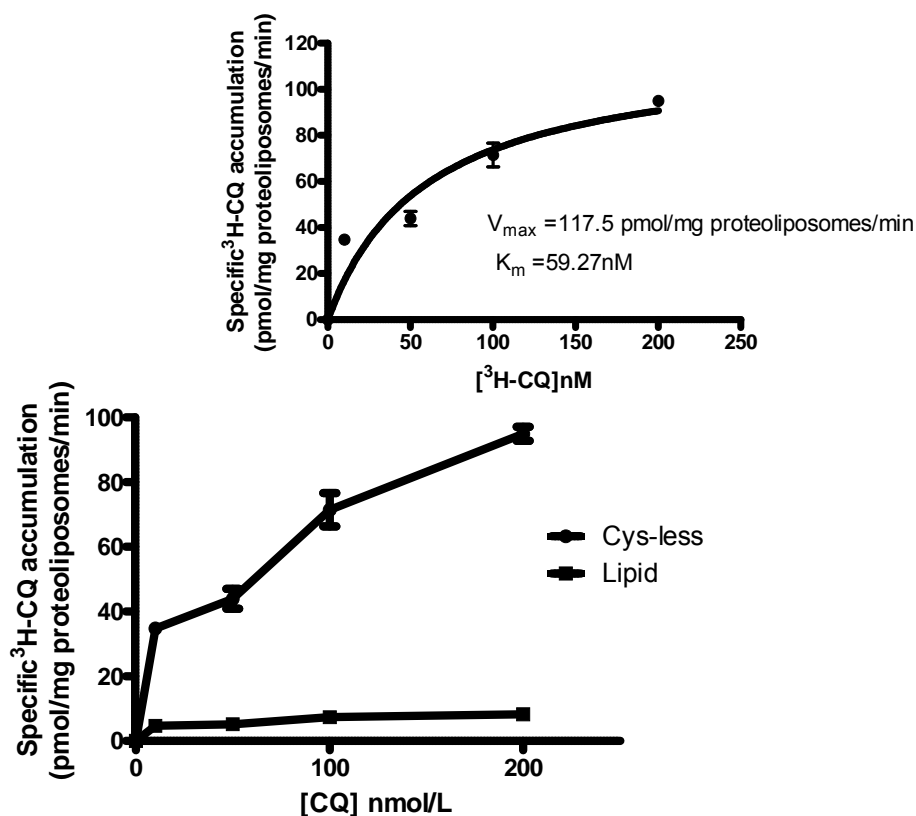


Figure 4-3 Dependence of ³H-CQ uptake on ³H-CQ concentration in proteoliposome
³H-CQ uptake into of liposome (20 μ g, no reconstituted PfCRT) and Dd2-Cys-less proteoliposomes (20 μ g) were measured using indicated ³H-CQ concentrations. Incubation time was for 1 minute. Specific ³H-CQ uptake (dot) was calculated by subtracting nonspecific ³H-CQ count from total ³H-CQ count (lower). Non-linear regression analysis using Michaelis-Menten model $Y = (V_{max} \cdot X) / (K_m + X)$ is shown in the inset. Data points represent means \pm S.E. (n=3).

4.3.3 Dependence of ³H-CQ uptake on proteoliposome concentration and incubation time

To determine the working concentration of reconstituted proteoliposomes in the reaction system, the ³H-CQ accumulation activity was characterized with Dd2-Cys-less PfCRT reconstituted proteoliposomes. The effect of proteoliposome concentration on CQ accumulation was studied by varying the amount of reconstituted proteoliposomes per

assay. As the reconstituted proteoliposomes increased, the specific accumulation increased (Figure 3-3). The accumulation activity almost reached saturation when 10 μg of microsomes was used.

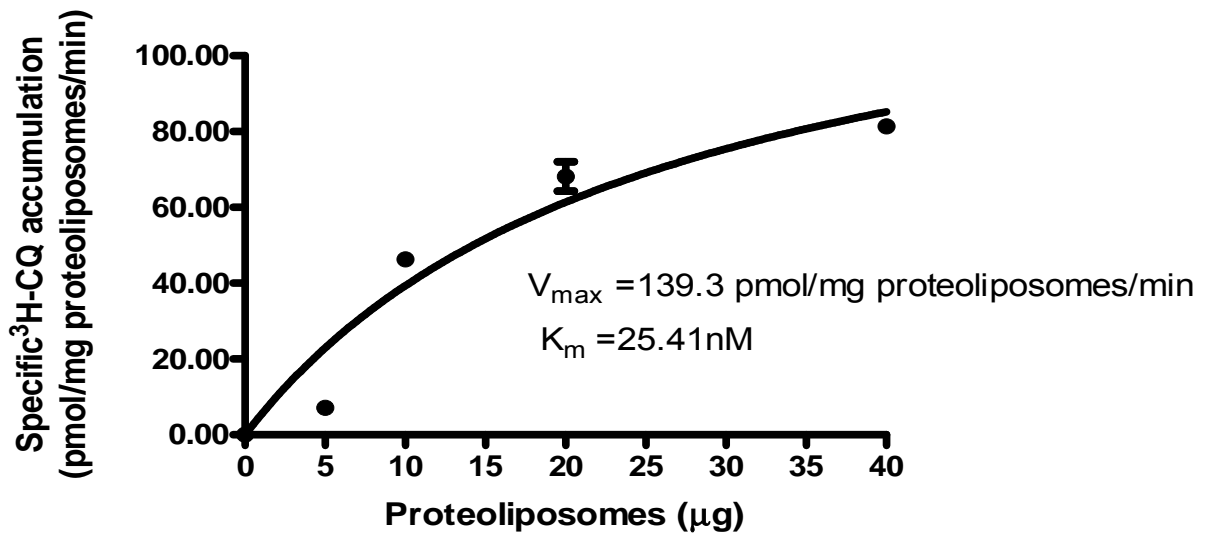


Figure 4-4 Dependence of $^3\text{H-CQ}$ uptake on concentration of proteoliposomes
Measurements were performed in triplicate. Samples containing 5-40 μg of reconstituted Dd2-Cys-less PfCRT proteoliposomes were incubated with 150 nM $^3\text{H-CQ}$ for 1 minute. Data points represent means \pm S.E. (n=3).

To determine the time course of CQ transport of reconstituted proteoliposomes in the reaction system, the $^3\text{H-CQ}$ accumulation activity was characterized with Dd2-Cys-less PfCRT reconstituted proteoliposomes. The initial accumulation within the first minute was linearly proportional to incubation time. It almost reached saturation within 60 sec and the level remained the same for a period of 60 min (see inset of Figure 4-5).

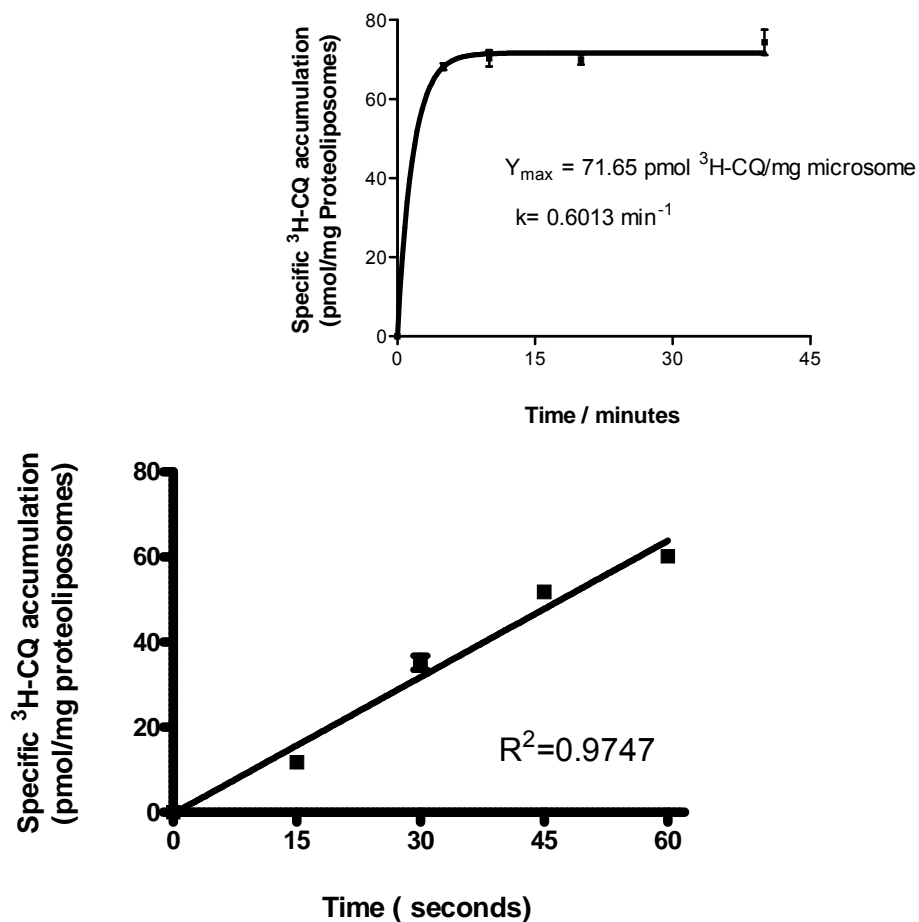


Figure 4-5 Time course of ³H-CQ accumulation in proteoliposomes
Proteoliposomes (20 μ g) were incubated with 150 nM ³H-CQ. Specific ³H-CQ accumulation activities were measured in triplicate for 3 independent experiments and expressed in pmol/mg proteoliposomes. Data points represent means \pm S.E. (n=3).

4.3.4 The specific ³H-CQ accumulation activity of single cysteine substitution mutants

The specific ³H-CQ accumulation activity of the reconstituted proteoliposomes Dd2-Cys-less-Y62C, Dd2-Cys-less-I67C, Dd2-Cys-less-V71C, Dd2-Cys-less-V73C and Dd2-Cys-less-T76C were analyzed (Figure 4-6). All of the reconstituted proteoliposomes showed

abilities to accumulate CQ. These variants showed considerable variation of specific activity ranging from about 50 to 70 pmol/mg proteoliposomes/min.

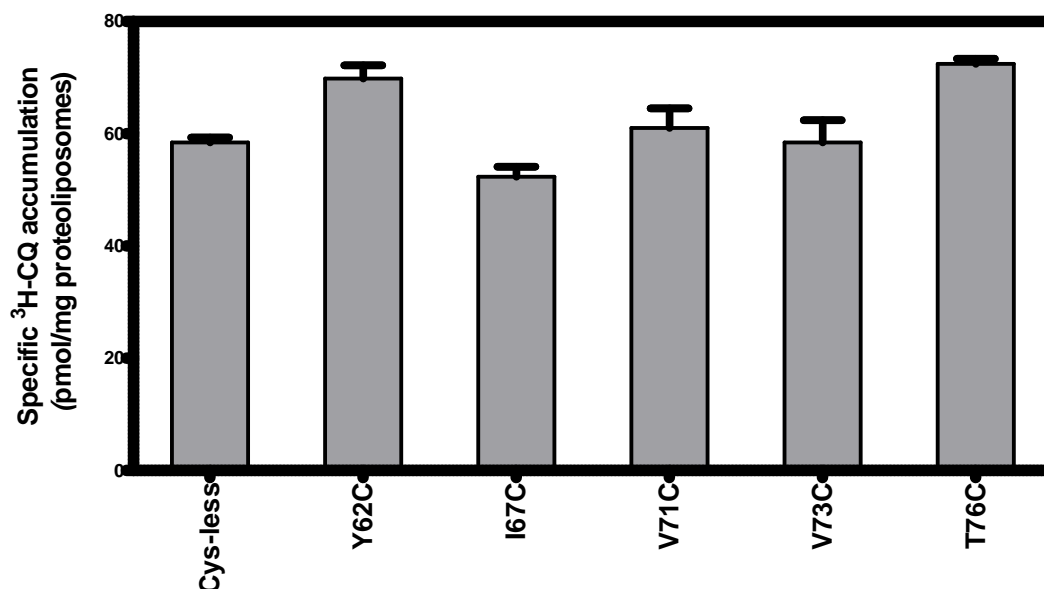


Figure 4-6 The specific ³H-CQ accumulation activity of proteoliposomes
The Specific ³H-CQ accumulation of reconstituted proteoliposomes (20µg): Dd2-Cys-less-Y62C, Dd2-Cys-less-I67C, Dd2-Cys-less-V71C, Dd2-Cys-less-V73C and Dd2-Cys-less-T76C within TMD1 were analyzed. The ability of ³H-CQ accumulation is expressed as pmol/mg liposomes/min. Data points represent means±S.E. (n=3).

4.3.5 MTS concentration dependence modification

To determine the optimal reaction conditions, MTS reagent concentration dependence assays were carried out. Varied concentrations of MTSES, MTSET and MTSEA were used. The ability of CQ accumulation of reconstituted proteoliposomes (Dd2-Cys-less-T76C and Dd2-Cys-less) under the effects of MTS was indicated as the specific accumulation ability (pmol/mg proteoliposomes/min). The concentration of each MTS reagent used in these assays is indicated in Figure 4-7, Figure 4-8 and Figure 4-9. The concentrations of MTSES, MTSET and MTSEA ranged from 0-12 mM, 0-3 mM and 0-

Chapter 4 Proteoliposomes and Cys-scanning TMD1

1.2 mM respectively. The specific accumulation of $^3\text{H-CQ}$ under the effects of MTSES, MTSET and MTSEA was saturable at approximately 8 mM, 1.5 mM and 0.6 mM respectively. The ability of CQ accumulation of proteoliposomes containing mutagenic PfCRT (Dd2-Cys-less-T76C) under the effects of MTSES increased as the concentration of MTSES increased. Meanwhile, MTSET and MTSEA led to a decrease of CQ accumulation as the concentration of these two MTS reagents increased. This suggests that high concentrations of MTSES can enhance CQ accumulation of Dd2-Cys-less-T76C PfCRT. MTSET and MTSEA have adverse effects. In the meantime, Dd2-Cys-less-T76C and Dd2-Cys-less PfCRT modified by MTS reagent did not show significant changes of CQ accumulation as the concentration of these three MTS reagents increased.

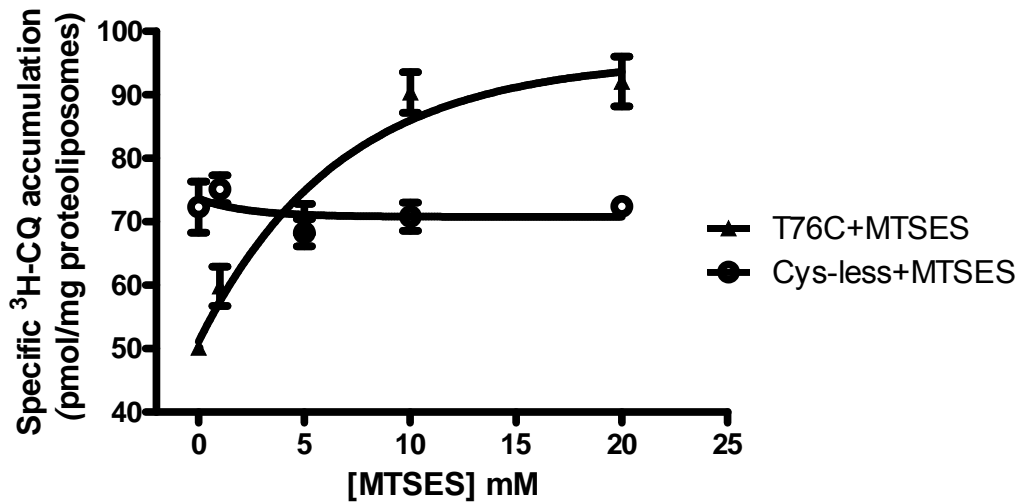


Figure 4-7 MTSES concentration dependence of the ability of CQ accumulation of proteoliposomes containing mutagenic PfCRT
 Proteoliposomes (20 μ g) were incubated with 150 nM 3 H-CQ. Specific 3 H-CQ accumulation activities were measured in triplicate for 3 independent experiments and expressed in pmol/mg proteoliposomes. The ability of CQ accumulation of proteoliposomes containing mutagenic PfCRT (Dd2-Cys-less-T76C and Dd2-Cys-less) is indicated as the specific accumulation ability (pmol/mg proteoliposomes/min). MTSES concentration ranges from 0-12 nM. Data points represent means \pm S.E. (n=3).

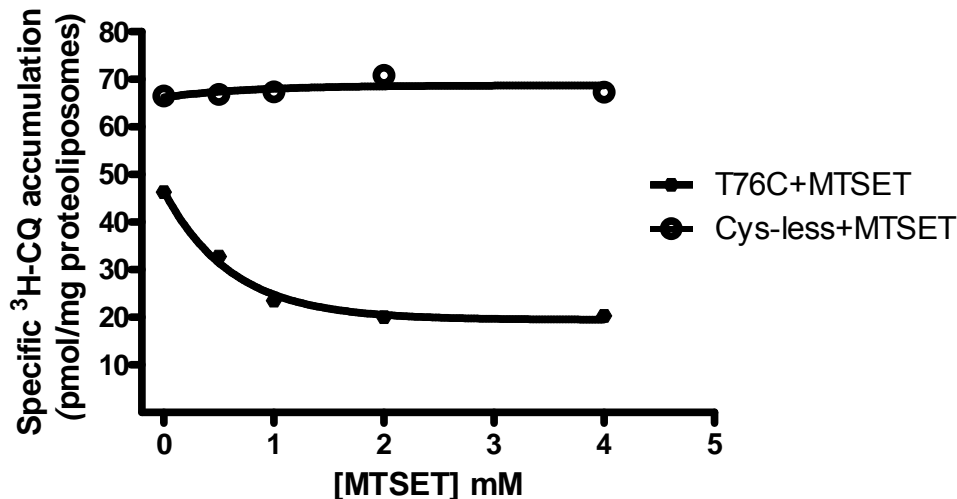


Figure 4-8 MTSET concentration dependence of the ability of CQ accumulation of proteoliposomes containing mutagenic PfCRT
 Proteoliposomes (20 μ g) were incubated with 150 nM 3 H-CQ. Specific 3 H-CQ accumulation activities were measured in triplicate for 3 independent experiments and expressed in pmol/mg proteoliposomes. The ability of CQ accumulation of proteoliposomes containing mutagenic PfCRT (Dd2-Cys-less-T76C and Dd2-Cys-less) is indicated as the specific accumulation ability (pmol/mg proteoliposomes/min). MTSET concentration ranges from 0-12 nM. Data points represent means \pm S.E. (n=3).

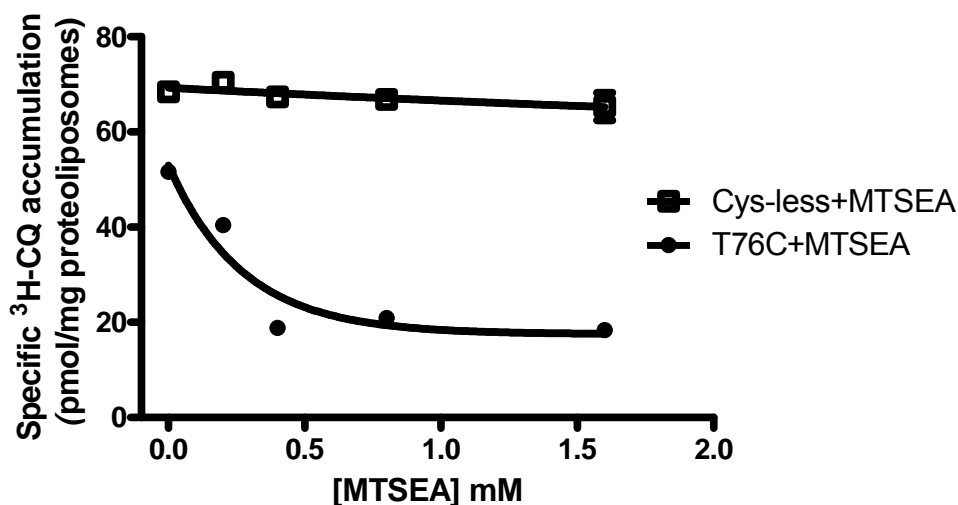


Figure 4-9 MTSEA concentration dependence of the ability of CQ accumulation of reconstituted proteoliposomes

Proteoliposomes (20 μ g) were incubated with 150 nM 3 H-CQ. Specific 3 H-CQ accumulation activities were measured in triplicate for 3 independent experiments and expressed in pmol/mg proteoliposomes. The ability of CQ accumulation of proteoliposomes containing mutagenic PfCRT (Dd2-Cys-less-T76C and Dd2-Cys-less) is indicated as the specific accumulation ability (pmol/mg proteoliposomes/min). MTSEA concentration ranges from 0-12 nM. Data points represent means \pm S.E. (n=3).

4.3.6 The sensitivity of single cysteine substitution mutants to MTSES

To further verify the characteristic property of Dd2-Cys-less-Y62C, Dd2-Cys-less-I67C, Dd2-Cys-less-V71C, Dd2-Cys-less-V73C and Dd2-Cys-less-T76C, these reconstituted proteoliposomes were studied. Their ability to accumulate CQ after exposure to MTS reagents are show in Figure 4-10 and Figure 4-11.

Chapter 4 Proteoliposomes and Cys-scanning TMD1

The relative activity of proteoliposomes is represented as percent of specific CQ accumulation of untreated MTSES (no MTSES modification) (Figure 4-10).

Among these mutants, Dd2-Cys-less-T76C displayed a higher relative activity (SD >125% of the mean) and Dd2-Cys-less-I67C, Dd2-Cys-less-V71C and Dd2-Cys-less-V73C displayed a lower relative activity (SD <50% of the mean). Dd2-Cys-less displayed approximately the same activity as untreated with MTSES.

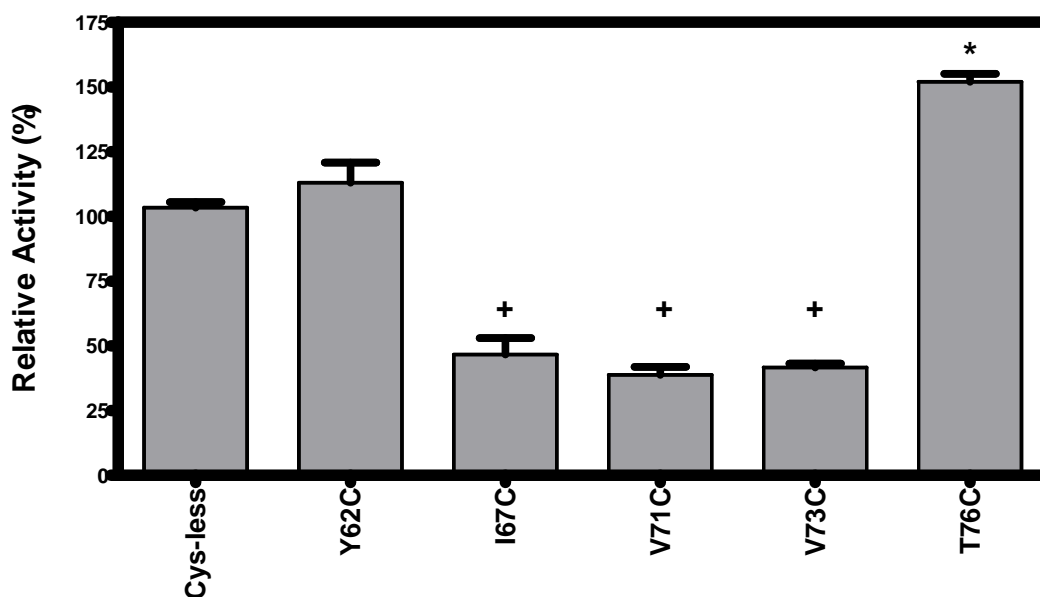


Figure 4-10 Sensitivity of single cysteine substitution mutants to MTSES

Incubate MTSES (10mM) with proteoliposomes (20 μ g) for 10 min. The relative activity of single cysteine-substitution mutants is expressed as percent of specific CQ accumulation ability of untreated MTSES (no MTSES reagent). + indicates the related activity SD <25% of the mean; * indicates the related activity SD >125% of the mean. Data are means \pm S.E. (n=3).

4.3.7 The sensitivity of single cysteine substitution mutants to MTSET

As described in Section 4.3.6, the relative activity of proteoliposomes is represented as percent of specific CQ accumulation of untreated MTSET (no MTSET modification) (Figure 4-11 Sensitivity of single cysteine substitution mutants to MTSET).

Among these mutants, Dd2-Cys-less-I67C and Dd2-Cys-less-V73C displayed a lower relative activity (SD <50% of the mean). Dd2-Cys-less displayed approximately the same activity as untreated with MTSET.

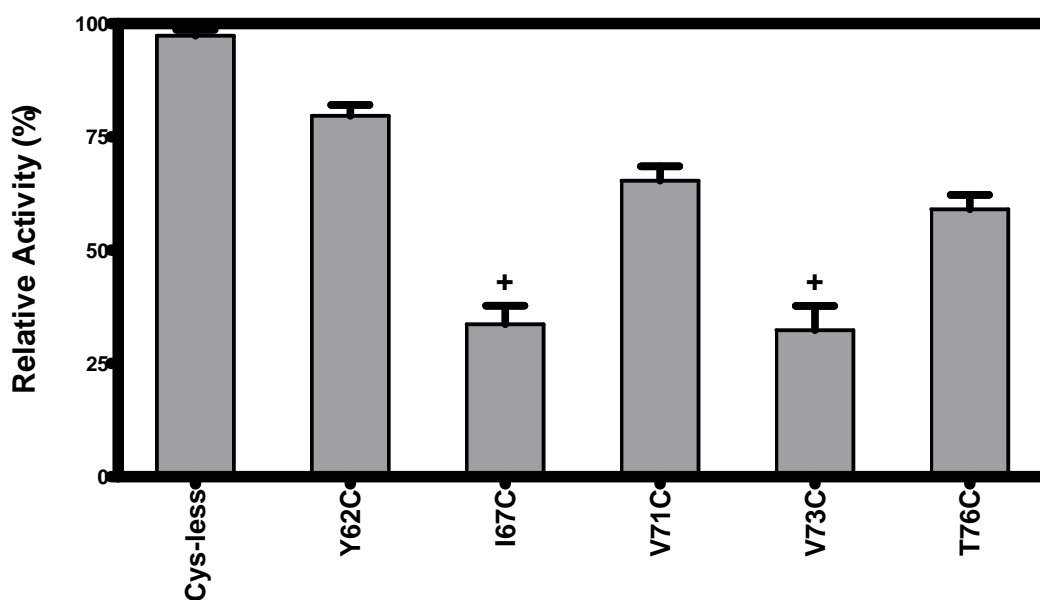


Figure 4-11 Sensitivity of single cysteine substitution mutants to MTSET
Incubate MTSET (2mM) with proteoliposomes (20 μ g) for 10 min. The relative activity of single cysteine-substitution mutants is expressed as percent of specific CQ accumulation ability of untreated MTSET (no MTSET reagent). + indicates the related activity SD <50% of the mean. Data are means \pm S.E. (n=3).

4.3.8 CQ protection of MTS modification

To study CQ protection of MTSES modification, proteoliposomes were incubated with MTSES reagents in the presence of non-radiolabeled CQ (Refer to Section 3.2.5). In this experiment, Dd2-Cys-less-T76C, which displayed a higher relative activity (SD >125% of the mean) and Dd2-Cys-less-I67C, Dd2-Cys-less-V71C and Dd2-Cys-less-V73C, which displayed a lower relative activity (SD <25% of the mean), were chosen for further studies (see section 3.3.6 and Figure 4-12).

The relative activity of single cysteine-substitution mutants is expressed as percent of specific CQ accumulation ability of untreated MTSES (no MTSES reagent).

Figure 4-12 shows that CQ pre-incubation weakened the enhancing effect of MTSES on the CQ accumulation ability of Dd2-Cys-less-T76C. Meanwhile, Dd2-Cys-less-I67C, Dd2-Cys-less-V71C and Dd2-Cys-less-V73C were not affected. This suggests that CQ prevents PfCRT from modification by MTSES and the 76th amino acid of PfCRT may be involved in the site where MTSET modification takes place.

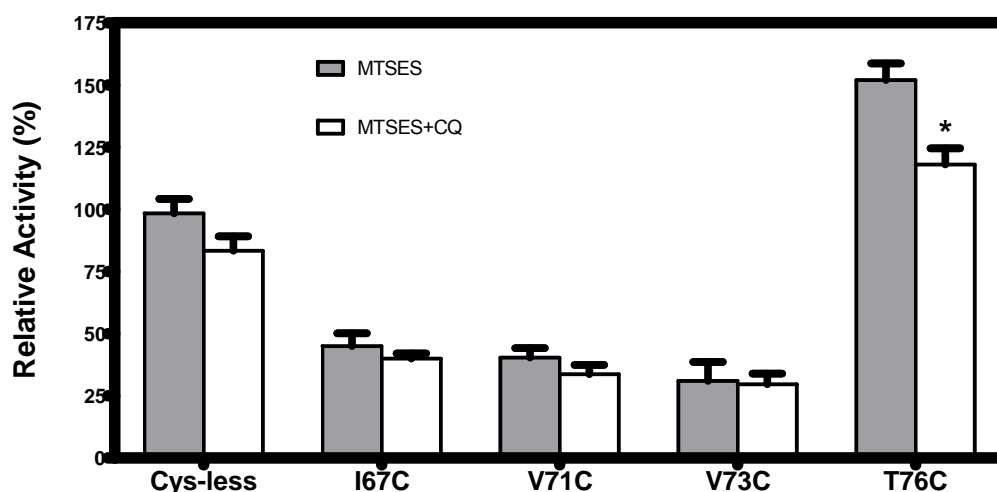


Figure 4-12 CQ protection to MTSES modification

Proteoliposomes (20 μ g) of Dd2-Cys-less-T76C, Dd2-Cys-less-I67C, Dd2-Cys-less-V71C and Dd2-Cys-less-V73C incubate with non-radiolabeled CQ (1nM) at 37°C for 10 min. Re-suspend the PEG precipitates and incubate with MTSES (10mM). Afterwards procedure is the same as that of non-protection. *, significant difference ($P<0.05$) compared to non-protection (in absence of non-radiolabeled CQ). Data are means \pm S.E. (n=3).

4.3.9 CQ protection to MTSET modification

The assay of CQ protection of MTSET modification was carried out in the presence of non-radiolabeled CQ. In this experiment, Dd2-Cys-less-I67C and Dd2-Cys-less-V73C and Dd2-Cys-less-T76C, which displayed a lower relative activity (SD <25% of the mean), were chosen for further studies (see section 3.3.6 and Figure 4-13).

The method was the same as described in Section 3.3.9. The result is displayed in Figure 4-13. It shows that CQ pre-incubation weakened the decreasing effect of MTSET on Dd2-Cys-less-T76C CQ accumulation. Meanwhile, Dd2-Cys-less-I67C and Dd2-Cys-less-V73C were not affected. This suggests that CQ prevents PfCRT from modification by MTSET and the 76th amino acid of PfCRT may be involved in the site where MTSET modification takes place.

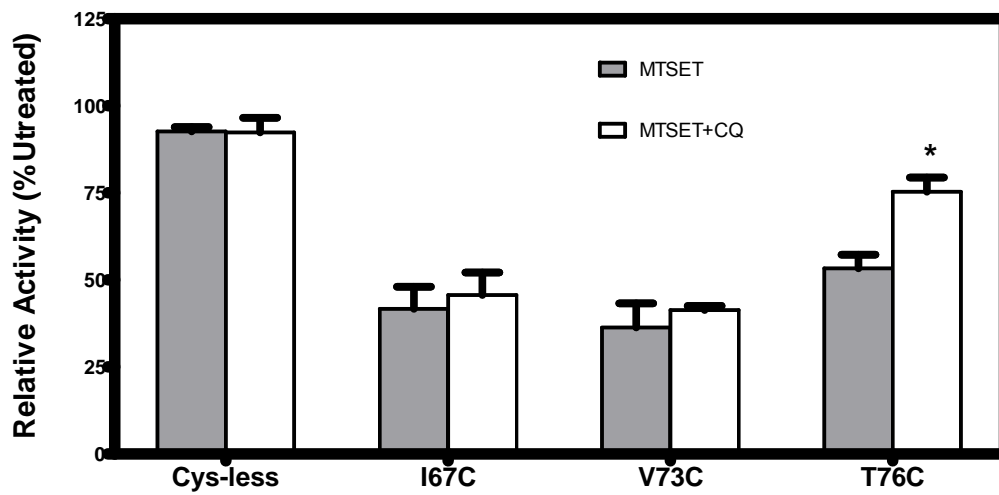


Figure 4-13 CQ protection to MTSET modification

Proteoliposomes (20µg) of Dd2-Cys-less-I67C and Dd2-Cys-less- V73C and Dd2-Cys-less- I76C incubate with non-radiolabeled CQ (1nM) at 37°C for 10 min. Re-suspend the PEG precipitates and incubate with MTSET (2mM). Afterwards procedure is the same as that of non-protection (see Section 3.2.4). *, significant difference (P<0.05) compared to non-protection (in absence of non-radiolabeled CQ). Data are means±S.E. (n=3).

4.4 Discussion

Reconstituted proteoliposomes were used in this project to study PfCRT. Dd2-Cys-less-Y62C, Dd2-Cys-less-I67C, Dd2-Cys-less-V71C, Dd2-Cys-less-V73C and Dd2-Cys-less-T76C were chosen for they demonstrated relative activity SD >125% of the mean or SD <25% of the mean when exposed to MTS reagents. All of them were purified with Ni²⁺-NTA agarose gel. Analysis of SDS-PAGE gels and western blots by densitometry showed that PfCRT protein could be isolated at a high level of purity (Figure 4-2). Western blot analyses showing the amount of PfCRT before and after reconstitution were compared. About 31% of PfCRT remained in the proteoliposomes after reconstitution. (Table 4-1)

Dd2-Cys-less reconstituted proteoliposomes could accumulate ³H-CQ in a concentration-dependent manner. The ³H-CQ transport activity was specific because it could be competed for by excess unlabeled CQ. This suggests that Dd2-Cys-less reconstituted proteoliposomes have significant specific CQ accumulation activity. The specific ³H-CQ accumulation activity of reconstituted proteoliposomes was analyzed (Figure 4-6). All of the reconstituted proteoliposomes showed abilities of accumulation of CQ. So we performed MTS treatment assays afterwards.

Since MTSEA demonstrated similar properties in microsomes to MTSET (Figure 3-8, Figure 3-7, Figure 3-11, Figure 3-10, Figure 3-15 and Figure 3-14), MTSES and MTSET were chosen for proteoliposome studies. Among these mutants, after modification by MTSES, Dd2-Cys-less-T76C demonstrated a higher relative activity (SD >125% of the

Chapter 4 Proteoliposomes and Cys-scanning TMD1

mean) and Dd2-Cys-less-I67C and Dd2-Cys-less-V73C displayed a lower relative activity (SD <50% of the mean). After modification by MTSET, only Cys-less-I67C and Dd2-Cys-less-V73C displayed a lower relative activity (SD <50% of the mean). These suggest that the 76th, 73rd and 67th amino acid residues are accessible to MTS. These results are the same as those obtained from experiments involving microsomes (Refer to Section3.3 and Section 3.4).

In the CQ protection assay, CQ prevented the 76th amino acid residue from modification by MTSES and the 76th amino acid of PfCRT may be involved in the site where MTSET modification takes place. (Figure 4-12 and Figure 4-13). These results were the same as for microsomes (Refer to Section3.3 and Section 3.4).

Chapter 5

Cysteine Scanning of Transmembrane Domain 4 of PfCRT

Abstract

The effect of residue 163 seemed to overwhelm that of residue 76, which was regarded as the determinant of the CQR phenotype. The gain of positive charge by S163R may block the efflux of positively charged molecules from the DV, thereby trapping protonated CQ in the DV, resulting in susceptibility. To verify this, MTSES and MTSET were chosen to carry out the SCAM assay. On the Dd2-cysteine-less background, seven single cysteine substituted mutants were constructed for this assay.

Modified by MTSET, only S163C displayed a lower relative activity. This result suggests that inducing a positive charge at 163 may lead to a CQ accumulation decrease, thus supporting the “charge” hypothesis. Our results showed that the CQ accumulation ability of 163 was not affected by CQ protection. This suggests that 163 is different from 76, which may be a CQ binding site within PfCRT.

5.1 Introduction

The mutation S163R (TMD4) of PfCRT results in both loss of chloroquine resistance and verapamil-reversible CQ resistance with K76T in TMD1 (Johnson et al., 2004). It is proposed that S163R introduces a positive charge to the PfCRT protein and could block CQ through the DV (Figure 5-1).

On the Dd2-cysteine-less background, seven single cysteine-substituted mutants, Yeast-Dd2-Cys-less-V159C, Yeast-Dd2-Cys-less-L160C, Yeast-Dd2-Cys-less-Q161C, Yeast-Dd2-Cys-less-S163C, Yeast-Dd2-Cys-less-I164C, Yeast-Dd2-Cys-less-P165C and Yeast-Dd2-Cys-less-N167C, were constructed for SCAM. The study aimed to understand the properties of TMD4 in CQR.

The gain of positive charge at residue 163, by S163R mutation, may block the efflux of positively charged molecules from the DV, thereby trapping protonated CQ in the DV, resulting in susceptibility. This proposed mechanism relies on the assumption that residue 163 is located on the luminal side of the PfCRT channel, the 76th and 163rd residues together line the PfCRT lumen and S163R mutation can compensate for the loss of positive charge in the K76T mutation in Dd2, thereby blocking the exit of positively charged CQ from the DV and resulting in susceptibility. To verify this, MTSES and MTSET were chosen to carry out the SCAM assay.

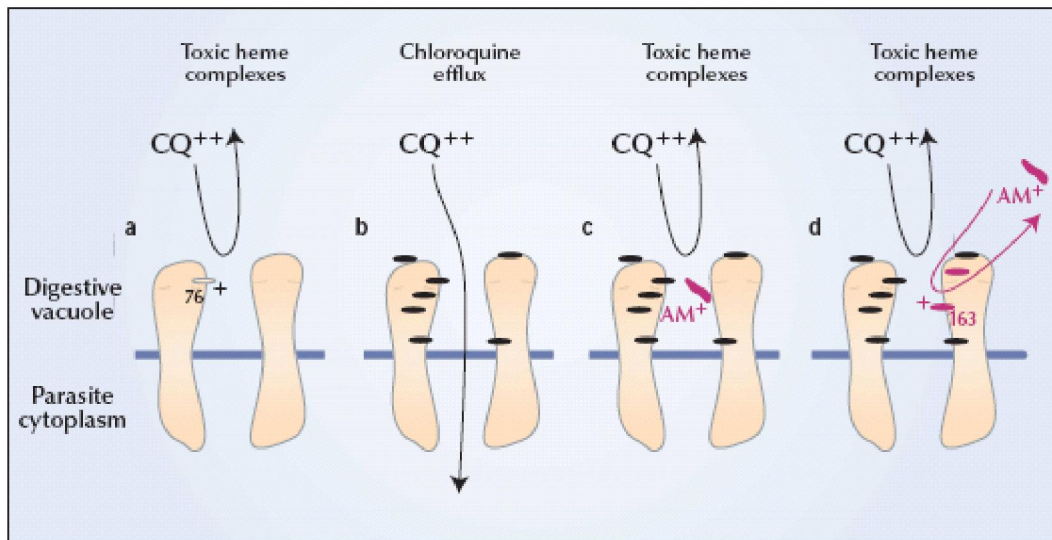


Figure 5-1 PfCRT point mutations and drug effects in *P. falciparum*

(a) PfCRT of wild-type parasites that carry K76 cannot expel chloroquine out from the DVs and thus is killed by interference of detoxification of heme (b) Point mutation of K76T introduce a energy-dependent transport of chloroquine and thus result in CQR (c) Positively charged amantadine that bind in the PfCRT pore of chloroquine-resistant parasites will interrupt chloroquine efflux. As the result, the CQR is reversed, leading to chloroquine sensitivity. (d) Point mutation of S163R confers the amantadine-resistance as well as a loss of CQR. As the result, the binding of amantadine and CQ efflux are inhibited. I356V is the second mutation introduced by amantadine selective pressure. CQ⁺⁺⁺, protonated chloroquine; AM⁺, amantadine (charged from). (Johnson et al., 2004)

5.2 Materials and Methods

5.2.1 Materials

Refer to Section 3.2.1

5.2.2 Culture of *P. pastoris* cells and preparation of microsomes from *P. pastoris*

Refer to Section 3.2.2

5.2.3 Determination of the orientation of PfCRT within membrane of microsomes

Refer to Section 3.2.3

5.2.4 Assay of the accumulation of ^3H -CQ in microsomes

Refer to Section 3.2.4

5.2.5 Treatment with MTS-linked reagents

Refer to Section 3.2.5

5.3 Results

5.3.1 The specific $^3\text{H-CQ}$ accumulation activity of single cysteine substitution mutants

The specific $^3\text{H-CQ}$ accumulation activity of the Dd2-Cys-less parent and seven single cysteine recovery mutants were analyzed (Figure 5-2). All of the mutants showed discrepant abilities of accumulating CQ. These discrepancies of specific activity ranged from about 7 to 15 pmol/mg microsomes/min.

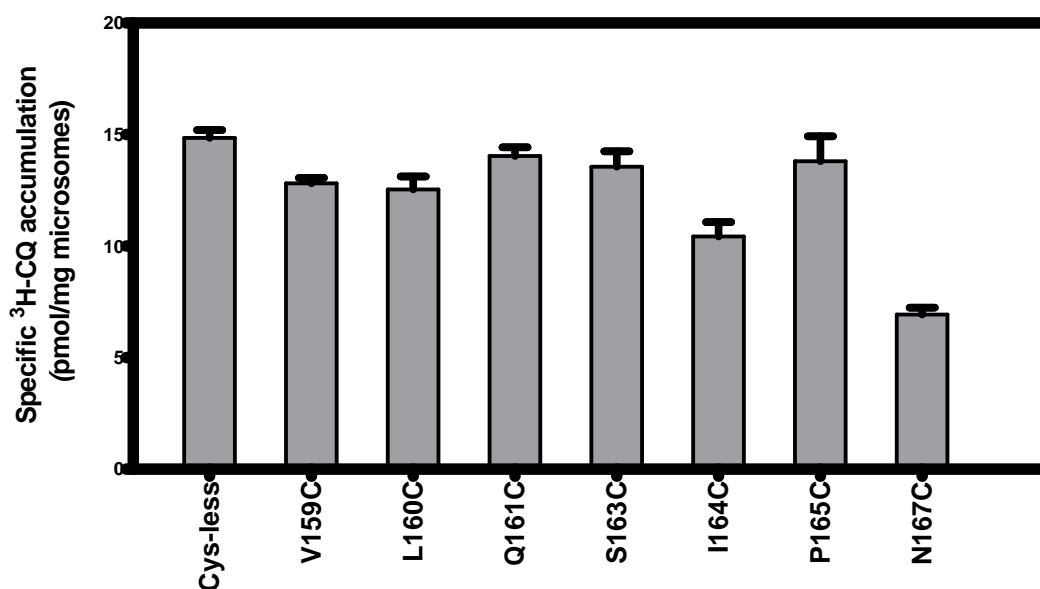


Figure 5-2 The specific $^3\text{H-CQ}$ accumulation of Pfert of Dd2-Cys-less seven single cysteine recovery mutants within TM4

Microsomes (50 μg) were incubated with 150 nM $^3\text{H-CQ}$. Specific $^3\text{H-CQ}$ accumulation activities were measured in triplicate for 3 independent experiments and expressed in pmol/mg microsomes. Data points represent means \pm S.E. (n=3).

5.3.2 The sensitivity of single cysteine substitution mutants to MTSES and MTSET

To scan TMD4 residues, seven single cysteine-substitution mutants were studied. Their ability to accumulate CQ after exposure to MTS reagents are show in Figure 5-3 and Figure 5-4.

Modified by MTSES, Dd2-Cys-less-L160C and Dd2-Cys-less-P156C displayed a lower relative activity (SD <75% of the mean). Dd2-Cys-less displayed approximately the same activity as untreated with MTSES.

Modified by MTSET, only Dd2-Cys-less-S163C displayed a lower relative activity (SD <25% of the mean). Dd2-Cys-less displayed approximately the same activity as untreated with MTSET.

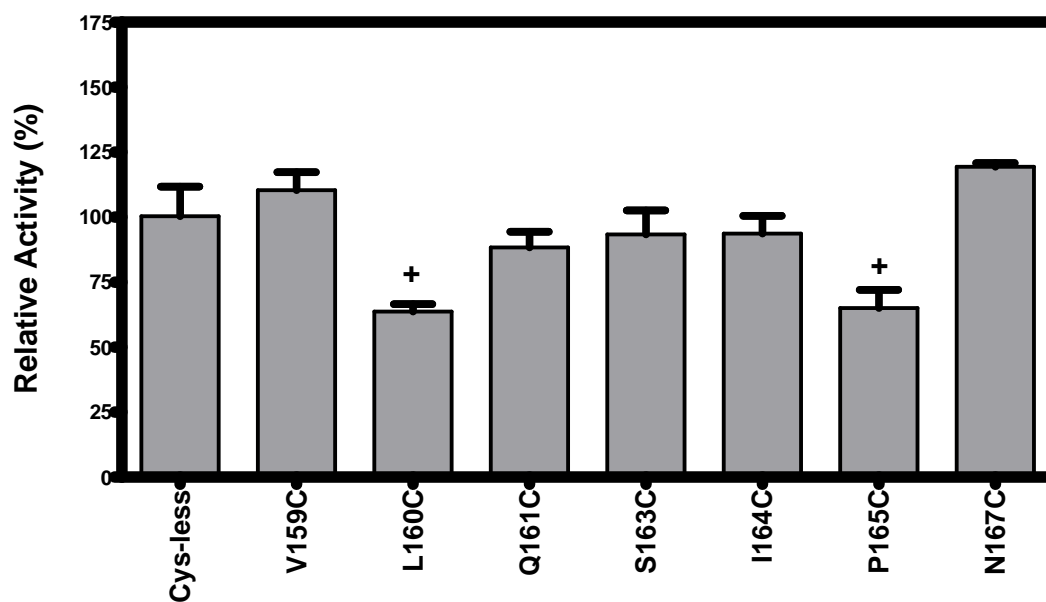


Figure 5-3 Sensitivity of single cysteine substitution mutants to MTSES

Incubate MTSES (10mM) solution in prepared microsomes (50 μ g) for 10 min. The relative activity of single cysteine-substitution mutants is expressed as percent of specific CQ accumulation ability of untreated MTSES (no MTSES reagent). + indicates the related activity SD <75% of the mean. Data are means \pm S.E. (n=3).

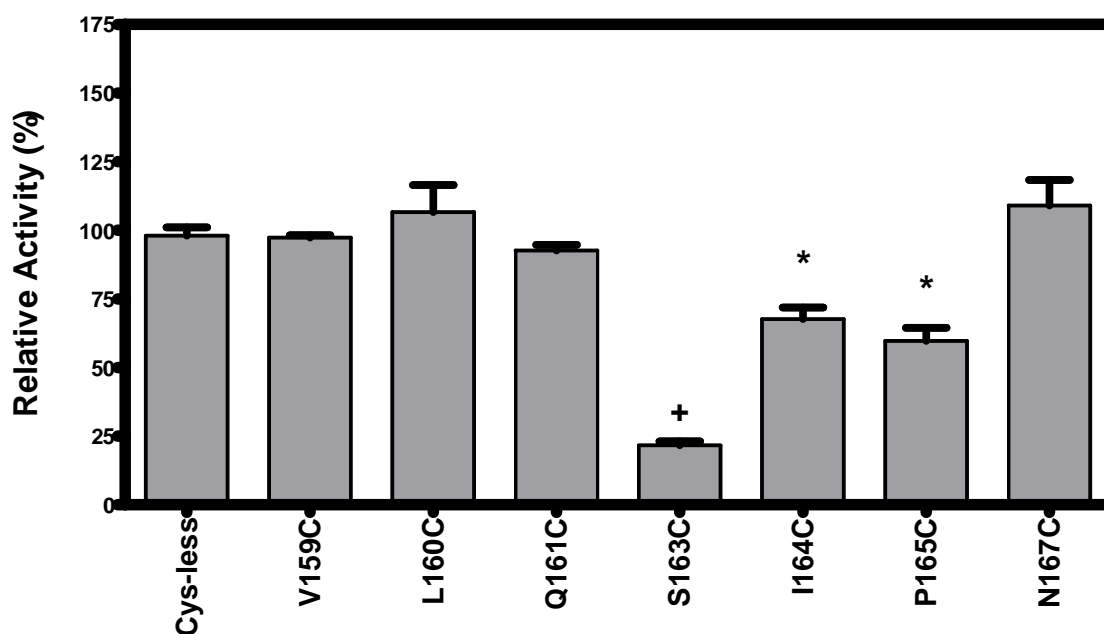


Figure 5-4 Sensitivity of single cysteine substitution mutants to MTSET

Incubate MTSET (2mM) solution in prepared microsomes (50 μ g) for 10 min. The relative activity of single cysteine-substitution mutants is expressed as percent of specific CQ accumulation ability of untreated MTSET (no MTSET reagent). + indicates the related activity SD <25% of the mean; * indicates the related activity SD <75% of the mean. Data are means \pm S.E. (n=3).

5.3.3 CQ protection to MTSES modification

To study the CQ protection of MTSES modification, microsomes were incubated with MTSES reagents in the presence of non-radiolabeled CQ (Refer to Section 3.2.5). In this experiment, Dd2-Cys-less-L160C and Dd2-Cys-less-P165C, which displayed a lower relative activity (SD <75% of the mean), were chosen for further studies (see section 3.3.6 and Figure 5-5).

The relative activity of single cysteine-substitution mutants is expressed as percent of specific CQ accumulation ability of untreated MTSES (no MTSES reagent).

Figure 5-5 shows that the CQ accumulation ability of Dd2-Cys-less-L160C and Dd2-Cys-less-P165C were not affected by CQ protection.

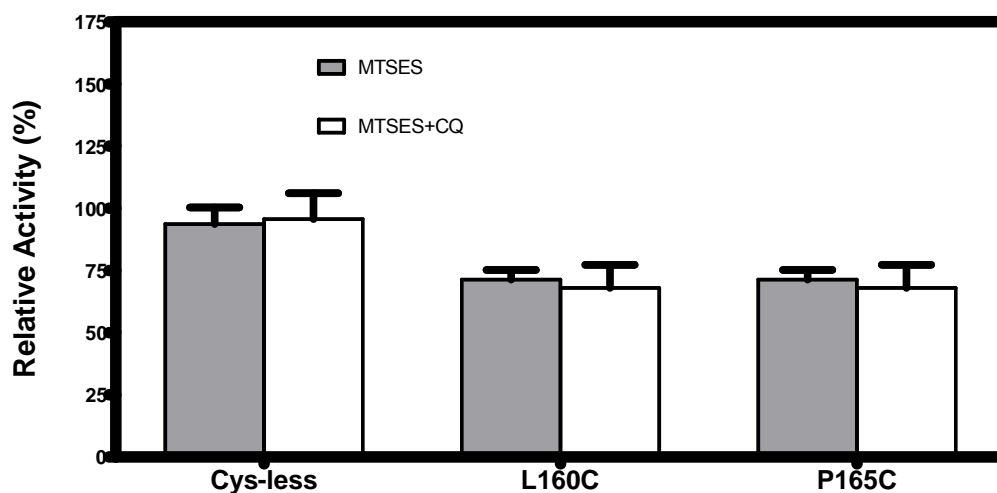


Figure 5-5 CQ protection to MTSES modification

Microsomes (50 μ g) of Dd2-Cys-less, Dd2-Cys-less-L160C and Dd2-Cys-less-P165C incubate with non-radiolabeled CQ (1nM) at 37°C for 10 min. Re-suspend the PEG precipitates and incubate with MTSES (10mM). Afterwards procedure is the same as that of non-protection (see Section 3.2.4).

Data are means \pm S.E. (n=3).

5.3.4 CQ protection of MTSET modification

The assay of CQ protection of MTSET modification was carried out in the presence of non-radiolabeled CQ. In this experiment, Dd2-Cys-less-S163C, Dd2-Cys-less-I164C and Dd2-Cys-less-P165C, which displayed a lower relative activity (SD <75% of the mean), were chosen for further studies (see section 3.3.6 and Figure 5-6).

Figure 5-6 shows that the CQ accumulation ability of Dd2-Cys-less-S163C, Dd2-Cys-less-I164C and Dd2-Cys-less-P165C were not affected by CQ protection.

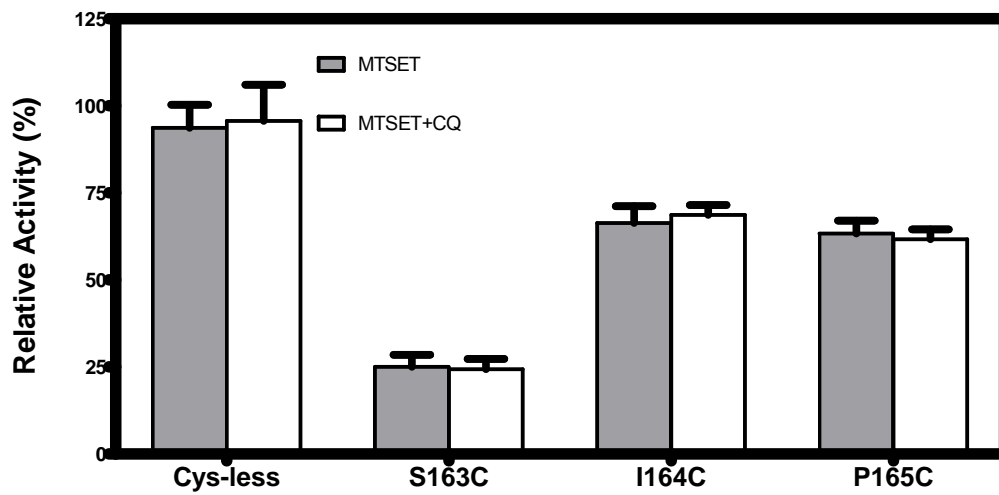


Figure 5-6 CQ protection to MTSET modification

Microsomes (50 μ g) of Dd2-Cys-less, Dd2-Cys-less- S163C, Dd2-Cys-less- I164C and Dd2-Cys-less- P165C incubate with non-radiolabeled CQ (1nM) at 37°C for 10 min. Re-suspend the PEG precipitates and incubate with MTSET (2mM). Afterwards procedure is the same as that of non-protection (see Section 3.2.4). Data are means \pm S.E. (n=3).

5.4 Discussion

The susceptible mutant at position 76K has a lower CQ accumulation when compared with the CQR mutant T⁷⁶ in microsomes and proteoliposomes (Tan et al., 2006). The charge hypothesis assumes that the positively-charged Lysine residue in the PfCRT lumen of the susceptible mutant tends to repel protonated CQ which would otherwise be able to pass through the lumen. The effect of residue 163 seemed to overwhelm that of residue 76, which was regarded as the determinant of CQR phenotype. One hypothesis suggests that this is due to the side chain volume of 163R. The side chain of Lysine is 366.25 Å while that of Arginine is 421.32 Å³. The larger size of Arginine may make R¹⁶³ more effective in blocking CQ from passing through the channel. It is expected that residue 76 lies on the surface of the PfCRT transmembrane lumen, where interaction with drug molecules is easy and unimpeded. The S163R (TMD4) of PfCRT results in both loss of chloroquine resistance and verapamil-reversible CQ resistance with K76T in TMD1 (Johnson et al., 2004).

The other explanation is that the gain of positive charge by S163R may block the efflux of positively charged molecules from the DV, thereby trapping protonated CQ in the DV, resulting in susceptibility. This proposed mechanism relies on the assumption that residue 163 is located on the luminal side of the PfCRT channel, the 76th and 163rd residues together line the PfCRT lumen and S163R mutation can compensate for the loss of positive charge in the K76T mutation in Dd2, thereby blocking the exit of positively charged CQ from DV and resulting in susceptibility. To verify this, MTSES and MTSET

were chosen to carry out the SCAM assay. On the Dd2-cysteine-less background, seven single cysteine-substituted mutants were constructed for this assay.

Modified by MTSET, only S163C displayed a lower relative activity. This result suggests that inducing a positive charge at 163 may lead to a CQ accumulation decrease, thus supporting the “charge hypothesis”.

Our results showed that the CQ accumulation ability of 163 was not affected by CQ protection. This suggest that 163 is different from 76 (refer to Section 3.4 and Figure 3-13, Figure 3-14 and Figure 3-15), which may be a CQ binding site within PfCRT.

Conclusion

PfCRT resides in a subcellular membrane within an intracellular parasite. It is extremely difficult to experimentally manipulate *in vivo*, so an *in vitro* system is definitely necessary. Heterologous expression of PfCRT in *Pichia* is helpful for further analysis of PfCRT transport function. Our laboratory and Rope's group have successfully expressed PfCRT in *Pichia* (Tan et al., 2006; Zhang et al., 2002) and function studies have been carried out. This project used this expression system to perform the Substituted-cysteine Accessibility Method (SCAM) to elucidate the structure of PfCRT and understand the mechanism of CQR.

Using site-directed mutagenesis, Cys-less encoding *pfcrts* (twenty-one cysteine substituted *pfcrts* within TMD1 and ten within TMD4) were constituted. *Pfcrts* of Cys-less and recoveries within TMD1 were all expressed. But only seven substituted PfCRTs within TMD4 were expressed. Although the expression level was low (approximately 1-2% of the total amount of microsomes), the PfCRT proteins were purified to apparent homogeneity. Purified PfCRT proteins were used to reconstitute into proteoliposomes for further studies.

PfCRT is directly or indirectly involved in a transporter-mediated CQ efflux system in CQR parasites (Sanchez et al., 2004; Sanchez et al., 2003). PfCRT has been predicted have ten transmembrane domains and localize to the DV membrane (Fidock et al., 2000b). Bioinformatics analyses predict that the N- and C-termini of PfCRT are located on the cytoplasmic side of the parasite's DV

Conclusion

membrane (Martin and Kirk, 2004). Within ten putative TMDs, positively-charged residues (Lysine or Arginine) are predicted to lie in the extra-membrane segments or in the termini regions. (Martin and Kirk, 2004; Tran and Saier, 2004)

Substitution of Threonine (T) for lysine (K) at position 76 (K76T) is the most pivotal change of CQR parasites (Djimde et al., 2001a; Fidock et al., 2000b). Using SCAM, it is possible to find detailed functional and structure information about TMD1, within which 76 is localized. Twenty-one cysteine-substituted *pfcrts* within TM1 were constituted and PfCRTs of Cys-less and recoveries within TM1 were all successfully expressed.

The microsomes isolated from each *P. pastoris* were used to determine the transport activity. Dd2-Cys-less PfCRT could accumulate $^3\text{H-CQ}$ in a concentration-dependent manner. The $^3\text{H-CQ}$ transport activity was specific (Figure 3-2, Figure 3-3 and Figure 3-4). There were significantly different CQ accumulation activities among these mutants (Figure 3-5). This suggests that CQ might interact with the internal (intra-DV) lumen of PfCRT, supporting the hypothesis that CQR parasites result from the presence of PfCRT-mediated CQ transport out of the DV. Results showed that cysteine substitution to obligate amino acids affected the function via the amino acid composition of the TMD1 helix.

SCAM and charged MTS reagents (MTSES, MTSET and MTSEA) have been successfully applied to the structural and functional elucidation of channels and transporters (Akabas and Karlin, 1995; Akabas et al., 1994; Akabas et al., 1992).

Conclusion

In this subject, modified by MTSES, Dd2-Cys-less-T76C PfCRT microsomes accumulated more CQ when the concentration of MTSES increased (Figure 3-6). Meanwhile, MTSET and MTSEA led to a decrease of specific CQ accumulation as the concentration of these two MTS reagents increased (Figure 3-7 and Figure 3-8). This suggests that high concentrations of MTSES can improve the ability of CQ accumulation of Dd2-Cys-less-T76C PfCRT, and MTSET and MTSEA have adverse effects. In the meantime, Dd2-Cys-less PfCRT did not show significant decrease or increase of specific CQ accumulation as the concentration of these three MTS reagents increased. This suggests that the charged 76th amino acid affects the CQ accumulation (Pochini et al., 2004; Ye et al., 2008). According to the reduced positivity model (Warhurst, 2001) (Figure 3-16), with a positively-charged 76th position, susceptible forms repel CQ from the PfCRT pathway. The 76-neutralized (76T) CQR allows CQ to enter the channel of PfCRT and in turn expel CQ. These results can be interpreted as the 76 negatively charged by MTSES facilitates CQ binding to PfCRT, thus increasing the CQ accumulation in microsomes. When modified by MTSET and MTSEA, the positively-charged 76 impedes the CQ binding and so CQ accumulation.

In scanning experiments on the sensitivity of single cysteine substitution mutants to MTSES reagent (Figure 3-9, Figure 3-10 and Figure 3-11), 62, 71 and 73h displayed a lower relative activity (SD <25% of the mean). These four amino acids somewhat face the same lumen of the helix (Figure 3-17). Thus they may have higher accessibility to be modified and impede CQ transport. This may due to a special pathway for MTS access (Akabas et al., 1992;

Conclusion

Altenbach et al., 1990; Frillingos and Kaback, 1997). This hypothesis needs more evidences to be verified. We noted that only negatively-charged 76 demonstrated a higher CQ accumulation, so a different interpretation is needed for 76.

Substrate (CQ) protection of MTS reagent modification was carried out in the presence of non-radiolabeled CQ. In these assays, only 76 showed protection effects. This result strongly suggests that 76 is a binding site of CQ in PfCRT. More kinetic tests are needed to verify this hypothesis.

Reconstituted proteoliposomes were used in this project to study the PfCRT. Dd2-Analysis showing the amount of PfCRT before and after reconstitution was compared. About 31% of PfCRT remained in the proteoliposomes after reconstitution (Table 4-1). Dd2-Cys-less reconstituted proteoliposomes could accumulate $^3\text{H-CQ}$ in a concentration-dependent manner. The $^3\text{H-CQ}$ transport activity was specific. This suggests that Dd2-Cys-less reconstituted proteoliposomes have significant specific CQ accumulation activity. The specific $^3\text{H-CQ}$ accumulation activity of reconstituted proteoliposomes was analyzed (Figure 4-6). All of the reconstituted proteoliposomes showed abilities to accumulate CQ. So we performed MTS treatment assays afterwards.

Since MTSEA demonstrated similar properties in microsomes to MTSET (Figure 3-8, Figure 3-7, Figure 3-11, Figure 3-10, Figure 3-15 and Figure 3-14), MTSES and MTET were chosen for proteoliposome studies. Among these mutants, after modification by MTSES, Dd2-Cys-less-T76C demonstrated a higher relative activity (SD >125% of the mean) and Dd2-Cys-less-I67C and

Conclusion

Dd2-Cys-less-V73C displayed a lower relative activity (SD <50% of the mean). After modification by MTSET, only Cys-less-I67C and Dd2-Cys-less-V73C displayed a lower relative activity (SD <50% of the mean). These suggest that 76, 73 and 67 are accessible to MTS. These results are the same as obtained from microsomes (refer to Section 3.3 and Section 3.4). In the CQ protection assay, CQ prevented 76 from modification by MTSES and the 76th amino acid of PfCRT may be involved in the site where MTSET modification takes place (Figure 4-12 and Figure 4-13). These results are the same as for microsomes (refer to Section 3.3 and Section 3.4).

The effect of residue 163 is regarded as the determinant for CQR phenotype. One hypothesis suggests that this is due to the side chain volume of R¹⁶³. The larger size of Arginine may make 163R more effective in blocking CQ from passing through the channel (Johnson et al., 2004).

The other hypothesis is that the gain of positive charge by S163R may block the efflux of positively-charged molecules from the DV. To verify this, MTSES and MTSET were chosen to carry out the SCAM assay. Modified by MTSET, only S163C displays the significant lower relative activity. This result suggests that inducing a positive charge at 163 may lead to CQ accumulation decrease, thus supporting the “charge” hypothesis. Our results showed that the CQ accumulation ability of 163 was not affected by CQ protection. This suggest that 163 is different from 76 (refer to Section 3.4 and Figure 3-13, Figure 3-14 and Figure 3-15), which may be a CQ binding site within PfCRT.

Summary

Malaria is a major public health problem in the world. It contributes to a considerable burden in endemic communities with premature deaths, disability from illness and impedes social and economic development. Malaria is caused by a parasite called *Plasmodium*, which is found worldwide in tropical and subtropical areas and can cause severe, potentially fatal malaria. WHO forecasts a 16% growth in malaria cases annually. About 1.5 million to 3 million people die of malaria every year (85% of these occur in Africa), accounting for about 4-5% of all fatalities in the world. A persistent effort to control malaria worldwide has been carried out the last two decades with effective tools and methods for prevention and cure.

CQ remains one of the best antimalarial drugs because of its high efficacy, its relative safety and its low cost. The most spectacular characteristic of chloroquine is its capacity to concentrate itself from nanomolar levels outside the parasite to millimolar levels in the DV of the intraerythrocytic trophozoite. CQ inhibits heme crystallization and heme decomposition, resulting in accumulation of toxic free heme and initiating the irreversible demise of the parasite. CQR accumulates significantly less chloroquine than susceptible parasites, and this is thought to be the basis of their resistance. Other studies suggest that the lower level of CQ accumulated in CQR parasite DVs is due to reduced import of CQ rather than increased drug export.

Summary

The gene *pfcr1* has a coding region spanning 3.1 kb in 13 exons ranging in size from 45–269 base pairs. Translation of the Dd2 *pfcr1* coding region predicts a 424 amino acid, 48.6 kDa protein. The protein product of *pfcr1*, PfCRT, belongs to a previously uncharacterized family of putative transporters, with 10 transmembrane segments.

Eight point mutations in PfCRT distinguish chloroquine-resistant from chloroquine-sensitive progeny of the cross. Some authors suggest that the codon 76 changes in PfCRT may reduce chloroquine influx into, or increase chloroquine efflux from the lysosome and/or alter drug action by pH modulation. The mutation in *pfcr1*, S163R in TMD4, results in both loss of chloroquine resistance and verapamil-reversible CQ resistance, despite of the presence of K76T in TMD1.

Our laboratory and Rope's group have successfully expressed PfCRT in *Pichia* and function studies have been carried out. Using this expression system, this project aimed to process the Substituted-cysteine Accessibility Method (SCAM) to elucidate the structure of PfCRT and understand the mechanism of CQR. In this study, using site-directed mutagenesis, Cys-less *pfcr1*, twenty-one cysteine substituted *pfcr1*s within TMD1 and 10 within TMD4 were constituted. Pfcr1s of Cys-less and recoveries within TMD1 were all expressed. But only seven out of ten within TMD4 were expressed. In the *Pichia* expression system, it is familiar to unexpectedly express some membrane proteins. The reason for failure is not clearly understood. In this project, failed expression may be a disadvantage, but it was still suitable for studying the notable position, 163 within TMD4. Purified PfCRT was reconstituted into proteoliposomes for further studies.

Summary

The microsomes isolated from each *P. pastoris* were used to determine the transport activity. Dd2-Cys-less PfCRT could accumulate $^3\text{H-CQ}$ in a concentration-dependent manner. We found that there were significantly different CQ accumulation activities among these mutants. This suggests that CQ might interact with the internal (intra-DV) lumen of PfCRT, supporting the hypothesis that the CQR parasite results from the presence of PfCRT-mediated CQ transport out of the DV. Different reconstituted PfCRTs may contribute to the variation of CQ accumulation. This suggests that cysteine substitution to obligate amino acids affects the function via the amino acid composition of the TMD1 helix.

Modified by MTSES, Dd2-Cys-less-T76C PfCRT microsomes accumulated more CQ when the concentration of MTSES increased. Meanwhile, MTSET and MTSEA led to a decrease of specific CQ accumulation as the concentration of these two MTS reagents increased. This suggests that high concentrations of MTSES can improve the ability of CQ accumulation of Dd2-Cys-less-T76C PfCRT. Nevertheless, MTSET and MTSEA had adverse effects. In the meantime, Dd2-Cys-less PfCRT did not show significant decrease or increase of specific CQ accumulation as the concentration of these three MTS reagents increased. This suggests that a charged 76th amino acid affects the CQ accumulation. According to the reduced positivity model, position 76 positively charged susceptible forms repel CQ from PfCRT pathway. The 76-neutralized (76T) CQR allows CQ to enter the PfCRT channel and expel CQ. Our study experimentally supports this hypothesis. The results can be interpreted as the 76 negatively charged by MTSES facilitates CQ binding to PfCRT, thus increasing

the CQ accumulation in microsomes. When modified by MTSET and MTSEA, positively charged 76 impedes the CQ binding and so CQ accumulation.

In scanning experiments on the sensitivity of single cysteine substitution mutants to MTSES reagent, 62, 71 and 73 displayed a lower relative activity. These four amino acids somewhat face the same lumen the helix. Thus they may have higher accessibility to be modified and impede CQ transport. 67, which is opposite to 76 within the helix, demonstrated higher accessibility to MTS. This may be due to a special pathway for MTS to access it. Substrate (CQ) protection of MTS reagent modification was carried out in the presence of non-radiolabeled CQ. In these assay, only 76 showed protection effects. This result strongly suggests that 76 is a binding site of CQ in PfCRT, More kinetic tests are needed to verify this hypothesis.

Reconstituted proteoliposomes contain a single type of transporter and can be assayed for transport activity. Transport activity can be measured more conclusively in a reconstituted system than in microsomes. In this study, we found that Dd2-Cys-less reconstituted proteoliposomes could accumulate ^3H -CQ in a concentration-dependent manner. This suggests that Dd2-Cys-less reconstituted proteoliposomes have significant specific CQ accumulation activities. The specific ^3H -CQ accumulation activity of reconstituted proteoliposomes was analyzed. All of the reconstituted proteoliposomes showed abilities to accumulate CQ. So we performed MTS treatment assays afterwards. Since MTSEA treatment demonstrated a similar property to MTSET treatment in microsome assays, MTSES and MTET were chosen for proteoliposome studies. Among the mutants, after modification by MTSES, Dd2-Cys-less-T76C

Summary

demonstrated a higher relative activity and Dd2-Cys-less-I67C and Dd2-Cys-less-V73C displayed a lower relative activity. After modification by MTSET, only Cys-less-I67C and Dd2-Cys-less-V73C displayed a lower relative activity. These suggest that 76, 73 and 67 are accessible to MTS. These results are the same as those obtained from microsomeassays. In the CQ protection assay, CQ prevented 76 from modification of MTSES and the 76th amino acid of PfCRT may be involved in the site where MTSET modification takes place.

The gain of positive charge by S163R may block the efflux of positively charged molecules from the DV, thereby trapping protonated CQ in the DV, resulting in susceptibility. To verify this, MTSES and MTSET were chosen to carry out the SCAM assay. On the Dd2-cysteine-less background, seven single cysteine substituted mutants were constructed for this assay. Modified by MTSET, only S163C displayed a lower relative activity. This result suggests that inducing a positive charge at 163 may lead to a CQ accumulation decrease, thus supporting the “charge” hypothesis. Our results showed that the CQ accumulation ability of 163 was not affected by CQ protection. This suggests that 163 is different from 76, which may be a CQ binding site within PfCRT.

Future Work

Using site-directed mutagenesis, Cys-less *pfcr1*, twenty-one cysteine substituted *pfcr1*s within TMD1 and 10 within TMD4 were constituted. PfCRT of Cys-less and 21 cysteine-substituted recoveries in TMD1 were all expressed. Because only seven cysteine-substituted PfCRT mutants in TMD4 were expressed, other cysteine-substituted PfCRT mutants of TMD4 should be constructed for farther study. Since only TMD1 and TMD4 were involved in this project, it is essential to study other TMDs in the future, especially TMD5, TMD3, TMD6, TMD8 and TMD10. It is known that TMDs 5 and 10 have a role in mediating the formation of homo-dimers by the NST and TPT transporters. This is needed to verify that the helix packing motifs in TMDs 5 and 10 may make PfCRT function as a dimer. Since certain residues in TMDs 3 and 8 in DMT transporters assist in the binding and translocation of the substrate and both domains also influence the substrate specificity of the transporter, future workers should focus on these two TMDs. Since amino acid 220S (TMD6) substitution is always required for conversion to a CQR phenotype, so TMD6 should be included in future work.

Using charged MTS reagents, MTSES, MTSET and MTSEA reagents, SCAM was carried out in this project to elucidate the properties of PfCRT. Because these thiol reagents introduce positive or negative charges at the position of previously neutral cysteine residues, they frequently cause a functional change that then can be measured. There are other functional thiol reagents that can be

Future Work

used to understand this protein. The spin-labeled derivative (1-Oxyl-2,2,5,5-tetramethyl- Æ^3 -pyrrolin-3-yl)methyl methanethiosulfonate (MTSL) exhibits high sulfhydryl selectivity and reactivity. Site-directed spin labeling (SDSL) and analysis of the EPR of spin-labeled PfCRT can be used to map the topography of the protein, to determine secondary structure, and to identify sites of tertiary interaction. The MTS-fluorophores could be applied in real-time monitoring of conformational changes, and to get information about distances and molecular motion in PfCRT.

Substrate protection of modification of MTS reagents demonstrated that only 76 has protective effects. Though these results strongly suggest that 76 is a binding site of CQ in PfCRT, farther studies are needed to verify this hypothesis. We can use more specific MTS reagents, e.g. (MTSL) and MTS-fluorophores, to investigate the role of 76. If we can identify sites of tertiary interaction of PfCRT, monitor the conformational changes and gain information about distances and molecular motion in PfCRT, a clearer profiling of 76 then could be obtained.

To avoid the complexity of microsomes, reconstitution proteoliposomes were used in this project to study the PfCRT. But only six substituted PfCRTs have been reconstituted. We should have more reconstituted PfCRTs to carry out SCAM in order to elucidate more properties of PfCRT. Verapamil and two other calcium channels slow the release and increase the accumulation of chloroquine by resistant *P. falciparum*. Verapamil partially reverses CQR *in vitro*. Thus the energy-dependent rapid efflux mechanism was proposed. It is suggested that verapamil inhibits the rapid efflux in CQR parasites resulting in a

Future Work

readily detectable increase in chloroquine accumulation. The chloroquine efflux carrier could be a primary active transporter, such as a pump, or a secondary active transporter that co- or counter-transport chloroquine with or against a substrate. SCAM and co-reconstituted PfCRT and other related transporters or channels, e.g. ATPase or chloride channels, can be applied to elucidate these hypotheses. With coupling between PfCRT and related transporters, and using SCAM to find the possible reaction center and binding sites of related drugs (such as Verapamil) in PfCRT, we may elucidate the role of PfCRT in CQ transport function and help define molecular partners in regulating PfCRT-mediated transport.

Previous work suggested that PfCRT mediates a pH change by cooperating with an unknown ATPase in *P. pastoris* microsomes. Our group found that CQ transport in proteoliposomes is dependent on pH gradient (Tan W, 2006). We suggest that the pH gradient might be caused by PfCRT itself, and these gradients seem to drive CQ transport. Our experiments showed that CQ transport in proteoliposomes is dependent on membrane potential, which are consistent with what was observed in microsomes. This implies that PfCRT by itself can maintain membrane potential without other accessory proteins. This project also found (data not show) that valinomycin and nigericin (acting as an H⁺, K⁺, and Pb²⁺ ionophore) inhibit CQ transport. It seems that PfCRT might mediate CQ transport indirectly through some other means, for example, PfCRT regulates pH across the membrane and the subsequent pH gradient could drive CQ transport. Using SCAM, more experiments should to be carried out to

Future Work

elucidate this hypothesis by finding the possible action center or binding sites of these drugs.

It is known that inducing a positive charge at 163 may lead to CQ accumulation decrease and 163 does not demonstrate a CQ protection effect. So we still need to understand the relationship between 163 and 76. In cross-linking experiments, our group (Chung Yik To's Master of Philosophy thesis) tried to examine the spatial proximity of the 76th and 163rd residues. The apparent reaction of these residues with a homobifunctional cross-linker (bBBr) implied their distance within 6 Å and the inhibition of cross-linking by substrate competition suggested their involvement in the drug-binding pocket. Using MTS cross-linkers of various lengths, future work should try to map the PfCRT channel. If a panel of cross-linkers with different lengths could interact with the residues on the PfCRT lumen, we can construct a spatial configuration of PfCRT and provide a possible structural image to explain the accommodation of different compounds. This should contribute to understand the flexibility of the substrate-binding site of PfCRT.

Appendix

Solution

SDS-PAGE Running Buffer

25 mM Tris base
192 mM Glycine
0.1% SDS

Western Transfer Buffer

192 mM Glycine
25 mM Tris base
20% Methanol

TTBS Washing Buffer

10 mM Tris base pH 7.5
150 mM Sodium chloride
0.05% Tween 20

12% SDS-PAGE separating gel (for 2 gels of 1 mm comb)

4 ml	30% Acrylamide/Bis
2.5 ml	1.5 M Tris-Cl, pH 8.8
100 μ l	10% SDS
50 μ l	10% APS
10 μ l	TEMED
3.35 ml	Distilled water

5% SDS-PAGE stacking gel (for 2 gels of 1 mm comb)

0.66 ml	30% Acrylamide/Bis
1.26 ml	0.5 M Tris-Cl, pH 6.8
50 μ l	10% SDS
25 μ l	10% ammonium persulphate
10 μ l	TEMED

3.00 ml Distilled water

4X SDS loading buffer

40%	glycerol
20%	-mercaptoethanol
12%	SDS
240 mM	Tris-HCl, pH 6.8
0.4%	bromophenol blue

PTM1 Trace Salts (500 ml)

3.0 g	Cupric sulfate-5H ₂ O
0.04 g	Sodium iodide
1.5 g	Manganese sulfate-H ₂ O
0.1 g	Sodium molybdate-2H ₂ O
0.01 g	Boric Acid
0.25 g	Cobalt chloride
10.0 g	Zinc chloride
32.5 g	Ferrous sulfate-7H ₂ O
0.1 g	Biotin
2.5 ml	Sulfuric Acid

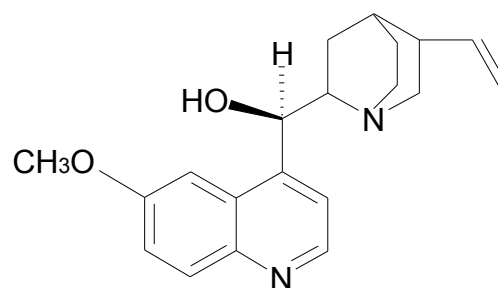
added water to a final volume of 500 ml

Drug Structure

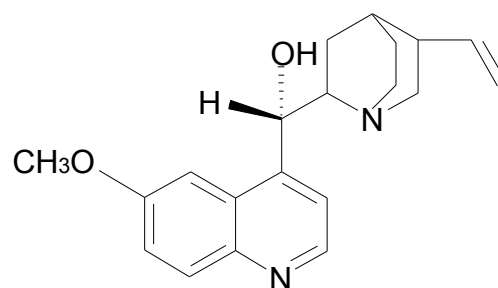
<i>Chemical name</i>	<i>Structures</i>
<p>MTSES</p> <p>Sodium(2-Sulfonatoethyl) methanethiosulfonate</p>	
<p>MTSET</p> <p>[2-(Trimethylammonium)ethyl] methanethiosulfonate</p>	
<p>MTSEA</p> <p>2-Aminoethyl Methanethiosulfonate</p>	
<p>Amodiaquine</p>	
<p>Mefloquine</p>	

Appendix

Quinine



Quinidine



References

- Abe, M., Hashimoto, H., and Yoda, K. (1999). Molecular characterization of Vig4/Vrg4 GDP-mannose transporter of the yeast *Saccharomyces cerevisiae*. *FEBS Lett* 458, 309-312.
- Akabas, M.H., and Karlin, A. (1995). Identification of acetylcholine receptor channel-lining residues in the M1 segment of the alpha-subunit. *Biochemistry* 34, 12496-12500.
- Akabas, M.H., Kaufmann, C., Cook, T.A., and Archdeacon, P. (1994). Amino acid residues lining the chloride channel of the cystic fibrosis transmembrane conductance regulator. *J Biol Chem* 269, 14865-14868.
- Akabas, M.H., Stauffer, D.A., Xu, M., and Karlin, A. (1992). Acetylcholine receptor channel structure probed in cysteine-substitution mutants. *Science* 258, 307-310.
- Akompong, T., Kadekoppala, M., Harrison, T., Oksman, A., Goldberg, D.E., Fujioka, H., Samuel, B.U., Sullivan, D., and Haldar, K. (2002). Trans expression of a *Plasmodium falciparum* histidine-rich protein II (HRPII) reveals sorting of soluble proteins in the periphery of the host erythrocyte and disrupts transport to the malarial food vacuole. *J Biol Chem* 277, 28923-28933.
- Altenbach, C., Marti, T., Khorana, H.G., and Hubbell, W.L. (1990). Transmembrane protein structure: spin labeling of bacteriorhodopsin mutants. *Science* 248, 1088-1092.
- Altschul, S.F., Madden, T.L., Schaffer, A.A., Zhang, J., Zhang, Z., Miller, W., and Lipman, D.J. (1997). Gapped BLAST and PSI-BLAST: a new generation of protein database search programs. *Nucleic Acids Res* 25, 3389-3402.
- Audia, J.P., Roberts, R.A., and Winkler, H.H. (2006). Cysteine-scanning mutagenesis and thiol modification of the *Rickettsia prowazekii* ATP/ADP translocase: characterization of TMs IV-VII and IX-XII and their accessibility to the aqueous translocation pathway. *Biochemistry* 45, 2648-2656.

Reference

- Ayesh, S., Litman, T., and Stein, W.D. (1997). Drug accumulation in the presence of the multidrug resistance pump: dissociation between verapamil accumulation and the action of P-glycoprotein. *Receptors Channels* 5, 175-183.
- Babiker, H.A., Pringle, S.J., Abdel-Muhsin, A., Mackinnon, M., Hunt, P., and Walliker, D. (2001). High-level chloroquine resistance in Sudanese isolates of *Plasmodium falciparum* is associated with mutations in the chloroquine resistance transporter gene *pfcr1* and the multidrug resistance Gene *pfmdr1*. *J Infect Dis* 183, 1535-1538.
- Bannister, L., and Mitchell, G. (2003). The ins, outs and roundabouts of malaria. *Trends Parasitol* 19, 209-213.
- Basco, L.K., and Ringwald, P. (2001). Analysis of the key *pfcr1* point mutation and in vitro and in vivo response to chloroquine in Yaounde, Cameroon. *J Infect Dis* 183, 1828-1831.
- Basivireddy, J., and Balasubramanian, K.A. (2003). A simple method of rat renal brush border membrane preparation using polyethylene glycol precipitation. *Int J Biochem Cell Biol* 35, 1248-1255.
- Bathori, G., Sahin-Toth, M., Fonyo, A., and Ligeti, E. (1993). Transport properties and inhibitor sensitivity of isolated and reconstituted porin differ from those of intact mitochondria. *Biochim Biophys Acta* 1145, 168-176.
- Bayoumi, R.A., Babiker, H.A., and Arnot, D.E. (1994). Uptake and efflux of chloroquine by chloroquine-resistant *Plasmodium falciparum* clones recently isolated in Africa. *Acta Trop* 58, 141-149.
- Beaudet, L., Urbatsch, I.L., and Gros, P. (1998). High-level expression of mouse Mdr3 P-glycoprotein in yeast *Pichia pastoris* and characterization of ATPase activity. *Methods Enzymol* 292, 397-413.
- Becker, K., and Kirk, K. (2004). Of malaria, metabolism and membrane transport. *Trends Parasitol* 20, 590-596.
- Begum, K., Kim, H.S., Kumar, V., Stojiljkovic, I., and Wataya, Y. (2003). In vitro antimalarial activity of metalloporphyrins against *Plasmodium falciparum*. *Parasitol Res* 90, 221-224.

Reference

- Bendrat, K., Berger, B.J., and Cerami, A. (1995). Haem polymerization in malaria. *Nature* 378, 138-139.
- Bevans, C.G., Kordel, M., Rhee, S.K., and Harris, A.L. (1998). Isoform composition of connexin channels determines selectivity among second messengers and uncharged molecules. *J Biol Chem* 273, 2808-2816.
- Blauer, G., and Akkawi, M. (2000). On the preparation of beta-haematin. *Biochem J* 346 Pt 2, 249-250.
- Bonday, Z.Q., Taketani, S., Gupta, P.D., and Padmanaban, G. (1997). Heme biosynthesis by the malarial parasite. Import of delta-aminolevulinate dehydrase from the host red cell. *J Biol Chem* 272, 21839-21846.
- Bowsher, C.G., Scrase-Field, E.F., Esposito, S., Emes, M.J., and Tetlow, I.J. (2007). Characterization of ADP-glucose transport across the cereal endosperm amyloplast envelope. *J Exp Bot* 58, 1321-1332.
- Bray, P.G., Howells, R.E., Ritchie, G.Y., and Ward, S.A. (1992). Rapid chloroquine efflux phenotype in both chloroquine-sensitive and chloroquine-resistant *Plasmodium falciparum*. A correlation of chloroquine sensitivity with energy-dependent drug accumulation. *Biochem Pharmacol* 44, 1317-1324.
- Bray, P.G., Jannah, O., and Ward, S.A. (1999). Chloroquine uptake and activity is determined by binding to ferriprotoporphyrin IX in *Plasmodium falciparum*. *Novartis Found Symp* 226, 252-260; discussion 260-254.
- Bray, P.G., Mungthin, M., Ridley, R.G., and Ward, S.A. (1998). Access to hematin: the basis of chloroquine resistance. *Mol Pharmacol* 54, 170-179.
- Bray, P.G., Saliba, K.J., Davies, J.D., Spiller, D.G., White, M.R., Kirk, K., and Ward, S.A. (2002). Distribution of acridine orange fluorescence in *Plasmodium falciparum*-infected erythrocytes and its implications for the evaluation of digestive vacuole pH. *Mol Biochem Parasitol* 119, 301-304; discussion 307-309, 311-303.
- Buckholz, R.G., and Gleason, M.A. (1991). Yeast systems for the commercial production of heterologous proteins. *Biotechnology (N Y)* 9, 1067-1072.
- Burckhardt, G., Di Sole, F., and Helmle-Kolb, C. (2002). The Na⁺/H⁺ exchanger gene family. *J Nephrol* 15 Suppl 5, S3-21.

Reference

- Chen, N., Russell, B., Staley, J., Kotecka, B., Nasveld, P., and Cheng, Q. (2001). Sequence polymorphisms in *pfCRT* are strongly associated with chloroquine resistance in *Plasmodium falciparum*. *J Infect Dis* *183*, 1543-1545.
- Chervitz, S.A., and Falke, J.J. (1996). Molecular mechanism of transmembrane signaling by the aspartate receptor: a model. *Proc Natl Acad Sci U S A* *93*, 2545-2550.
- Choi, C.Y., Cerda, J.F., Chu, H.A., Babcock, G.T., and Marletta, M.A. (1999). Spectroscopic characterization of the heme-binding sites in *Plasmodium falciparum* histidine-rich protein 2. *Biochemistry* *38*, 16916-16924.
- Cole, K.A., Ziegler, J., Evans, C.A., and Wright, D.W. (2000). Metalloporphyrins inhibit beta-hematin (hemozoin) formation. *J Inorg Biochem* *78*, 109-115.
- Cooper, R.A., Ferdig, M.T., Su, X.Z., Ursos, L.M., Mu, J., Nomura, T., Fujioka, H., Fidock, D.A., Roepe, P.D., and Wellems, T.E. (2002). Alternative mutations at position 76 of the vacuolar transmembrane protein PfCRT are associated with chloroquine resistance and unique stereospecific quinine and quinidine responses in *Plasmodium falciparum*. *Mol Pharmacol* *61*, 35-42.
- Cooper, R.A., Hartwig, C.L., and Ferdig, M.T. (2005). *pfCRT* is more than the *Plasmodium falciparum* chloroquine resistance gene: a functional and evolutionary perspective. *Acta Trop* *94*, 170-180.
- Cregg, J.M., Vedvick, T.S., and Raschke, W.C. (1993). Recent advances in the expression of foreign genes in *Pichia pastoris*. *Biotechnology (N Y)* *11*, 905-910.
- Dean, R.M., Rivers, R.L., Zeidel, M.L., and Roberts, D.M. (1999). Purification and functional reconstitution of soybean nodulin 26. An aquaporin with water and glycerol transport properties. *Biochemistry* *38*, 347-353.
- Demirev, P.A. (2004). Mass spectrometry for malaria diagnosis. *Expert Rev Mol Diagn* *4*, 821-829.
- Diez-Sampedro, A., Loo, D.D., Wright, E.M., Zampighi, G.A., and Hirayama, B.A. (2004). Coupled sodium/glucose cotransport by SGLT1 requires a negative charge at position 454. *Biochemistry* *43*, 13175-13184.

Reference

- Djimde, A., Doumbo, O.K., Cortese, J.F., Kayentao, K., Doumbo, S., Diourte, Y., Dicko, A., Su, X.Z., Nomura, T., Fidock, D.A., *et al.* (2001a). A molecular marker for chloroquine-resistant falciparum malaria. *N Engl J Med* 344, 257-263.
- Djimde, A., Doumbo, O.K., Steketee, R.W., and Plowe, C.V. (2001b). Application of a molecular marker for surveillance of chloroquine-resistant falciparum malaria. *Lancet* 358, 890-891.
- Djimde, A.A., Doumbo, O.K., Traore, O., Guindo, A.B., Kayentao, K., Diourte, Y., Niare-Doumbo, S., Coulibaly, D., Kone, A.K., Cissoko, Y., *et al.* (2003). Clearance of drug-resistant parasites as a model for protective immunity in *Plasmodium falciparum* malaria. *Am J Trop Med Hyg* 69, 558-563.
- Doring, F., Theis, S., and Daniel, H. (1997). Expression and functional characterization of the mammalian intestinal peptide transporter PepT1 in the methylotropic yeast *Pichia pastoris*. *Biochem Biophys Res Commun* 232, 656-662.
- Dorn, A., Stoffel, R., Matile, H., Bubendorf, A., and Ridley, R.G. (1995). Malarial haemozoin/beta-haematin supports haem polymerization in the absence of protein. *Nature* 374, 269-271.
- Dorn, A., Vippagunta, S.R., Matile, H., Bubendorf, A., Vennerstrom, J.L., and Ridley, R.G. (1998). A comparison and analysis of several ways to promote haematin (haem) polymerisation and an assessment of its initiation in vitro. *Biochem Pharmacol* 55, 737-747.
- Dorsey, G., Kanya, M.R., Singh, A., and Rosenthal, P.J. (2001). Polymorphisms in the *Plasmodium falciparum* *pfert* and *pfmdr-1* genes and clinical response to chloroquine in Kampala, Uganda. *J Infect Dis* 183, 1417-1420.
- Dzekunov, S.M., Ursos, L.M., and Roepe, P.D. (2000). Digestive vacuolar pH of intact intraerythrocytic *P. falciparum* either sensitive or resistant to chloroquine. *Mol Biochem Parasitol* 110, 107-124.
- England, P.M., Zhang, Y., Dougherty, D.A., and Lester, H.A. (1999). Backbone mutations in transmembrane domains of a ligand-gated ion channel: implications for the mechanism of gating. *Cell* 96, 89-98.
- Eytan, G.D., Regev, R., and Assaraf, Y.G. (1996a). Functional reconstitution of P-glycoprotein reveals an apparent near stoichiometric drug transport to ATP hydrolysis. *J Biol Chem* 271, 3172-3178.

Reference

- Eytan, G.D., Regev, R., Oren, G., and Assaraf, Y.G. (1996b). The role of passive transbilayer drug movement in multidrug resistance and its modulation. *J Biol Chem* 271, 12897-12902.
- Ferrari, V., and Cutler, D.J. (1990). Uptake of chloroquine by human erythrocytes. *Biochem Pharmacol* 39, 753-762.
- Fidock, D.A., Nomura, T., Cooper, R.A., Su, X., Talley, A.K., and Wellems, T.E. (2000a). Allelic modifications of the *cg2* and *cg1* genes do not alter the chloroquine response of drug-resistant *Plasmodium falciparum*. *Mol Biochem Parasitol* 110, 1-10.
- Fidock, D.A., Nomura, T., Talley, A.K., Cooper, R.A., Dzekunov, S.M., Ferdig, M.T., Ursos, L.M., Sidhu, A.B., Naude, B., Deitsch, K.W., *et al.* (2000b). Mutations in the *P. falciparum* digestive vacuole transmembrane protein PfCRT and evidence for their role in chloroquine resistance. *Mol Cell* 6, 861-871.
- Fidock, D.A., Nomura, T., Talley, A.K., Cooper, R.A., Dzekunov, S.M., Ferdig, M.T., Ursos, L.M., Sidhu, A.B., Naude, B., Deitsch, K.W., *et al.* (2000c). Mutations in the *P. falciparum* digestive vacuole transmembrane protein PfCRT and evidence for their role in chloroquine resistance
- Allelic modifications of the *cg2* and *cg1* genes do not alter the chloroquine response of drug-resistant *Plasmodium falciparum*. *Mol Cell* 6, 861-871.
- Fidock, D.A., Takashi, N., Talley, A.K., Cooper, R.A., Dzekunov, S.M., Ferdig, M.T., Ursos, L.M.B., Sidhu, A.S., Naude, B., Deitsch, K.W., *et al.* (2000d). Mutations in the *P. falciparum* digestive vacuole transmembrane protein PfCRT and evidence for their role in chloroquine resistance. *Mol Cell* 6, 861-871.
- Fitch, C.D. (1970). *Plasmodium falciparum* in owl monkeys: drug resistance and chloroquine binding capacity. *Science* 169, 289-290.
- Fitch, C.D. (1998). Involvement of heme in the antimalarial action of chloroquine. *Trans Am Clin Climatol Assoc* 109, 97-105; discussion 105-106.
- Foley, M., Deady, L.W., Ng, K., Cowman, A.F., and Tilley, L. (1994). Photoaffinity labeling of chloroquine-binding proteins in *Plasmodium falciparum*. *J Biol Chem* 269, 6955-6961.
- Foley, M., and Tilley, L. (1998). Quinoline antimalarials: mechanisms of action and resistance and prospects for new agents. *Pharmacol Ther* 79, 55-87.

Reference

- Francis, S.E., Gluzman, I.Y., Oksman, A., Banerjee, D., and Goldberg, D.E. (1996). Characterization of native falcipain, an enzyme involved in *Plasmodium falciparum* hemoglobin degradation. *Mol Biochem Parasitol* 83, 189-200.
- Frillingos, S., and Kaback, H.R. (1997). The role of helix VIII in the lactose permease of *Escherichia coli*: II. Site-directed sulfhydryl modification. *Protein Sci* 6, 438-443.
- Fritz, F., Howard, E.M., Hoffman, M.M., and Roepe, P.D. (1999). Evidence for altered ion transport in *Saccharomyces cerevisiae* overexpressing human MDR 1 protein. *Biochemistry* 38, 4214-4226.
- Fu, D., Ballesteros, J.A., Weinstein, H., Chen, J., and Javitch, J.A. (1996). Residues in the seventh membrane-spanning segment of the dopamine D2 receptor accessible in the binding-site crevice. *Biochemistry* 35, 11278-11285.
- Fu, D., Sarker, R.I., Abe, K., Bolton, E., and Maloney, P.C. (2001). Structure/function relationships in OxIT, the oxalate-formate transporter of *Oxalobacter formigenes*. Assignment of transmembrane helix 11 to the translocation pathway. *J Biol Chem* 276, 8753-8760.
- Fu, J., and Kirk, K.L. (2001). Cysteine substitutions reveal dual functions of the amino-terminal tail in cystic fibrosis transmembrane conductance regulator channel gating. *J Biol Chem* 276, 35660-35668.
- Gao, X.D., Nishikawa, A., and Dean, N. (2001). Identification of a conserved motif in the yeast golgi GDP-mannose transporter required for binding to nucleotide sugar. *J Biol Chem* 276, 4424-4432.
- Gillen, C.M., and Forbush, B., 3rd (1999). Functional interaction of the K-Cl cotransporter (KCC1) with the Na-K-Cl cotransporter in HEK-293 cells. *Am J Physiol* 276, C328-336.
- Gluzman, I.Y., Krogstad, D.J., Orjih, A.U., Nkangineme, K., Wellems, T.E., Martin, J.T., and Schlesinger, P.H. (1990). A rapid in vitro test for chloroquine-resistant *Plasmodium falciparum*. *Am J Trop Med Hyg* 42, 521-526.
- Goldberg, D.E., Sharma, V., Oksman, A., Gluzman, I.Y., Wellems, T.E., and Piwnica-Worms, D. (1997). Probing the chloroquine resistance locus of *Plasmodium falciparum* with a novel class of multidentate metal(III) coordination complexes. *J Biol Chem* 272, 6567-6572.

Reference

- Grinius, L., Stanton, D.T., Morris, C.M., Howard, J.M., and Curnow, A.W. (2002). Profiling of drugs for membrane activity using liposomes as an in vitro model system. *Drug Dev Ind Pharm* 28, 193-202.
- Grinius, L.L., and Goldberg, E.B. (1994). Bacterial multidrug resistance is due to a single membrane protein which functions as a drug pump. *J Biol Chem* 269, 29998-30004.
- Guizouarn, H., Gabillat, N., and Borgese, F. (2004). Evidence for up-regulation of the endogenous Na-K-2Cl co-transporter by molecular interactions with the anion exchanger tAE1 expressed in *Xenopus* oocyte. *J Biol Chem* 279, 11513-11520.
- Hanscheid, T., Valadas, E., and Grobusch, M.P. (2000). Automated malaria diagnosis using pigment detection. *Parasitol Today* 16, 549-551.
- Hawley, S.R., Bray, P.G., O'Neill, P.M., Naisbitt, D.J., Park, B.K., and Ward, S.A. (1996). Manipulation of the N-alkyl substituent in amodiaquine to overcome the verapamil-sensitive chloroquine resistance component. *Antimicrob Agents Chemother* 40, 2345-2349.
- Henderson, R., Baldwin, J.M., Ceska, T.A., Zemlin, F., Beckmann, E., and Downing, K.H. (1990). Model for the structure of bacteriorhodopsin based on high-resolution electron cryo-microscopy. *J Mol Biol* 213, 899-929.
- Herwaldt, B.L., Schlesinger, P.H., and Krogstad, D.J. (1990). Accumulation of chloroquine by membrane preparations from *Plasmodium falciparum*. *Mol Biochem Parasitol* 42, 257-267.
- Hill, A.V. (2006). Pre-erythrocytic malaria vaccines: towards greater efficacy. *Nat Rev Immunol* 6, 21-32.
- Holmgren, M., Liu, Y., Xu, Y., and Yellen, G. (1996). On the use of thiol-modifying agents to determine channel topology. *Neuropharmacology* 35, 797-804.
- Ivanina, T., Perets, T., Thornhill, W.B., Levin, G., Dascal, N., and Lotan, I. (1994). Phosphorylation by protein kinase A of RCK1 K⁺ channels expressed in *Xenopus* oocytes. *Biochemistry* 33, 8786-8792.
- Iwata, S., Ostermeier, C., Ludwig, B., and Michel, H. (1995). Structure at 2.8 Å resolution of cytochrome c oxidase from *Paracoccus denitrificans*. *Nature* 376, 660-669.

Reference

- Jaburek, M., and Garlid, K.D. (2003). Reconstitution of recombinant uncoupling proteins: UCP1, -2, and -3 have similar affinities for ATP and are unaffected by coenzyme Q10. *J Biol Chem* 278, 25825-25831.
- Jack, D.L., Yang, N.M., and Saier, M.H., Jr. (2001). The drug/metabolite transporter superfamily. *Eur J Biochem* 268, 3620-3639.
- Javitch, J.A., Ballesteros, J.A., Weinstein, H., and Chen, J. (1998). A cluster of aromatic residues in the sixth membrane-spanning segment of the dopamine D2 receptor is accessible in the binding-site crevice. *Biochemistry* 37, 998-1006.
- Javitch, J.A., Fu, D., Chen, J., and Karlin, A. (1995). Mapping the binding-site crevice of the dopamine D2 receptor by the substituted-cysteine accessibility method. *Neuron* 14, 825-831.
- Johnson, D.J., Fidock, D.A., Mungthin, M., Lakshmanan, V., Sidhu, A.B., Bray, P.G., and Ward, S.A. (2004). Evidence for a central role for PfCRT in conferring *Plasmodium falciparum* resistance to diverse antimalarial agents. *Mol Cell* 15, 867-877.
- Juge, N., Yoshida, Y., Yatsushiro, S., Omote, H., and Moriyama, Y. (2006). Vesicular glutamate transporter contains two independent transport machineries. *J Biol Chem* 281, 39499-39506.
- Kaback, H.R. (1997). A molecular mechanism for energy coupling in a membrane transport protein, the lactose permease of *Escherichia coli*. *Proc Natl Acad Sci U S A* 94, 5539-5543.
- Karlin, A. (2001). Scam feels the pinch. *J Gen Physiol* 117, 235-238.
- Karlin, A., and Akabas, M.H. (1998). Substituted-cysteine accessibility method. *Methods Enzymol* 293, 123-145.
- Kirk, K., and Saliba, K.J. (2001). Chloroquine resistance and the pH of the malaria parasite's digestive vacuole. *Drug Resist Updat* 4, 335-337.
- Knappe, S., Flugge, U.I., and Fischer, K. (2003). Analysis of the plastidic phosphate translocator gene family in *Arabidopsis* and identification of new phosphate translocator-homologous transporters, classified by their putative substrate-binding site. *Plant Physiol* 131, 1178-1190.

Reference

- Knol, J., Veenhoff, L., Liang, W.J., Henderson, P.J., Leblanc, G., and Poolman, B. (1996). Unidirectional reconstitution into detergent-destabilized liposomes of the purified lactose transport system of *Streptococcus thermophilus*. *J Biol Chem* 271, 15358-15366.
- Kocken, C.H., Dubbeld, M.A., Van Der Wel, A., Pronk, J.T., Waters, A.P., Langermans, J.A., and Thomas, A.W. (1999). High-level expression of *Plasmodium vivax* apical membrane antigen 1 (AMA-1) in *Pichia pastoris*: strong immunogenicity in *Macaca mulatta* immunized with *P. vivax* AMA-1 and adjuvant SBAS2. *Infect Immun* 67, 43-49.
- Kohler, T., Michea-Hamzehpour, M., Henze, U., Gotoh, N., Curty, L.K., and Pechere, J.C. (1997). Characterization of MexE-MexF-OprN, a positively regulated multidrug efflux system of *Pseudomonas aeruginosa*. *Mol Microbiol* 23, 345-354.
- Kolakovich, K.A., Gluzman, I.Y., Duffin, K.L., and Goldberg, D.E. (1997). Generation of hemoglobin peptides in the acidic digestive vacuole of *Plasmodium falciparum* implicates peptide transport in amino acid production. *Mol Biochem Parasitol* 87, 123-135.
- Krogstad, D.J., Gluzman, I.Y., Kyle, D.E., Oduola, A.M., Martin, S.K., Milhous, W.K., and Schlesinger, P.H. (1987). Efflux of chloroquine from *Plasmodium falciparum*: mechanism of chloroquine resistance. *Science* 238, 1283-1285.
- Krogstad, D.J., and Herwaldt, B.L. (1988). Chemoprophylaxis and treatment of malaria. *N Engl J Med* 319, 1538-1540.
- Krogstad, D.J., and Schlesinger, P.H. (1987). The basis of antimalarial action: non-weak base effects of chloroquine on acid vesicle pH. *Am J Trop Med Hyg* 36, 213-220.
- Krogstad, D.J., Schlesinger, P.H., and Gluzman, I.Y. (1989). Chloroquine and acid vesicle function. *Prog Clin Biol Res* 313, 53-59.
- Kumar, A., Zhang, J., and Yu, F.S. (2006). Toll-like receptor 3 agonist poly(I:C)-induced antiviral response in human corneal epithelial cells. *Immunology* 117, 11-21.
- Kumar, S., Guha, M., Choubey, V., Maity, P., and Bandyopadhyay, U. (2007). Antimalarial drugs inhibiting hemozoin (beta-hematin) formation: a mechanistic update. *Life Sci* 80, 813-828.

Reference

- Kuner, T., Wollmuth, L.P., Karlin, A., Seeburg, P.H., and Sakmann, B. (1996). Structure of the NMDA receptor channel M2 segment inferred from the accessibility of substituted cysteines. *Neuron* *17*, 343-352.
- Leed, A., DuBay, K., Ursos, L.M., Sears, D., De Dios, A.C., and Roepe, P.D. (2002). Solution structures of antimalarial drug-heme complexes. *Biochemistry* *41*, 10245-10255.
- Lerner-Marmarosh, N., Gimi, K., Urbatsch, I.L., Gros, P., and Senior, A.E. (1999). Large scale purification of detergent-soluble P-glycoprotein from *Pichia pastoris* cells and characterization of nucleotide binding properties of wild-type, Walker A, and Walker B mutant proteins. *J Biol Chem* *274*, 34711-34718.
- Liu, Y., Jurman, M.E., and Yellen, G. (1996). Dynamic rearrangement of the outer mouth of a K⁺ channel during gating. *Neuron* *16*, 859-867.
- Livshits, V.A., Zakataeva, N.P., Aleshin, V.V., and Vitushkina, M.V. (2003). Identification and characterization of the new gene *rhtA* involved in threonine and homoserine efflux in *Escherichia coli*. *Res Microbiol* *154*, 123-135.
- Loo, T.W., and Clarke, D.M. (1995a). Membrane topology of a cysteine-less mutant of human P-glycoprotein. *J Biol Chem* *270*, 843-848.
- Loo, T.W., and Clarke, D.M. (1995b). Rapid purification of human P-glycoprotein mutants expressed transiently in HEK 293 cells by nickel-chelate chromatography and characterization of their drug-stimulated ATPase activities. *J Biol Chem* *270*, 21449-21452.
- Loria, P., Miller, S., Foley, M., and Tilley, L. (1999). Inhibition of the peroxidative degradation of haem as the basis of action of chloroquine and other quinoline antimalarials. *Biochem J* *339*, 363-370.
- Mannuzzu, L.M., Moronne, M.M., and Isacoff, E.Y. (1996). Direct physical measure of conformational rearrangement underlying potassium channel gating. *Science* *271*, 213-216.
- Margolles, A., Putman, M., van Veen, H.W., and Konings, W.N. (1999). The purified and functionally reconstituted multidrug transporter LmrA of *Lactococcus lactis* mediates the transbilayer movement of specific fluorescent phospholipids. *Biochemistry* *38*, 16298-16306.

Reference

- Martin, C., Requero, M.A., Masin, J., Konopasek, I., Goni, F.M., Sebo, P., and Ostolaza, H. (2004). Membrane restructuring by *Bordetella pertussis* adenylate cyclase toxin, a member of the RTX toxin family. *J Bacteriol* *186*, 3760-3765.
- Martin, R.E., and Kirk, K. (2004). The malaria parasite's chloroquine resistance transporter is a member of the drug/metabolite transporter superfamily. *Mol Biol Evol* *21*, 1938-1949.
- Martin, S.K., Oduola, A.M., and Milhous, W.K. (1987). Reversal of chloroquine resistance in *Plasmodium falciparum* by verapamil. *Science* *235*, 899-901.
- Martiney, J.A., Cerami, A., and Slater, A.F. (1995). Verapamil reversal of chloroquine resistance in the malaria parasite *Plasmodium falciparum* is specific for resistant parasites and independent of the weak base effect. *J Biol Chem* *270*, 22393-22398.
- Mayor, A.G., Gomez-Olive, X., Aponte, J.J., Casimiro, S., Mabunda, S., Dgedge, M., Barreto, A., and Alonso, P.L. (2001). Prevalence of the K76T mutation in the putative *Plasmodium falciparum* chloroquine resistance transporter (pfcrt) gene and its relation to chloroquine resistance in Mozambique. *J Infect Dis* *183*, 1413-1416.
- Nalbandian, R.M., Sammons, D.W., Manley, M., Xie, L., Sterling, C.R., Egen, N.B., and Gingras, B.A. (1995). A molecular-based magnet test for malaria. *Am J Clin Pathol* *103*, 57-64.
- Naude, B., Brzostowski, J.A., Kimmel, A.R., and Wellems, T.E. (2005). *Dictyostelium discoideum* expresses a malaria chloroquine resistance mechanism upon transfection with mutant, but not wild-type, *Plasmodium falciparum* transporter PfCRT. *J Biol Chem* *280*, 25596-25603.
- Nessler, S., Friedrich, O., Bakouh, N., Fink, R.H., Sanchez, C.P., Planelles, G., and Lanzer, M. (2004). Evidence for Activation of Endogenous Transporters in *Xenopus laevis* Oocytes Expressing the *Plasmodium falciparum* Chloroquine Resistance Transporter, PfCRT. *J Biol Chem* *279*, 39438-39446.
- Orjih, A.U. (1996). Haemolysis of *Plasmodium falciparum* trophozoite-infected erythrocytes after artemisinin exposure. *Br J Haematol* *92*, 324-328.
- Pagola, S., Stephens, P.W., Bohle, D.S., Kosar, A.D., and Madsen, S.K. (2000). The structure of malaria pigment beta-haematin. *Nature* *404*, 307-310.

Reference

- Palmieri, F., Indiveri, C., Bisaccia, F., and Kramer, R. (1993). Functional properties of purified and reconstituted mitochondrial metabolite carriers. *J Bioenerg Biomembr* 25, 525-535.
- Pascual, J.M., Shieh, C.C., Kirsch, G.E., and Brown, A.M. (1995). K⁺ pore structure revealed by reporter cysteines at inner and outer surfaces. *Neuron* 14, 1055-1063.
- Paternostre, M.T., Roux, M., and Rigaud, J.L. (1988). Mechanisms of membrane protein insertion into liposomes during reconstitution procedures involving the use of detergents. 1. Solubilization of large unilamellar liposomes (prepared by reverse-phase evaporation) by triton X-100, octyl glucoside, and sodium cholate. *Biochemistry* 27, 2668-2677.
- Pebay-Peyroula, E., Rummel, G., Rosenbusch, J.P., and Landau, E.M. (1997). X-ray Structure of Bacteriorhodopsin at 2.5 Å from Microcrystals Grown in Lipidic Cubic Phases. *Science* 277, 1676-1681.
- Peters, W., Ekong, R., Robinson, B.L., Warhurst, D.C., and Pan, X.Q. (1989). Antihistaminic drugs that reverse chloroquine resistance in *Plasmodium falciparum*. *Lancet* 2, 334-335.
- Pillai, D.R., Labbe, A.C., Vanisaveth, V., Hongvangthong, B., Pomphida, S., Inkathone, S., Zhong, K., and Kain, K.C. (2001). *Plasmodium falciparum* malaria in Laos: chloroquine treatment outcome and predictive value of molecular markers. *J Infect Dis* 183, 789-795.
- Platel, D.F., Mangou, F., and Tribouley-Duret, J. (1999). Role of glutathione in the detoxification of ferriprotoporphyrin IX in chloroquine resistant *Plasmodium berghei*. *Mol Biochem Parasitol* 98, 215-223.
- Pochini, L., Oppedisano, F., and Indiveri, C. (2004). Reconstitution into liposomes and functional characterization of the carnitine transporter from renal cell plasma membrane. *Biochim Biophys Acta* 1661, 78-86.
- Prabhu, R., and Balasubramanian, K.A. (2003). Simple method of preparation of rat colonocyte apical membranes using polyethylene glycol precipitation. *J Gastroenterol Hepatol* 18, 809-814.
- Prapunwattana, P., Sirawaraporn, W., Yuthavong, Y., and Santi, D.V. (1996). Chemical synthesis of the *Plasmodium falciparum* dihydrofolate reductase-thymidylate synthase gene. *Mol Biochem Parasitol* 83, 93-106.

Reference

- Putman, M., van Veen, H.W., Degener, J.E., and Konings, W.N. (2001). The lactococcal secondary multidrug transporter LmrP confers resistance to lincosamides, macrolides, streptogramins and tetracyclines. *Microbiology* *147*, 2873-2880.
- Putman, M., van Veen, H.W., Poolman, B., and Konings, W.N. (1999). Restrictive use of detergents in the functional reconstitution of the secondary multidrug transporter LmrP. *Biochemistry* *38*, 1002-1008.
- Racker, E. (1979). Reconstitution of membrane processes. *Methods Enzymol* *55*, 699-711.
- Ramirez-Latorre, J., Yu, C.R., Qu, X., Perin, F., Karlin, A., and Role, L. (1996). Functional contributions of alpha5 subunit to neuronal acetylcholine receptor channels. *Nature* *380*, 347-351.
- Ridley, R.G. (1998). Malaria: dissecting chloroquine resistance. *Curr Biol* *8*, R346-349.
- Riordan, J.R., Deuchars, K., Kartner, N., Alon, N., Trent, J., and Ling, V. (1985). Amplification of P-glycoprotein genes in multidrug-resistant mammalian cell lines. *Nature* *316*, 817-819.
- Roberts, D.D., Lewis, S.D., Ballou, D.P., Olson, S.T., and Shafer, J.A. (1986). Reactivity of small thiolate anions and cysteine-25 in papain toward methyl methanethiosulfonate. *Biochemistry* *25*, 5595-5601.
- Romanos, M.A., Scorer, C.A., and Clare, J.J. (1992). Foreign gene expression in yeast: a review. *Yeast* *8*, 423-488.
- Rubio, J.P., and Cowman, A.F. (1996). The ATP-binding cassette (ABC) gene family of *Plasmodium falciparum*. *Parasitol Today* *12*, 135-140.
- Saier, M.H., Jr. (2000). A functional-phylogenetic classification system for transmembrane solute transporters. *Microbiol Mol Biol Rev* *64*, 354-411.
- Saliba, K.J., Folb, P.I., and Smith, P.J. (1998). Role for the *Plasmodium falciparum* digestive vacuole in chloroquine resistance. *Biochem Pharmacol* *56*, 313-320.

Reference

- Sanchez, C.P., McLean, J.E., Stein, W., and Lanzer, M. (2004). Evidence for a substrate specific and inhibitable drug efflux system in chloroquine resistant *Plasmodium falciparum* strains. *Biochemistry* *43*, 16365-16373.
- Sanchez, C.P., Rohrbach, P., McLean, J.E., Fidock, D.A., Stein, W.D., and Lanzer, M. (2007a). Differences in trans-stimulated chloroquine efflux kinetics are linked to PfCRT in *Plasmodium falciparum*. *Mol Microbiol* *64*, 407-420.
- Sanchez, C.P., Stein, W., and Lanzer, M. (2003). Trans stimulation provides evidence for a drug efflux carrier as the mechanism of chloroquine resistance in *Plasmodium falciparum*. *Biochemistry* *42*, 9383-9394.
- Sanchez, C.P., Stein, W.D., and Lanzer, M. (2007b). Is PfCRT a channel or a carrier? Two competing models explaining chloroquine resistance in *Plasmodium falciparum*. *Trends Parasitol* *23*, 332-339.
- Schmitt, C., and Burckhardt, G. (1993). p-Aminohippurate/2-oxoglutarate exchange in bovine renal brush-border and basolateral membrane vesicles. *Pflugers Arch* *423*, 280-290.
- Schumann, R.R. (2007). Malarial fever: hemozoin is involved but Toll-free. *Proc Natl Acad Sci U S A* *104*, 1743-1744.
- Sentjurc, M., Vrhovnik, K., and Kristl, J. (1999). Liposomes as a topical delivery system: the role of size on transport studied by the EPR imaging method. *J Control Release* *59*, 87-97.
- Sha, Q., Lansbery, K.L., Distefano, D., Mercer, R.W., and Nichols, C.G. (2001). Heterologous expression of the Na(+),K(+)-ATPase gamma subunit in *Xenopus* oocytes induces an endogenous, voltage-gated large diameter pore. *J Physiol* *535*, 407-417.
- Shapiro, A.B., Corder, A.B., and Ling, V. (1997). P-glycoprotein-mediated Hoechst 33342 transport out of the lipid bilayer. *Eur J Biochem* *250*, 115-121.
- Shear, H.L., Grinberg, L., Gilman, J., Fabry, M.E., Stamatoyannopoulos, G., Goldberg, D.E., and Nagel, R.L. (1998). Transgenic mice expressing human fetal globin are protected from malaria by a novel mechanism. *Blood* *92*, 2520-2526.

Reference

Sidhu, A.B., Verdier-Pinard, D., and Fidock, D.A. (2002). Chloroquine resistance in *Plasmodium falciparum* malaria parasites conferred by *pfcr* mutations. *Science* 298, 210-213.

Silvius, J.R. (1992). Solubilization and functional reconstitution of biomembrane components. *Annu Rev Biophys Biomol Struct* 21, 323-348.

Sirawaraporn, W., Sirawaraporn, R., Cowman, A.F., Yuthavong, Y., and Santi, D.V. (1990). Heterologous expression of active thymidylate synthase-dihydrofolate reductase from *Plasmodium falciparum*. *Biochemistry* 29, 10779-10785.

Slater, A.F. (1993). Chloroquine: mechanism of drug action and resistance in *Plasmodium falciparum*. *Pharmacol Ther* 57, 203-235.

Slater, A.F., and Cerami, A. (1992). Inhibition by chloroquine of a novel haem polymerase enzyme activity in malaria trophozoites. *Nature* 355, 167-169.

Slomianny, C., Prensier, G., and Charet, P. (1985). [Comparative ultrastructural study of the process of hemoglobin degradation by *P. berghei* (Vincke and Lips, 1948) as a function of the state of maturity of the host cell]. *J Protozool* 32, 1-5.

Sonnhammer, E.L., von Heijne, G., and Krogh, A. (1998). A hidden Markov model for predicting transmembrane helices in protein sequences. *Proc Int Conf Intell Syst Mol Biol* 6, 175-182.

Stauffer, D.A., and Karlin, A. (1994). Electrostatic potential of the acetylcholine binding sites in the nicotinic receptor probed by reactions of binding-site cysteines with charged methanethiosulfonates. *Biochemistry* 33, 6840-6849.

Su, X., and Wellems, T.E. (1996). Toward a high-resolution *Plasmodium falciparum* linkage map: polymorphic markers from hundreds of simple sequence repeats. *Genomics* 33, 430-444.

Sullivan, A.D., Ittarat, I., and Meshnick, S.R. (1996a). Patterns of haemozoin accumulation in tissue. *Parasitology* 112 (Pt 3), 285-294.

Sullivan, D.J., Jr., Gluzman, I.Y., Russell, D.G., and Goldberg, D.E. (1996b). On the molecular mechanism of chloroquine's antimalarial action. *Proc Natl Acad Sci U S A* 93, 11865-11870.

Reference

- Sun, J., and Kaback, H.R. (1997). Proximity of periplasmic loops in the lactose permease of *Escherichia coli* determined by site-directed cross-linking. *Biochemistry* 36, 11959-11965.
- Sun, J., Li, J., Carrasco, N., and Kaback, H.R. (1997). The last two cytoplasmic loops in the lactose permease of *Escherichia coli* comprise a discontinuous epitope for a monoclonal antibody. *Biochemistry* 36, 274-280.
- Sun, J., Wu, J., Carrasco, N., and Kaback, H.R. (1996). Identification of the epitope for monoclonal antibody 4B1 which uncouples lactose and proton translocation in the lactose permease of *Escherichia coli*. *Biochemistry* 35, 990-998.
- Tan, W., Gou, D.M., Tai, E., Zhao, Y.Z., and Chow, L.M. (2006). Functional reconstitution of purified chloroquine resistance membrane transporter expressed in yeast. *Arch Biochem Biophys* 452, 119-128.
- Tinto, H., Guekoun, L., Zongo, I., Guiguemde, R.T., D'Alessandro, U., and Ouedraogo, J.B. (2008). Chloroquine-resistance molecular markers (Pfcrt T76 and Pfmdr-1 Y86) and amodiaquine resistance in Burkina Faso. *Trop Med Int Health* 13, 238-240.
- Towbin, H., Staehelin, T., and Gordon, J. (1979). Electrophoretic transfer of proteins from polyacrylamide gels to nitrocellulose sheets: procedure and some applications. *Proc Natl Acad Sci U S A* 76, 4350-4354.
- Trager, W. (2003). The formation of haemozoin--further intrigue. *Trends Parasitol* 19, 388.
- Tran, C.V., and Saier, M.H., Jr. (2004). The principal chloroquine resistance protein of *Plasmodium falciparum* is a member of the drug/metabolite transporter superfamily. *Microbiology* 150, 1-3.
- Trape, J.F., Pison, G., Preziosi, M.P., Enel, C., Desgrees du Lou, A., Delaunay, V., Samb, B., Lagarde, E., Molez, J.F., and Simondon, F. (1998). Impact of chloroquine resistance on malaria mortality. *C R Acad Sci III* 321, 689-697.
- Trape, J.F., Pison, G., Spiegel, A., Enel, C., and Rogier, C. (2002). Combating malaria in Africa. *Trends Parasitol* 18, 224-230.

Reference

- Tschopp, J.F., Brust, P.F., Cregg, J.M., Stillman, C.A., and Gingeras, T.R. (1987). Expression of the lacZ gene from two methanol-regulated promoters in *Pichia pastoris*. *Nucleic Acids Res* *15*, 3859-3876.
- Ursos, L.M., Dzekunov, S.M., and Roepe, P.D. (2000). The effects of chloroquine and verapamil on digestive vacuolar pH of *P. falciparum* either sensitive or resistant to chloroquine. *Mol Biochem Parasitol* *110*, 125-134.
- van Klompenburg, W., Nilsson, I., von Heijne, G., and de Kruijff, B. (1997). Anionic phospholipids are determinants of membrane protein topology. *Embo J* *16*, 4261-4266.
- Vieira, P.P., das Gracias Alecrim, M., da Silva, L.H., Gonzalez-Jimenez, I., and Zalis, M.G. (2001). Analysis of the PfCRT K76T mutation in *Plasmodium falciparum* isolates from the Amazon region of Brazil. *J Infect Dis* *183*, 1832-1833.
- Wadia, J.S., and Dowdy, S.F. (2002). Protein transduction technology. *Curr Opin Biotechnol* *13*, 52-56.
- Wagner, C.A., Broer, A., Albers, A., Gamper, N., Lang, F., and Broer, S. (2000). The heterodimeric amino acid transporter 4F2hc/LAT1 is associated in *Xenopus* oocytes with a non-selective cation channel that is regulated by the serine/threonine kinase *sgk-1*. *J Physiol* *526 Pt 1*, 35-46.
- Walliker, D., Hunt, P., and Babiker, H. (2005). Fitness of drug-resistant malaria parasites. *Acta Trop* *94*, 251-259.
- Wang, X., Sarker, R.I., and Maloney, P.C. (2006). Analysis of substrate-binding elements in OxIT, the oxalate:formate antiporter of *Oxalobacter formigenes*. *Biochemistry* *45*, 10344-10350.
- Ward, S.A., Bray, P.G., and Hawley, S.R. (1997). Quinoline resistance mechanisms in *Plasmodium falciparum*: the debate goes on. *Parasitology* *114 Suppl*, S125-136.
- Warhurst, D. (2001). New developments: chloroquine-resistance in *Plasmodium falciparum*. *Drug Resist Updat* *4*, 141-144.
- Warhurst, D. (June 23, 2002:). *Plasmodium falciparum* chloroquine-resistance transporter: one of the usual channels? Paper presented at: COST B9 meeting on antiprotozoal chemotherapy (London).

Reference

- Warhurst, D.C. (2002). Resistance to antifolates in *Plasmodium falciparum*, the causative agent of tropical malaria. *Sci Prog* 85, 89-111.
- Warhurst, D.C., Craig, J.C., and Adagu, I.S. (2002). Lysosomes and drug resistance in malaria. *Lancet* 360, 1527-1529.
- Wellems, T.E., Panton, L.J., Gluzman, I.Y., do Rosario, V.E., Gwadz, R.W., Walker-Jonah, A., and Krogstad, D.J. (1990). Chloroquine resistance not linked to *mdr*-like genes in a *Plasmodium falciparum* cross. *Nature* 345, 253-255.
- Wellems, T.E., and Plowe, C.V. (2001). Chloroquine-resistant malaria. *J Infect Dis* 184, 770-776.
- Wellems, T.E., Walker-Jonah, A., and Panton, L.J. (1991). Genetic mapping of the chloroquine-resistance locus on *Plasmodium falciparum* chromosome 7. *Proc Natl Acad Sci U S A* 88, 3382-3386.
- WHO <http://www.who.int/mediacentre/factsheets/fs094/en/>.
- WHO (2008). World Malaria Report 2008.
- Wiesner, J., Ortmann, R., Jomaa, H., and Schlitzer, M. (2003). New antimalarial drugs. *Angew Chem Int Ed Engl* 42, 5274-5293.
- Winograd, E., Clavijo, C.A., Bustamante, L.Y., and Jaramillo, M. (1999). Release of merozoites from *Plasmodium falciparum*-infected erythrocytes could be mediated by a non-explosive event. *Parasitol Res* 85, 621-624.
- Wootton, J.C., Feng, X., Ferdig, M.T., Cooper, R.A., Mu, J., Baruch, D.I., Magill, A.J., and Su, X.Z. (2002). Genetic diversity and chloroquine selective sweeps in *Plasmodium falciparum*. *Nature* 418, 320-323.
- Wright, C.W., Addae-Kyereme, J., Breen, A.G., Brown, J.E., Cox, M.F., Croft, S.L., Gokcek, Y., Kendrick, H., Phillips, R.M., and Pollet, P.L. (2001). Synthesis and evaluation of cryptolepine analogues for their potential as new antimalarial agents. *J Med Chem* 44, 3187-3194.
- Xie, H., Patching, S.G., Gallagher, M.P., Litherland, G.J., Brough, A.R., Venter, H., Yao, S.Y., Ng, A.M., Young, J.D., Herbert, R.B., *et al.* (2004). Purification and

properties of the Escherichia coli nucleoside transporter NupG, a paradigm for a major facilitator transporter sub-family. *Mol Membr Biol* 21, 323-336.

Xu, M., and Akabas, M.H. (1993). Amino acids lining the channel of the gamma-aminobutyric acid type A receptor identified by cysteine substitution. *J Biol Chem* 268, 21505-21508.

Xu, M., and Akabas, M.H. (1996). Identification of channel-lining residues in the M2 membrane-spanning segment of the GABA(A) receptor alpha1 subunit. *J Gen Physiol* 107, 195-205.

Yan, R.T., and Maloney, P.C. (1993). Identification of a residue in the translocation pathway of a membrane carrier. *Cell* 75, 37-44.

Yang, G., Liu, R.Q., Taylor, K.L., Xiang, H., Price, J., and Dunaway-Mariano, D. (1996). Identification of active site residues essential to 4-chlorobenzoyl-coenzyme A dehalogenase catalysis by chemical modification and site directed mutagenesis. *Biochemistry* 35, 10879-10885.

Yayon, A. (1985). The antimalarial mode of action of chloroquine. *Rev Clin Basic Pharm* 5, 99-139.

Yayon, A., Cabantchik, Z.I., and Ginsburg, H. (1984). Identification of the acidic compartment of Plasmodium falciparum-infected human erythrocytes as the target of the antimalarial drug chloroquine. *Embo J* 3, 2695-2700.

Yayon, A., Cabantchik, Z.I., and Ginsburg, H. (1985). Susceptibility of human malaria parasites to chloroquine is pH dependent. *Proc Natl Acad Sci U S A* 82, 2784-2788.

Ye, L., and Maloney, P.C. (2002). Structure/function relationships in OxIT, the oxalate/formate antiporter of Oxalobacter formigenes: assignment of transmembrane helix 2 to the translocation pathway. *J Biol Chem* 277, 20372-20378.

Ye, L., McKinney, C.C., Feng, M., and Maloney, P.C. (2008). Cysteine Scanning Mutagenesis of TM5 Reveals Conformational Changes in OxIT, the Oxalate Transporter of *Oxalobacter formigenes*. *Biochemistry* 47, 5709-5717.

Yerushalmi, H., Lebendiker, M., and Schuldiner, S. (1995). EmrE, an Escherichia coli 12-kDa multidrug transporter, exchanges toxic cations and H⁺ and is soluble in organic solvents. *J Biol Chem* 270, 6856-6863.

Reference

Zgurskaya, H.I., and Nikaido, H. (1999). Bypassing the periplasm: reconstitution of the AcrAB multidrug efflux pump of *Escherichia coli*. *Proc Natl Acad Sci U S A* 96, 7190-7195.

Zhang, H., Howard, E.M., and Roepe, P.D. (2002). Analysis of the antimalarial drug resistance protein Pfcrf expressed in yeast. *J Biol Chem* 277, 49767-49775.

Zhang, H., Paguio, M., and Roepe, P.D. (2004). The antimalarial drug resistance protein *Plasmodium falciparum* chloroquine resistance transporter binds chloroquine. *Biochemistry* 43, 8290-8296.

Ziegler, J., Linck, R., and Wright, D.W. (2001). Heme Aggregation inhibitors: antimalarial drugs targeting an essential biomineralization process. *Curr Med Chem* 8, 171-189.